HIGH-THROUGHPUT CHEMICAL ANALYSIS USING CAPILLARY ELECTROPHORESIS AND ELECTROSPRAY IONIZATION MASS SPECTROMETRY WITH APPLICATIONS TO DRUG SCREENING

by

Jian Pei

A dissertation submitted in partial fulfillment
of the requirements for the degree of
Doctor of Philosophy
(Chemistry)
in The University of Michigan
2010

Doctoral Committee:

Professor Robert T. Kennedy, Chair
Professor Michael D. Morris
Professor Richard R. Neubig
Associate Professor Kristina I. Hakansson

2010

To my family and friends, who warmed me up and gave me courage to get through the winters.

ACKNOWLEDGEMENTS

I owe my deepest gratitude to my advisor Professor Robert T. Kennedy, whose encouragement, guidance and support made my graduate school experience very rewarding. Also this thesis would not have been possible without the help and friendship from all past and present members of the Kennedy group. Special thanks go to Dr. Emily Jameson who taught me how to operate the fancy flow-gate CE system, Dr. Jennifer Cunliffe for insightful discussions about cellular signaling, Dr. Zechariah Sandlin for his electronics expertise and Qiang Li for pleasant and fruitful collaboration on the mass spectrometry projects.

It is an honor for me to have Dr. Richard Neubig, Dr. Kristina Hakansson and Dr. Michael Morris on my doctoral committee. I am grateful for their guidance and assistance throughout my tenure at the University of Michigan. Particularly I would like to thank Dr. Richard Neubig and his lab member David Roman for collaborating on the GPCR/RGS projects and for generously donating precious protein samples used in this work. I would also like to thank Dr. Roger Sunahara for some wonderful biochemistry laboratory experience. I also thank Dr. Gary Valaskovic from New Objective for generously donating the ESI emitter tips used in this work.

.

TABLE OF CONTENTS

CHAPTER 6 FUTURE DIRECTIONS

LIST OF FIGURES

Figure

LIST OF ABBREVIATIONS

α_{2A}AR	α_{2A} adrenoreceptor
Ach	Acetylcholine
AchE	Acetylcholinesterase
AD	Alzheimer's disease
AppNHp	Adenosine 5'-[(β,γ)-imido]triphosphate
BGDP	BODIPY® FL GDP
BGTP	BODIPY® FL GTP
C351I	α_{2A}AR – $G_{\alpha o1}$ C351I fusion
CAE	Capillary array electrophoresis
cAMP	Cyclic adenosine monophosphate
CCD	Charge-coupled device
CE	Capillary electrophoresis
CEC	Capillary electro-chromatography
CGE	Capillary gel electrophoresis
CIEF	Capillary isoelectric focusing
CZE	Capillary zone electrophoresis
DMSO	Dimethyl sulfoxide
EC	Electrochemical (detection)

EMMA	Electrophoretically mediated microanalysis
EOF	Electroosmotic flow
ESI	Electrospray ionization
FCPIA	Flow cytometry protein interaction assay
FIA	Flow injection analysis
FLIPR	Fluorometric imaging plate reader
FSCE	Free-solution capillary electrophoresis
G protein	Guanine nucleotide-binding protein
GAP	GTPase activating protein
GDP	Guanosine 5'-diphosphate
GE	Gel electrophoresis
GEF	Guanine nucleotide exchange factor
GPCR	G protein-coupled receptor
GTP	Guanosine 5'-triphosphate
$GTP_{\gamma}S$	Guanosine 5'-O-(thiotriphosphate)
$G_{\alpha i1}$	recombinant-myristolated $G_{\alpha i1}$
$G_{\alpha o}$	His_6-$G_{\alpha o}$
HTS	High-throughput screening
i.d.	Inner diameter
IS	Internal standard
k_{cat}	Turnover number
K_M	Michaelis-Menten constant

LIF	Laser-induced fluorescence
LOD	Limit of detection
MALDI	Matrix-assisted laser desorption/ionization
MEKC	Micellar electrokinetic capillary chromatography
MEMS	Microelectromechanical system
MS	Mass spectrometry/mass spectrometer
MTP	Multi-well plate
NMR	Nuclear magnetic resonance
o.d.	Outer diameter
OTCS	Octadecyltrichlorosilane
PMT	Photomultiplier tube
RFU	Relative fluorescence unit
RGS	Regulator of G protein signaling
RSD	Relative standard deviation
TG	Tris-glycine (buffer)
TGEM	TG buffer with 10 mM $MgCl_2$ and 1mM EDTA
TRF	Time-resolved fluorescence
uHTS	Ultrahigh-throughput screening
µTAS	Micro-total analysis system
UV	Ultraviolet (detection)
wt	Wild type
YJ34	Ac-Val-Lys-c(Et)[Cys-Thr-Gly-Ile-Cys]-Glu-NH_2

ABSTRACT

Ever increasing throughput in chemical analysis is of interest for many endeavors including biochemistry, genetics and pharmacology. One of the most prominent areas is drug discovery where combinatorial libraries are screened for their activities using biochemical assays. Although multi-well plate-based fluorescence assays are highly successful for high-throughput screening, more information rich and label-free assays would be more versatile and offer new opportunities for human therapeutics discovery. In this dissertation, methods for improving throughput of electrophoretic and mass spectrometric assays and their applications to drug screening will be described.

A fluorescent hydrolysis assay was first developed for G protein-coupled receptors (GPCRs). This assay utilized capillary electrophoresis (CE) for fast determination of GPCR activation and proved to be amenable for high-throughput applications. Throughput of assays of this kind was then improved by developing microfluidic chips with up to 36 parallel electrophoresis channels each capable of rapid separation. This system was applied to testing for inhibitors of RGS-G Protein interaction. Further improvement of assay throughput was sought by developing a sample introduction interface which allowed discrete samples in a two-phase flow to be continuously fed to parallel

CE separation. The ultimate throughput obtained was no longer limited by the time-consuming sample transferring step but only by speed of CE separation.

In the second approach, mass spectrometry (MS) was explored as an analytical method for label-free enzyme assays. In order to improve the throughput of MS-based assays and fully exploit the fast scanning speed of MS, nanoliter of sample plugs segmented by air were sequentially infused to a conductive nano-electrospray ionization (ESI) emitter tip for fast MS analysis. High-throughput screening (HTS) of acetylcholinesterase inhibitors was demonstrated using this method and a throughput of 0.65 Hz was achieved.

CHAPTER 1

INTRODUCTION

Overview

Analytical development for chemical analysis is in the transition from traditional expensive and bulky instruments to miniaturized, low-cost and functionally integrated devices. One of the promises offered by these 'chip'-sized devices is automated sample processing and high throughput. Increasing throughput for chemical analysis is of great interest and pursued for many endeavors including biochemistry, genetics, drug discovery, proteomics, clinical chemistry and pharmacology. One of the most prominent areas where high throughput analysis plays a pivotal role is drug discovery. In this case, lead compounds are discovered by testing libraries of candidate compounds. With the adoption of combinatorial synthesis, 10^5 – 10^7 of chemical entities can be generated for a screening library. In order to test such a huge number of compounds, both assay systems and robotics have evolved over the past two decades so that over 100,000 assays can be performed each day. Such systems are considered to be ultrahigh throughput screening (uHTS)[1].

Sample and reagent consumption of screening assays is another key issue for high-throughput analysis. With thousands of assays performed per day, reagent

consumption can become a significant portion of the R&D cost. Reagent consumption has been largely decreased by miniaturizing the HTS system and employing high-density microtiter plate (MTP). For example, by using 1536-well plate which has a working volume of 5 μL/well, a 20-fold decrease in reagent consumption and a 16-fold increase in throughput can be achieved compared to traditional 96-well plate. Recently even plates of 9,600 wells with a working volume of 0.2 μL/well have been introduced[2]. However, miniaturization adds to the technical difficulties of reagent dispensing and demands higher sensitivity for the detection methods used[3].

Pipetting and dispensing techniques for MTP-based HTS have been reviewed in several articles[3, 4]. These techniques use different mechanisms such as displacement, capillary force and droplet ejection. Evaporation and adsorption can become a major limitation of such techniques. Also detection schemes that are compatible with MTP screening are limited to techniques such as scintillation proximity assays (SPAs), fluorescence and luminescence[5-7]. As powerful as these detection systems are, they have relatively low information output. They always rely on changes in the total emitted signals from the sample which would indicate progression of the reactions. In most cases, only a single component in the assay, usually the one with special label or spectroscopic property, can be monitored. Also sometimes a suitable indicator or label is not readily available which limits the assays that can be performed on MTP. Moreover, the overall spectroscopic signal can be skewed due by the presence of background matrix which adds uncertainty to interpreting the screening results.

In considering these limitations, it is apparent that separation techniques may be desirable tools to be added to the repertoire of HTS. For example capillary electrophoresis (CE) has useful properties for HTS applications such as high speed, high resolution separation, low sample consumption and high mass sensitivity. In the first part of the work presented herein, we demonstrate all the steps necessary for applying CE to HTS including assay development (Chapter 2), system miniaturization and throughput improvement(Chapter 3), and finally automation (Chapter 4).

In the later part of the dissertation, use of mass spectrometry (MS) for HTS was explored. MS also offers several useful properties for HTS including rapid analysis and label-free detection. We envision that by employing MS we can further expand the applications of HTS. The throughput of MS has been limited by the rate at which samples are delivered to its inlet. In Chapter 5, a novel sample introduction scheme for electrospray ionization MS (ESI-MS) was presented and its application to drug screening was demonstrated.

Principles of Capillary Electrophoresis (CE)

We first developed CE-based HTS; hence its basics are discussed in the next three sections. Ever since Michaelis observed proteins migrate to their isoelectric points under an external electric field in 1909[8], electrophoresis-based separation techniques have evolved into a number of different modes. These include capillary zone electrophoresis (CZE) which is also known as free-solution CE (FSCE), micellar electrokinetic capillary chromatography (MEKC), capillary isoelectric focusing

(CIEF), capillary gel electrophoresis (CGE), and capillary electro-chromatography (CEC). The separation path in all these techniques is confined in a capillary that has an inner diameter ranging from 5 to 200 μm and a length from 5 to 100 cm. The micro-scale separation space in a capillary can effectively prevent convectional distortion of the analyte bands, which is similar to what polyacrylamide or agarose does in slab gel electrophoresis (GE). Furthermore, a capillary format offers advantages over traditional gels in that its high surface-to-volume ratio enables efficient dissipation of Joule heat thus allowing an electric field up to several thousand volts per centimeter to be applied compared to merely 15-40 V/cm for GE.

CZE, which is usually referred to as CE, is the simplest yet most widely used format of electrophoretic separation in capillary. In CZE bands of analytes migrate in the background electrolyte (BGE) solution when an electric field is applied across the capillary. The speed and direction of analyte migration are governed by two phenomena: electrophoresis and electroosmotic flow (EOF). Electrophoresis is the migration of charged particles experiencing an electric field. Its speed is measured by electrophoretic mobility (μ). μ is an intrinsic property of the analyte and is described by:

$$\mu = \frac{q}{6\pi\eta r}$$

where q is the charge of the particle, η is the viscosity of the electrophoresis buffer, r is the Stoke's radius of the particle. So the charge-to-size ratio of the analyte determines its electrophoretic mobility. Electroosmotic flow, on the other hand, is the result of ionized silanol groups on the inner capillary wall (the charged chemical

moiety can be different when material other than fused silica is used). The charged silanol groups cause a net positive charge for the bulk electrophoresis buffer and under the electric field the bulk solution migrates toward cathode. The electroosmotic mobility (μ_{eo}) is described by:

$$\mu_{eo} = \frac{\varepsilon\xi}{\eta}$$

where ε is the permittivity and η is the viscosity of the solution, and ξ is the potential in the Helmholtz plane. So the EOF is dependent on the ξ potential which is determined by the ionic properties at the capillary/buffer interface. The overall migration velocity (v) of the analyte is then proportional to the electric field strength (E) and given by:

$$v = (\mu_{eo} + \mu)E$$

Since the thickness of the diffusion layer at the capillary/buffer interface is negligible compared to the capillary i.d., EOF has a plug-shaped velocity profile compared to the parabolic profile of a laminar flow driven by pressure. This directly results in much less band broadening compared to techniques such as HPLC.

In the ideal situation, when factors such as Joule heating, injected sample plug width and adsorption are controlled or inconsequential, diffusion is the only dispersive phenomenon contributing to the peak broadening, quantified as:

$$\sigma^2 = \frac{2D_i L_d}{(\mu_{eo} + \mu)E}$$

where σ^2 is the variance of the zone. As can be seen in the equation, high diffusion coefficient, long migration length and slow migration velocity result in wider peaks.

To measure the efficiency of CZE separation, N, the number of theoretical plates, can be calculated as following:

$$N = \frac{L^2}{\sigma^2} = \frac{\mu_{ave} V}{2D_i}$$

where μ_{ave} is the average mobility of the analytes and L is the migration length. Since N is proportional to the voltage applied, the highest voltage (V) that can be applied without causing significant Joule heating or arcing is always desirable for achieving high-efficiency CZE separation.

Sample injection for CZE is also of great importance because the size of the injected sample plug determines both the separation efficiency/resolution and limit of detection (LOD). Both hydrostatic (such as using pressure or gravity) and electrokinetic (applying a voltage for injection) injection schemes are widely used and have their respective advantages/disadvantages. For example hydrostatic injection does not cause injection bias based on analyte mobility while electrokinetic injection is more suitable for rapid serial injections.

Overall when developing CZE separation conditions, an array of factors such as properties/concentrations of analytes, separation buffer pH and ionic strength, capillary diameter and length, and separation voltage need to optimized to achieve high efficiency within reasonable separation time. Readers can find more detailed discussion and guidance elsewhere[9].

Capillary Electrophoresis-based Enzyme Assay

Quantification of enzymatic activity is no longer the pure interest of fundamental research in the biochemistry labs; rather it has played an increasingly important role in biotechnology, pharmaceutical and clinical development. For example, abnormal enzymatic activities have been implicated in many disease states and those enzymes have presented themselves as valuable targets for therapeutic interventions. While photometric and radiochemical methods have been historically used to determine enzymatic activity, CE has gained popularity for the same purpose. CE allows fast determination of enzyme kinetics by separating enzymatic product from substrate thus eliminating the requirement that the product is distinguishable from the substrate.

Since Krueger et al. measured endopeptidase Arg-C activity using CE for the first time in 1991[10], hundreds of publications have emerged demonstrating different enzyme assays using CE. These assays can take different formats depending on the specific application and enzyme under study. Broadly there are heterogeneous and homogeneous enzyme assays. In the heterogeneous format, enzyme is usually immobilized onto some surface to form an enzyme microreactor. Mixing and reaction occur when solution containing enzyme substrate is passed through and the substrate turnover is monitored using CE post-reaction. This format has the advantages of improved enzyme stability and catalytic efficiency. Homogeneous format can be divided into three subcategories: 1. pre-column assay where enzyme reaction takes place before CE separation; 2. on-column assay where enzyme and substrate are mixed electrophoretically on column, which is also known as

electrophohretically mediated microanalysis (EMMA)[11, 12]; and 3. post-column assay where CE is used to separate a mixture of enzyme substrates before they react with the enzyme upon elution. While the on-column and post-column formats are considered on-line assay, their application is limited by their low throughput or instrumentation difficulties. To date pre-column enzyme assays have found the widest application and well over 100 enzymes have been characterized using this format[13]. More thorough discussions regarding all three assay formats can be found in a review by Glatz[13].

A variety of detection schemes have been implemented for CE-based enzyme assays, the most common of which are ultraviolet (UV) absorbance, electrochemical (EC) and laser-induced fluorescence (LIF) modes. UV detection is the most widely used because it requires no chemical derivatization and majority of analytes absorb somewhere in the UV region. However it can suffer from background interference from either the electrophoresis buffer or sample matrix. Also since absorbance intensity is proportional to the UV light pathlength, the micron-scale diameter of capillaries results in inherently low sensitivity of absorbance detection.

In contrast electrochemical detection is concentration-sensitive so its sensitivity is not constrained by the size of the capillary. Both universal detection using conductivity and specific detection using amperometry can be achieved using EC. Yet the number of literatures reporting CE-enzyme assay using EC detection has remained limited. This is probably due to the technical difficulties involved in the EC electrode fabrication and manipulation and decoupling separation voltage from the

EC signal output.

Laser-induced fluorescence detection is quite popular for fluorescent enzyme assays. Due to its low background, LOD down to several tens of molecules has been reported on CE[14]. LIF detection is suitable for CE because its sensitivity is not dependent on light pathlength thus allowing small i.d. capillary (5-10 μm) to be used for high-efficiency separation. Unfortunately most analytes are not natively fluorescent and this necessitates analyte derivatization (including pre-, on, and post-column derivatization) or indirect detection using coupled secondary reactions. Pre-column derivatization is the most common method for enzyme assay using CE-LIF where the substrate is labeled using a fluorophore before reacting with the enzyme. In fact fluorescent analogues of many enzyme substrates with fluorophores of different properties are now commercially available. However, extreme care must be taken when choosing the fluorophore and interpreting the enzyme assay results since addition of the bulky fluorophores to the substrate might adversely affect the substrate-enzyme interaction and alter the enzymatic kinetics.

Not only can CE be performed on single capillary it can also be performed in parallel on so-called capillary array electrophoresis (CAE) systems. While the application of these capillary array systems has mainly been limited to DNA genotyping and sequencing, enzyme assays have been demonstrated on such systems. For example Yeung's group demonstrated parallel assays for lactate dehydrogenase (LDH) using a custom-built 96-capillary system equipped with a UV-absorbance detector[15]. Similarly Tu et al. used a commercial CAE system from SpectruMedix

which had 96 parallel capillaries and a LIF detector to measure the activity of extracellular signal-regulated protein kinase (ERK) from in vitro cell extract[16].

Capillary Electrophoresis on Chip

In 1979 Terry et al. constructed a miniaturized gas chromatography (GC) on a 5-cm diameter silicon wafer[17]. Ever since then effort has been put forth by many researchers and this trend of miniaturization has promised to revolutionize chemical processing and analysis. People use microfabrication techniques adopted from the integrated-circuit manufacturing industry to create features of dimensions in the range of micrometers to millimeters on various materials such as silicon, glass and various polymers. These microfabrication techniques have been covered and discussed in several reviews[18-20]. Microfabrication not only creates analytical devices with significantly decreased footprint but also enables integrating all sorts of laboratory functions on a single device. These microfabricated devices are named microelectromechanical systems (MEMS) or micro-total analysis systems (μTAS) which are also known as lab-on-a-chip.

CE was first demonstrated on chip by Manz et al. in 1991[21]. To date CE is the dominant separation function that is applied to chips probably because the compatible dimension of microfabricated channels. A plethora of chemical analyses have been demonstrated using CE on chip including DNA, protein and small molecule analysis[22, 23]. CE-based enzyme assays, which have been performed extensively on capillary as discussed in previous part, have also been developed on chips. Pre-column[24, 25],

on-column[26-28] and post-column[29] assays have all be demonstrated on chip.

Microfabricated electrophoresis devices are mainly fabricated on glass due to its suitable surface chemistry (high density of negatively charged silanol groups) and optical transparency. As an alternative material, polymers have gained increasing popularity because of their tunable surface characteristics and potential for low-cost mass production. However, separation efficiency comparable to CE on glass chips has yet to be demonstrated.

Compared with traditional CE, CE on chip has a lot more advantages besides the small size. For example shorter separation channels (down to several millimeters) can be constructed on chip allowing extremely fast separation (sub-second separation). Sample injection on chip also allows flexible and fine control to allow shorter injection plug. But probably the biggest advantage about performing CE on chip is that multiple CE separation units can be fabricated on a single wafer without significantly increasing production cost and device size. Relatively simple detection schemes are also available compared to those of the capillary-array systems[30, 31].

Using such microfabricated electrophoresis channel-array devices multiple samples can be electrophoretically analyzed simultaneously allowing proportionally improved sample throughput. Over the past 20 years or so, the number of electrophoresis channels integrated on a single device has seen a dramatic increase. One key to fabricating such devices is how to arrange the separation channels (Figure 1-1). Radial design introduced by Mathies's group has produced the highest channel density so far by effectively utilizing the wafer surface area. Eight times more

channels were fit onto a glass wafer with only a four-fold increase in the wafer size (Figure 1-1 B and C). A four-color rotary confocal scanner was used for fluorescence detection of all channels. Parallel genotyping was demonstrated using CGE and 384 DNA samples were analyzed in 325 s. The highest number of separation channels that have been integrated on a single chip was reported by Aborn et al (Figure 1-1 D). However, this arrangement did not have as high channel density as that achieved with the radial design. Similar parallel operations for other purposes such as immunoassay have also been reported but in relatively limited number of publications[31-34]. Assays for several enzymes have been demonstrated in parallel including β-galactosidase[35], phospholipase A_2[36] and serine/threonine kinase[37]; however, only 4 parallel channels were used in these studies.

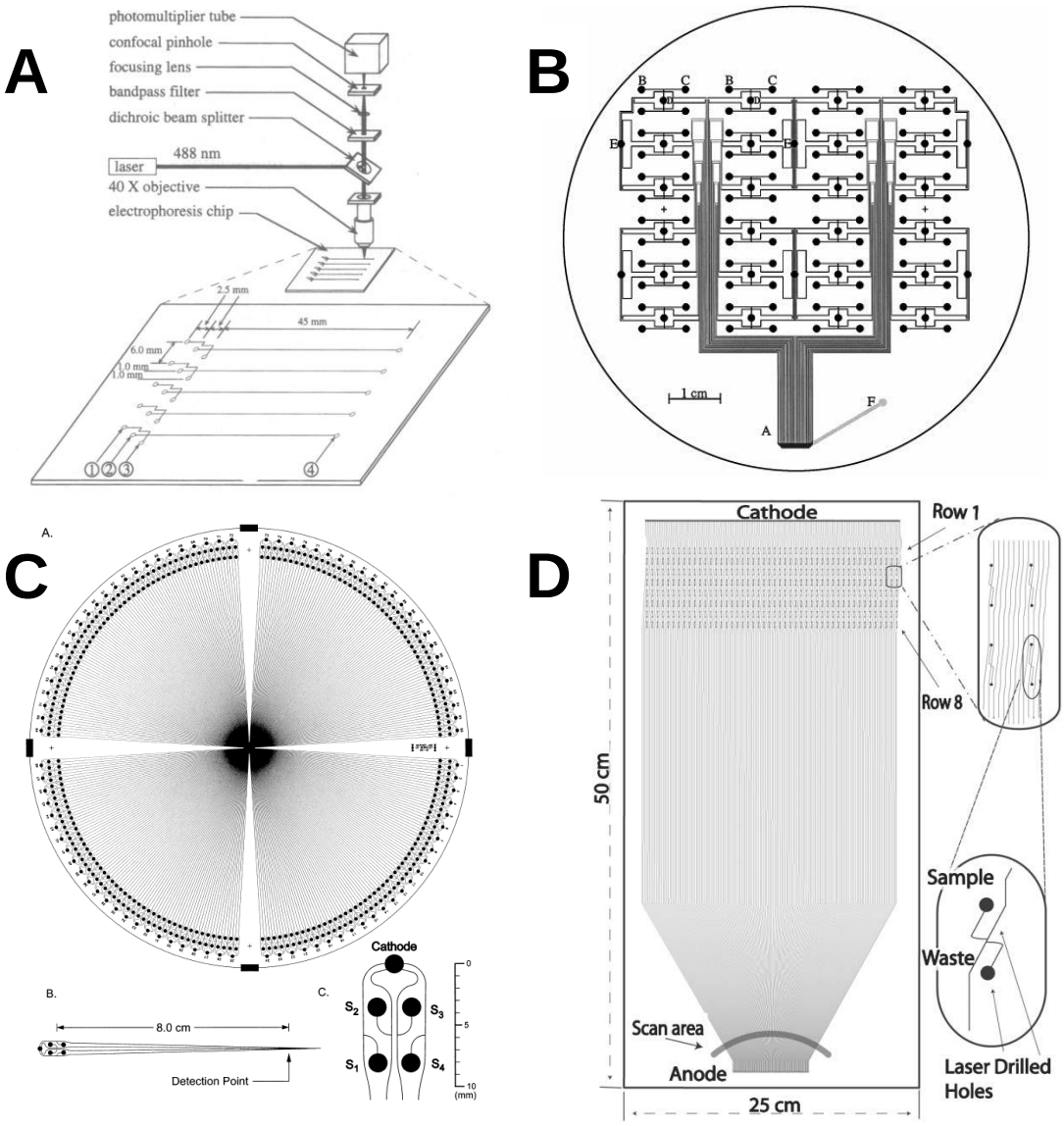

Figure 1-1. Geometric arrangement of electrophoresis channel arrays. A. Parallel arrangement of five separation channels (1994)[38]; B. 48 separation channels on a 10-cm-diameter wafer (1998)[39]; C. 384 separation channels on a 20-cm-diameter wafer (2000)[40]; D. 768 separation channels on a 25 cm ×50 cm wafer (2005)[41].

Since our research goal was to apply the developed analytical techniques to drug screening, two of the drug targets we studied and their related biochemistry were discussed in the next two parts.

Drug Targets Along the G Protein Signaling Pathway

Due to the prevalence of G protein signaling in cellular functions, derangement of G protein signaling is thought to be involved in a wide range of diseases such as diabetes, depression, cardiovascular defects and certain forms of cancer[42]. Therefore therapeutic interventions have hence been sought on these bases. In view of the significance of G protein signaling, we have developed assays for different aspects of this pathway as a model system.

G proteins, short for guanine nucleotide-binding proteins, are a family of proteins involved in many intracellular signaling pathways (Figure 1-2)[43]. They act as molecular switches controlling magnitude of signal transductions. There are two distinct families of G proteins: heterotrimeric and Ras G proteins. As the name suggests heterotrimeric G protein is made up of three subunits: α, β and γ. Ras proteins, on the other hand, are monomeric and are homologous to the α subunit of heterotrimeric G protein. In the work presented here we will refer to heterotrimeric G proteins as G proteins. G proteins can alternate between two states: when the α subunit binds to guanosine diphosphate (GDP) α, β and γ form an inactive trimer; when GDP is replaced by guanosine triphosphate (GTP), α subunit disassociates from β/γ dimer and both of them can interact with downstream effectors such as adenylyl cyclase, protein kinase and phospholipase and activate signaling cascades[44]. Conversion between these two states is mediated by G protein-coupled receptors (GPCRs). When an extracellular ligand binds to GPCR it can induce enough conformation change in the receptor which allows the receptor to function as so-called

guanine nucleotide exchange factor (GEF). Activation of GPCR then leads to GPCR-G protein coupling and activation of G protein. G protein signaling continues after activation until GTP bound to the α subunit is hydrolyzed to GDP by the intrinsic GTPase activity of the α subunit. A variety of intracellular proteins further accelerate this hydrolysis process (turning-off of the signaling) and are classified as GTPase-activating proteins (GAPs). RGS proteins, or regulators of G protein-signaling, is one such GAP. By stabilizing the G protein-GTP transition state during hydrolysis RGS proteins markedly reduce the lifetime of activated α subunit and attenuate the signaling[45].

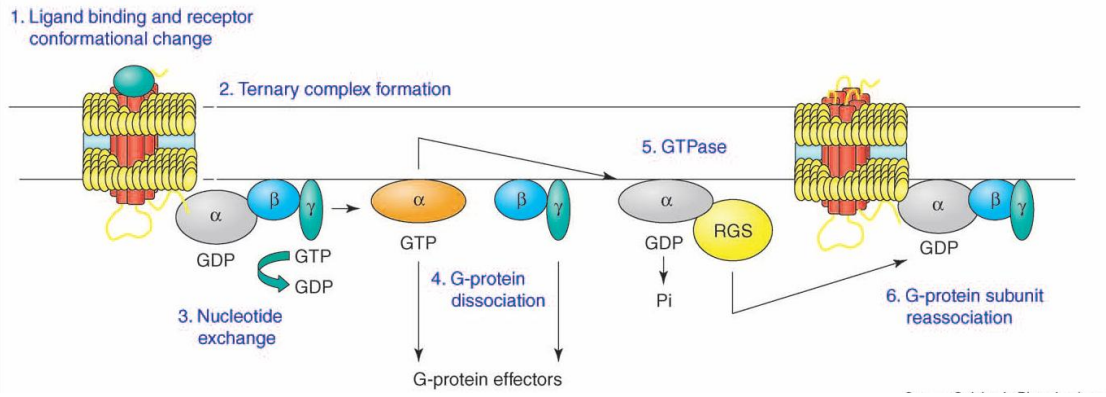

Figure 1-2. The G-protein activation/deactivation cycle. 1. The agonist–receptor interaction promotes a series of conformational changes favoring receptor coupling to G protein(s); 2. Formation of the agonist–receptor–G-protein ternary complex promotes a G-protein conformational change facilitating; 3. The exchange of α-subunit-bound GDP for GTP; 4. the activated G protein then dissociates to form the GTP-bound α subunit and the βγ complex. The GTP-bound α subunit and βγ complex regulate the activity of specific intracellular effector proteins, leading to changes in the levels of secondary messengers (e.g. cAMP and calcium) and regulation of select signal transduction pathways; 5. The activity of the GTP-bound α subunit is terminated by hydrolysis of GTP to GDP by intrinsic GTPase activity of the α subunit; 6. The cycle is completed through the reassociation of the GDP-bound α subunit with the βγ complex. The kinetics of the G-protein activation/deactivation cycle are modulated by several accessory proteins including regulators of G-protein signaling (RGS) proteins[3]. Reproduced with permission from Thomsen et al[43].

GPCRs, encoded by the largest gene family (800-1000 GPCR genes[46]) in human genome, interact with a variety of ligands such as biogenic amines, amino acids, ions, peptides and proteins[47]. GPCRs are one of the most studied drug targets in modern pharmaceutical research, and over 50% of clinically used drugs target GPCRs[48]. Desire to discover more effective and specific GPCR drugs, including drugs targeting those some 150 orphan GPCRs whose functions are unknown, remains to the driving force behind the development of more efficient, robust and cost-effective GPCR assays. Historically GPCR drug screening has focused on identifying compounds that bind to a receptor typically through displacement of a known ligand. Limitations of this approach include requirement of having a known ligand to start with (i.e., cannot be applied to drug screening for orphan GPCRs) and lack of quantification of GPCR activation. Functional assay has been replacing binding assay and a variety of platforms have been developed and even commercialized[43]. There are mainly two categories of GPCR functional assays: proximal point (directly reporting GPCR activation as a function of G protein activation) and distal point (measuring downstream secondary messengers such as cAMP, inositol phosphate and calcium levels). Proximal point assays can reduce the incidence of false positives; however, radiolabeled GTP analogues such as [^{35}S]GTPγS and [γ-^{32}P]GTP are usually used, imposing high cost and environmental hazards. A non-radioactive GTP analogue (europium-labeled GTP) has been introduced by Perkin Elmer to allow time-resolved fluorescence (TRF) binding assay. However all these assays require tedious filtration and are time-consuming, hence are not suitable for HTS. Distal

point assays have the benefit of amplified signal but suffer from false positives associated with stimulation of the secondary messengers independent of the GPCR. Actually several distal point assay kits have been commercialized and instruments such as fluorometric imaging plate reader (FLIPR) can be used for detection allowing HTS. However, these assays sometimes require modification of G proteins so that the GPCR can be coupled to a pre-selected second messenger system; thus response may not be representative of the in vivo signal pathway. In all an ideal GPCR assay should be simple, non-radioactive, reliable, homogenous and amenable to HTS. In Chapter 2, we developed such an assay based on fast CE separation and effects of GPCR drugs were successfully detected.

RGS proteins have recently emerged as an attractive drug target. These proteins have been implicated in diseases such as Alzheimer's, Parkinson's, epilepsy and depression[49]. Since RGS proteins accelerate GTPase activity, inhibitors of RGS can enhance G protein signaling and promise to potentiate GPCR agonists. Also the highly localized and dynamically regulated distribution of RGS proteins means that RGS protein drugs should have high specificity and low side effects[50]. However lack of high-throughput assays for RGS protein activity is hampering the rate of discovery of RGS inhibitors. Single-turnover hydrolysis assay using [γ-^{32}P]GTP is the most widely used assay for RGS functions[51]. To eliminate the requirement of radiolabeled chemical, a stopped-flow spectroscopic assay has been developed by the Neubig group[52]. This assay measures decrease of the intrinsic tryptophan fluorescence of G protein α subunit accompanying GTP hydrolysis allowing

millisecond-kinetics to be monitored. Yet this assay has not been applied to HTS. Flow cytometry protein interaction assay (FCPIA) based on RGS-G protein binding has been developed for identifying small molecule RGS inhibitors[53]. Commercial Luminex 100IS 96-well plate reading flow cytometer used in this study allows analyzing a 96-well plate in less than 30 min. Since binding results can not be directly translated to information regarding functional modulation, FCPIA is susceptible to false positives and negatives and additional confirmation of inhibitor activity is required. More recently, Jameson et al. developed a CE-LIF-based hydrolysis assay where a fluorescent GTP analogue, BODIPY® FL GTP (BGTP), was used to determine GTPase activity modulated by RGS proteins[54]. This functional assay showed promises to be used for HTS for RGS inhibitors. In Chapter 3, we increased the throughput of this assay by performing parallel CE on chip. Up to 36 assay reactions could be analyzed simultaneously.

Acetylcholinesterase as Drug Target

Acetylcholinesterase (AchE) is another important drug target that was explored in this work. It is present in cholinergic neurons playing a pivotal role in controlling cholinergic signal transduction by catalyzing the hydrolysis of acetylcholine (Ach) to its inactive product choline. Ach is an important neurotransmitter that carries nerve impulses across the cholinergic pathway. Based on the so-called cholinergic hypothesis[55-57], depletion of Ach in the synaptic cleft can be associated with Alzheimer's disease (AD), the most common neurologic disorder among aged

population. AchE inhibitors which prolong lifetime of Ach in the brain are currently be sought as potential treatment for AD[58, 59]. While a handful of AchE inhibitors have been approved for AD treatment, searching for compounds with improved pharmacological and toxicological properties remains to be of great importance[60-63].

The most widely used assay for AchE activity is based on a photometric method developed by Ellman et al[64]. Inhibitor screening based on this method has been demonstrated. For example, flow injection analysis (FIA) coupled to immobilized enzyme columns with UV detection was used for fast inhibitor screening at about 1 sample per 10 minutes[65, 66, 67]. Other more sensitive methods such as fluorometric[68], chemiluminescent[69], radiometric[70] assays have also been reported. However, either a fluorogenic substrate or a secondary reaction was used in these methods. This tends to cause false positives and negatives in the screening process. Mass spectrometry has been used to detect AchE inhibitors where unlabeled Ach was used. Hu et al. used immobilized AchE microspheres for AchE inhibitor detection[71]. Hydrolysis was quenched by removing the magnetic microspheres before ESI-MS analysis. Ozbal et al used a microfluidic system integrating on-line HPLC sample purification and ESI-MS for AchE inhibitor screening[72]. Highly sophisticated robotic system was used for flow injecting of individual samples and a throughput of 4-5 s per sample was achieved.

Sub-microliter Liquid Handing and Segmented Flow

As discussed earlier, multi-well plates are the main platform for HTS, and well

plates of increasing density are used to increase screening throughput and reduce cost of reagents. However, expensive robotics and sophisticated techniques are required for reagent dispensing and these approaches are limited by evaporation and surface tension. Confining nanoliter sample plugs segmented by gas or immiscible liquid has recently emerged as a promising alternative to well plate-based screening[73].

Three ways to generate such segmented flow are illustrated in Figure 1-3 A-C. These discrete sample plugs or droplets act as miniaturized reaction vessels and they can be manipulated automatically in a high-throughput fashion. A full spectrum of sample manipulating techniques including sampling[74], dilution[75], reagent addition[76, 77], splitting[75, 78] and mixing[79] have been demonstrated (Figure 1-3 D). A variety of chemical reactions have been performed in droplets including DNA analysis[80], enzyme assay[81], organic synthesis[82] and protein crystallization[83]. However, methods for chemically analyzing droplets have been largely limited to those optical methods such as fluorescence and X-ray diffraction. For example, a droplet-based fluorescence assay was develop for screening phosphatase activity of several proteins[84]. Also screening for protein crystallization conditions using x-ray diffraction was also demonstrated[83]. A few other techniques such as electrophoresis[85, 86], MS[82, 87, 88]and NMR[89] have also been explored for droplet analysis. Off-line collection and analysis of droplets by MALDI was demonstrated for screening organic reactions in droplets[82]. Also on-line extraction of droplets using microfluidic chip for CE and MS analysis was demonstrated by several groups[86-88]. It can be envisioned that combining enzyme assay in droplets with fast

and information-rich analytical techniques will open up new possibilities for HTS. In Chapter 4, we used segmented flow as a sample introduction tool and coupled it to parallel CE separation on chip to further improve the previously developed GTPase assay.

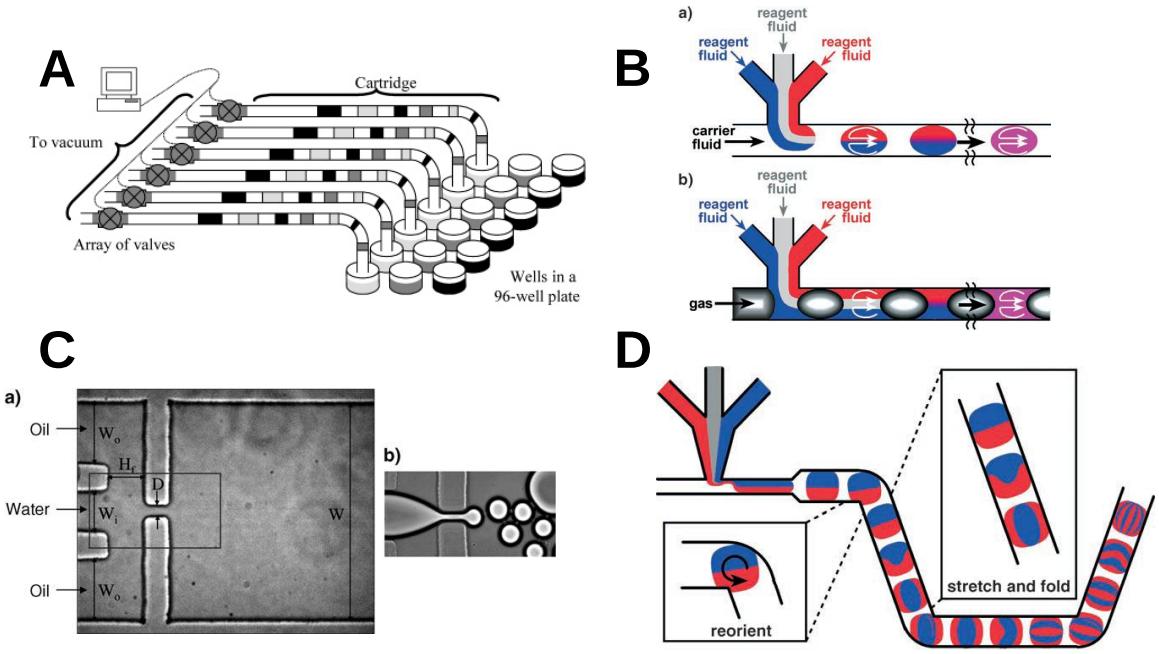

Figure 1-3. Examples of microfluidic droplet generation and manipulation. A. Generating droplets by sampling from a 96-well plate. Inlets of the tubing are inserted into sample and oil alternatively[90]; B. Droplet generation using a T-junction. Either oil (a) or gas (b) can be used as the immiscible phase. Aqueous sample breaks off from the T-junction and forms droplet[91]; C. Droplet generation using a flow-focusing geometry. Aqueous sample is pushed through a small orifice to form droplet emulsion[92]; D. Fast mixing using chaotic advection after reagent addition. Millisecond mixing can be achieved[79].

HTS using Mass Spectrometry

Assays based on the spectroscopic properties of analytes usually require the use of surrogate substrates or secondary reactions to produce detectable signals such as fluorescence. This can sometimes cause false reflection of enzyme activity (e.g. in enzyme assay) and produce false positives or negatives. Mass spectrometery

(MS)-based assays are an interesting alternative in this regard in that no labeling is required and native substrates or binding partners can be used[93]. Screening using MS generally falls into one of two categories: testing one compound at one time or testing all compounds at once (also known as one-pot screening)[94, 95].

The one-pot strategy is exclusively used for testing affinity interactions between test compounds and the target. The entire pool of combinatorial compounds are usually mixed with and competitively bind to the target protein before the non-covalent complexes and unbound species are separated and detected[96]. Various separation techniques can be used to separate the complexes from the unbound before MS detection, including size-exclusion chromatography[97], pulsed ultrafiltration[98], affinity CE[99] and frontal affinity chromatography[100, 101]. Stand-alone MS, termed bioaffinity MS, can also be used for screening affinity interactions without prior separation and achieving higher throughput[102, 103]. Non-covalent complexes are selected for fragmentation in tandem MS and bound ligands are then detected.

Testing individual compounds is more common for screening combinatorial libraries. Assay reactions are performed in individual wells containing the test compounds prior to MS analysis. Effects of compounds on both protein-protein interactions and enzyme activities can be tested this way. However, it requires pipetting individual samples and rinsing after each analysis and this limits the overall throughput. Multiplexed CE and HPLC have been employed and coupled to MS to process multiple samples simultaneously[15, 58, 72, 104]; however, the throughput still falls short of HTS needs. In Chapter 5, we again used segmented flow as the sample

introduction method and coupled it to ESI-MS. We demonstrated label-free inhibitor screening for acetylcholinesterase and throughput as high as 0.65 Hz was achieved

CHAPTER 2

CAPILLARY ELECTROPHORESIS ASSAY FOR G PROTEIN-COUPLED RECEPTOR-MEDIATED GTPASE ACTIVITY

Introduction

Heterotrimeric guanine nucleotide binding proteins (G proteins) play an important role in intracellular signaling pathways by coupling membrane bound receptors (G protein-coupled receptors or GPCRs) to downstream effectors. The G protein α subunit (G_α) switches from an inactive (GDP-bound) to an active (GTP-bound) form in response to agonist binding to GPCR. Signaling is terminated when the G protein, which is a GTPase, hydrolyzes bound GTP to GDP. G protein pathways regulate many processes related to cardiovascular, neural, and endocrine function, and as such an intense focus has been placed on the development of GPCRs as therapeutic drug targets. It is estimated that 30−50% of drugs used clinically act at GPCRs[105].

GPCR drug screening has historically focused on identifying compounds that bind to a receptor (typically through displacement of a known ligand), followed by functional assays to detect effects on downstream effectors or second messengers associated with the GPCR. Limitations of this approach include requirements of

having a known ligand to start and the use of radiolabeled species for the assays. The drive to screen based on functional response, along with concerns associated with the use of radioactivity, led to the development of whole cell, fluorescence-based assays. In these assays, G protein activation via the GPCR evokes a chemical change (such as intracellular Ca^{2+} concentration) that can be conveniently monitored using an appropriate instrument such as a Fluorometric Imaging Plate Reader (FLIPR) [106]. However, these whole-cell assays sometimes require modification of G proteins so that the GPCR can be coupled to a pre-selected second messenger system; thus response may not be representative of the *in vivo* signal pathway. These assays are also subject to false positives associated with stimulation of the second messenger independent of the GPCR. Finally, it can be difficult to detect modulation of GPCR signal downstream of the ligand binding.

A significant goal for GPCR screening therefore remains the development of non-radioactive assays capable of reporting GPCR activation directly as a function of GTP binding or GTPase activity using G proteins that maintain their *in vivo* coupling specificities. Progress has been made in the first goal by development of Eu-GTP, a non-hydrolyzable GTP analogue that exhibits fluorescence changes upon binding to G proteins[107]. This reagent has formed the basis of numerous assays for GPCR screening at the level of GTP binding[108]. Screening at the hydrolysis step is also of interest because of the potentiality of modulating hydrolysis for modulating activity of GPCRs. Fluorescent probes for the hydrolysis reaction have also been investigated[109, 110]. One intriguing example has been the use of the fluorescent GTP

analogue, BODIPY® FL GTP (BGTP) as a reporter substrate. Although there have been no reported differences in fluorescence properties of BGTP and the hydrolyzed form BODIPY® GDP (BGDP), it has been shown that the protein-bound forms have significant differences in fluorescence intensity[110]. Thus, under conditions where all the BODIPY-labeled nucleotide is bound (i.e., a single turnover assay), it is possible to record fluorescence changes from hydrolysis. The assays that were developed based on these fluorophores however were not extended to membrane preparations and therefore could not be used to detect a GPCR-mediated effect on GTPase activity; rather they were designed to investigate biochemical mechanisms that do not involve the membrane-bound receptor. Although it may be possible to extend these assays to membrane systems, several factors could make this difficult including nonspecific binding of BGTP to the membrane preparation components and the requirement of working under single turnover conditions.

Another approach to performing enzyme assays is by capillary electrophoresis with laser-induced fluorescence (CE-LIF) as recently reviewed[13, 111]. Two advantages of CE-LIF for enzyme assays that are relevant to this application are (1) the substrate and product can be separated, thus eliminating the requirement for a fluorescence difference between the two, and (2) the development of parallel CE-LIF instrumentation suggests the potential for high-throughput screening as demonstrated for other enzyme assay systems[15]. Previously, we have demonstrated that CE-LIF assays can be successfully employed to determine the GTPase activity of purified G proteins with a fluorescent GTP analogue, BGTP, as the substrate[112]. On the basis of

this result, we hypothesized that GPCR-mediated GTPase activity could also be detected using BGTP as substrate and CE-LIF as a read-out to yield a new approach to screen for drugs that modulate GPCRs. Herein, we describe such an assay and demonstrate that it is simple, rapid, automatable, and yields results similar to those obtained by more traditional radioactivity techniques.

Experimental Section

Materials

[^{3}H]-Yohimbine (80.5 Ci/mmol) was from Perkin-Elmer Life Sciences (Boston, MA). Lipofectamine 2000 was from Invitrogen (Carlsbad, CA). BGTP and BGDP were obtained from Molecular Probes (Eugene, OR). 10× Tris-glycine buffer was purchased from Bio-Rad Laboratories (Hercules, CA). Enzyme-grade sodium phosphate monobasic was purchased from Fisher (Fair Lawn, NJ). All other chemicals were from Sigma Chemical Co. (St.Louis, MO). RGS8 was expressed and purified as previously described[113, 114] and stored at −80 °C until used. Buffers were made with deionized water purified by an E-Pure water system (Barnestead International Co., Dubuque, IA) and filtered prior to use.

Construction of α_{2A}-Adrenergic Receptor-$G_{\alpha o}$ Fusion Plasmids, Cell Culture, and Transfection

Wild-type (wt) α_{2A} adrenoreceptor-$G_{\alpha o1}$ (α_{2A}AR-$G_{\alpha o1}$) fusion plasmid and α_{2A}AR-$G_{\alpha o1}$ C351I fusion plasmid (with a 351Cys→Ile mutation on $G_{\alpha o1}$) were

constructed as previously described[115]. HEK293T cells were maintained at 37 °C in 5% CO_2 in DMEM medium with 10% fetal bovine serum, 100 U/mL penicillin, and 100 μg/mL streptomycin. Cells were transiently transfected with either the α_{2A}-$G_{\alpha o1}$ fusion (wt) or α_{2A}-$G_{\alpha o1}$ C351I fusion (C351I) for 48 h using 10 μg of plasmid DNA and 30 μL of lipofectamine 2000 per 100 mm dish according to the manufacturer's instructions.

Membrane Preparation

Transfected HEK293T cells were lysed at 4 °C for 15 min in 1 mM Tris, pH 7.4, with 10 mM benzamidine, 1 μg/mL aprotinin, and 1 mM PMSF. Cell membranes were homogenized with 10 strokes using a Potter−Elvehjem tissue grinder. Nuclei and undisrupted cells were removed via centrifugation by a 10 min, 4 °C spin at 1000g. The supernatant was reserved. The pellet was resuspended in buffer, homogenized, and spun as above. The two supernatants were then combined. The membrane fraction was pelleted with a 30 min spin at 40000g at 4 °C. The pellet containing membrane was resuspended in 50 mM Tris, 10 mM $MgCl_2$, 1 mM EGTA, pH 7.6, with protease inhibitor (Roche Complete, Mini). Aliquots were snap frozen in liquid nitrogen and stored at −80 °C until use. Membrane protein content was determined via a Bradford assay (Bio-Rad, Hercules, CA). [^{3}H]-Yohimbine binding assays were performed on 10 μg of membrane protein in a final volume of 100 μL as previously described[116]. The results of these assays for both fusion preparations are as follows: wt, 1.565 mg of protein/mL, 2.9 pmol of α_{2A} receptor/mg of protein;

C351I, 1.465 mg of protein/mL, 3.2 pmol of α_{2A} receptor/mg of protein.

Capillary Electrophoresis Instrumentation

At the beginning of each day, the separation capillary was rinsed with 1 M NaOH, deionized water, and electrophoresis buffer for 2 min each. For rapid CE separations, a CE-LIF instrument equipped with "flow-gated" injection similar to that described elsewhere was used[117, 118]. Briefly, the sample was loaded into a chamber that was then pressurized so that sample flowed from the chamber to the flow-gate interface through a fused-silica capillary (Polymicro Technologies, Phoenix, AZ). The flow-gate controlled periodic injections (details below) onto the CE-LIF where sample was rapidly separated. Electrophoresis buffer was supplied as a gating-flow at 1.2 mL/min by a series I HPLC pump (LabAlliance, Fisher Scientific, Pittsburgh, PA) equipped with an external pulse dampener.

When the valve on the flow-gate line was open, electrophoresis buffer flowing through the flow-gate caused the sample to be washed to waste. To inject sample onto the electrophoresis capillary, the valve was closed so that buffer flow stopped, allowing sample to accumulate in the interface between the two capillaries. The injection voltage was then applied across the separation capillary by a high-voltage power supply (CZE 1000R, Spellman High Voltage Electronics, Plainview, NY) for a specified amount of time to load sample onto the capillary column. Once sample was injected, gating-flow of electrophoresis buffer was resumed by actuating the gating valve, and separation voltage was applied. Serial injections could be performed at a rate limited by separation time. All operations were controlled by a

personal computer equipped with a multi-function board (AT-MIO-16, National Instruments, Austin, TX) using software written in-house.

Detection was accomplished using LIF as described elsewhere[119]. The LIF detector used the 488-nm line of an air-cooled 15 mW Ar^+ laser (Spectra Physics, Mountain View, CA) as the excitation source. Fluorescence was collected 90° from the excitation source via a 40× microscope objective (Melles Griot, Irvine, CA). The fluorescence emission was spectrally filtered using a 520 ± 10 nm band-pass filter and a 488 nm notch filter (Corion, Holliston, MA), and spatially filtered through two pinholes (5 mm × 7 mm and 1.5 mm × 4 mm) before entering a photomultiplier tube (PMT) (model E717-21, Hamamatsu Photonics, Bridgewater, NJ). Signal from the PMT was amplified by a Keithley 428 current amplifier and collected using the same computer and software used for instrument control. Processing of electrophoresis data was performed with a program written in-house[120].

Buffers

For most of the BGTP assays, the electrophoresis buffer was 75% 25 mM Tris, 192 mM glycine pH 8.5, and 25% 100 mM sodium phosphate pH 7.1 (TGP). Samples were prepared in 50 mM Tris-HCl, pH 7.4 buffer supplemented with 1 mM EDTA, 5 mM $MgCl_2$, 1 mM DTT, 100 mM NaCl, and 10 μM GDP. All experiments were performed at room temperature (RT).

GTPase Assays

Samples containing 58.6 fmol of α_{2A} receptor (fused to either wt or C351I $G_{\alpha o1}$) in HEK293T membranes, 1 μM BGTP, 12.8 nM rhodamine 110 as the internal standard (IS), and indicated levels of UK14,304 (0.1 nM−0.4 mM), with and without 300 nM yohimbine were incubated in a total volume of 50 μL for 10 min at RT. Following incubation, membranes were removed from samples using 10 kDa MWCO Micron Centrifugal Filter Devices (Millipore Corporation, Bedford, MA) that had been rinsed three times with 50 μL of deionized water for 10 min at 13.4k rpm. Samples were spun at 13.4k rpm for 10 min, and the filtrate was analyzed by CE-LIF. Experiments with RGS were performed in a similar manner, with either 1.3 μM or 5.2 μM RGS8 added concomitant with the other sample components.

In some experiments, the filtration step was bypassed for a direct injection assay. In these experiments, 0.6 μg of membrane containing 6.8 fmol of receptor was incubated with the same buffer as the GTPase assay modified to contain 0.53 mM adenosine 3,5'-(β,γ-imino)triphosphate (App(NH)p). After 10 min of incubation, the samples were pumped into the flow-gated interface, without filtration. Separation was performed as for the GTPase assay except the electrophoresis buffer was 25 mM Tris, 192 mM glycine, and 1.5 mM $MgSO_4$ adjusted to pH 8.5.

The extent of BGDP product formation in each sample was assessed using the ratio of the peak areas of BGDP and IS (BGDP/IS). Conversion to BGDP concentration was made by comparison to an external calibration curve generated from standards (i.e., non-membrane containing samples) with various BGDP/IS ratios where the BGDP was varied over the range of expected concentrations. For all

samples, the BGDP/IS ratio was determined by averaging the data from 10 individual electropherograms.

Dose−response curves are reported as specific GTPase activity versus drug concentration. For this calculation, the concentration of total BGDP formed was measured for each drug concentration using the conditions above. The BGDP produced as a result of the specific (low K_M) GTPase activity was calculated by subtracting the BGDP due to nonspecific GTPase (high K_M) from the total BGDP formed. Nonspecific GTPase activity was determined by adding 10 μM GTP to a membrane incubation mixture in the absence of drug and recording the amount of BGDP formed. This background value was used for all subsequent assays on a given day. The fluorescence signal attributed to specific GTPase activity was converted to picomoles (milligram of protein)$^{-1}$ minute^{-1}. Complete dose−response curves were obtained 3 times each in the presence and absence of the antagonist yohimbine. Averaged dose−response data were fit to sigmoidal curves using GraphPad Prism 3.0 (GraphPad Software, San Diego, CA). Statistics calculations were also performed with GraphPad Prism, using a two-tailed t test. All data are reported as the mean ± SD.

Results and Discussion

Overview of GPCR Activation Assay

The principle of the CE-LIF assay is illustrated in Figure 2-1. Membranes expressing the α_{2A}AR-$G_{\alpha o1}$ fusion proteins were incubated in solution containing

GPCR ligand, 1 μM BGTP, and an internal standard (IS) for 10 min at RT. The BGTP hydrolysis reaction was subsequently quenched by removal of membranes from the sample via rapid filtering through a 10 kDa molecular weight cutoff filter. CE-LIF was used to separate BGTP (G protein substrate) from BGDP (product of G protein GTPase activity) in the resulting filtrate, allowing detection of agonist-stimulated activity based on the increase in hydrolysis product formation. Typical electropherograms from sample with (right) and without (left) the α2A receptor agonist UK14,304 are shown in Figure 2-1, demonstrating both the complete separation of all fluorescent components (IS, BGDP, and BGTP) as well as the increase of BGDP formation observed in the sample containing agonist. The CE separation step was a vital component of the assay, as fluorescence of the BGDP product is equivalent to that of the BGTP substrate (data not shown), meaning that no change would be observed if only total fluorescence had been monitored. Two electrophoretic peaks each are observed for BGDP and BGTP as BGTP is supplied as a mixture of the 2' and 3'-isomers. In agreement with previous studies using purified G proteins, both isomers are readily turned over with no detectable difference in kinetics[54].

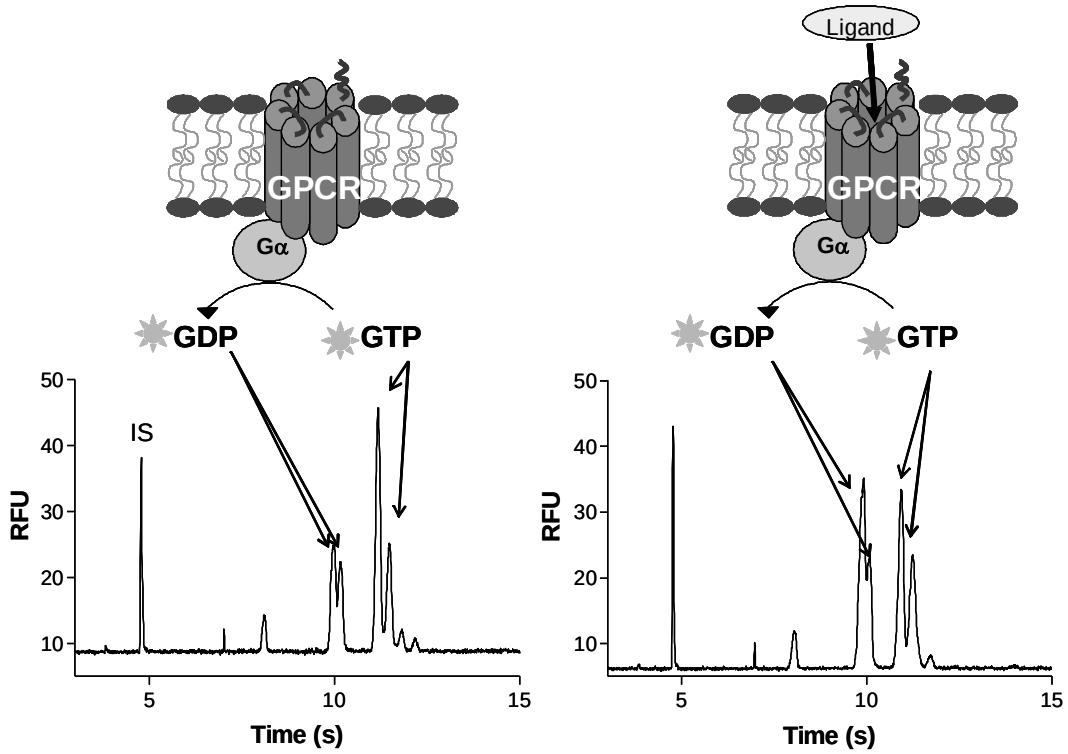

Figure 2-1. CE-based fluorescence assay for receptor-mediated G protein GTPase activity in cell membranes. The cartoon portion illustrates the hydrolysis of BODIPY FL GTP (BGTP) to BODIPY FL GDP (BGDP) by heterotrimeric G proteins in a sample containing cell membranes with (right) and without (left) GPCR ligand (in this case an agonist). The electropherograms (actual data) show how the fluorescent product BGDP is separated from the substrate BGTP by capillary electrophoresis (CE), with more BGDP produced in the sample containing agonist. Two peaks are observed for both BGTP and BGDP, due to the location of the fluorophore on either the 2' or 3' position of the ribose ring of the GTP substrate.

Agonist-stimulated hydrolysis of BGTP was measured in membranes expressing the α_{2A}AR fused to wt $G_{\alpha o1}$ or $G_{\alpha o1}$ with a 351Cys→Ile mutation (C351I $G_{\alpha o1}$). GPCR−G_α fusion systems were chosen for these studies as they typically translate into highly reproducible assays due to the defined 1:1 stoichiometry and ensured physical proximity of the signaling partners[105]. An added advantage is that the extent of nucleotide binding in the presence of agonist is significantly elevated in fusion systems as compared to unfused co-expressed receptors and G_α subunits. The

use of $G_{\alpha o1}$ with the 351Cys→Ile mutation has been shown to further enhance GTP binding and enhance sensitivity of GPCR activation assays[121].

Dose−Response Curves of Specific Activity

For quantification, the amount of BGDP produced in each sample was calculated from a calibration curve using the ratio of the sum of the two BGDP peak areas to the peak area of IS (BGDP/IS) as the signal. The calibration curve was constructed using BGDP standards prepared in the same buffer used for the assay, including IS, and a range of BGDP concentrations that spanned the concentrations generated by the assay. This method of calibration accounted for any effects of the assay buffer on separation and detection and ensured a response in the linear range allowing accurate determination of the BGDP produced in any of the membrane preparations used. (Effects of minor components, such as the drugs and GTP added to some preparations, on the calibration are negligible in CE-LIF measurements allowing the same BGDP calibration curve to be used for all samples.)

Figure 2-1 illustrates that although agonist induces an increase in BGDP formation, substantial GTPase activity is detectable without agonist (see BDGP formed without drug in left trace of Figure 2-1). This BGTP turn over occurs because tissue and cell lysate samples contain significant GTPase activity that is not due to G protein GTPase and is therefore not coupled to the GPCR. Similar background or nonspecific GTPase activity is observed with radiolabeled GTP[122]. To account for this nonspecific GTPase activity, radiochemical assays utilize a

background subtraction method. This background subtraction method takes advantage of the fact that G protein GTPases have high affinity (i.e., low K_M of 0.1 μM) whereas the nonspecific GTPases have low affinity (i.e., higher K_M > 1 μM). Therefore, GTPase activity measured the presence of micromolar unlabeled GTP (which should block turnover of nucleotide by G proteins) is deemed a result of the high K_M, nonspecific GTPase and is subtracted from the observed GTPase levels in all other samples. In this way, the low K_M GTPase associated with G proteins can be probed separately from all other GTPases. This same background subtraction method was used for the CE assays. Thus, to quantify the G protein-specific GTPase activity in the membrane samples, BGDP formed in a sample with 10 μM GTP added (but no drug) was subtracted from all subsequent measurements (see Experimental Procedures) to determine the specific GTPase activity.

The specific GTPase activity measured by this assay increased sigmoidally with the log of the concentration of α_{2A}AR agonist (UK14,304) added to the membranes expressing α_{2A}AR-C351I fusion, as expected for a classical agonist-induced effect (Figure 2-2). The observed EC_{50} (480 ± 200 nM) was in good agreement with a previously reported estimate of 207 ± 8 nM obtained under similar experimental conditions with radiolabeled GTP[123]. Maximal specific stimulation observed with UK14,304 was to 525% of basal levels. Without subtraction of nonspecific activity, maximum stimulation was to 125% of basal levels. The low percent stimulation without subtraction of nonspecific activity affirms the importance of probing G protein GTPase separately from total GTPase when designing high-sensitivity GPCR

activation assays. In the presence of the α_2 antagonist yohimbine, the magnitude of observed stimulated BGTP hydrolysis was not affected (525% of basal) but the EC_{50} for UK14,304 was shifted to the right, increasing to 9.4 ± 5 μM as expected. These results indicate that GPCR activation can be accurately assessed via hydrolysis of BGTP. These results also demonstrate that both agonists and antagonists can be detected.

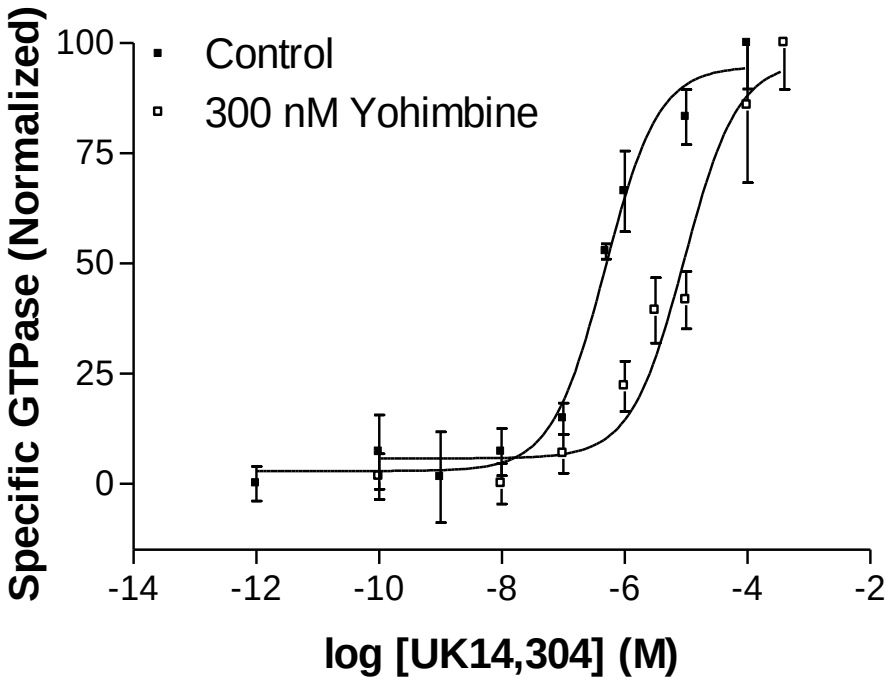

Figure 2-2. Dose response curves for UK14,304 in the absence (control) and presence of α_{2A}AR antagonist yohimbine. Data shown are for membranes expressing C351I fusion protein. The calculated EC_{50} values were 480 ± 200 nM (n = 3) and 9.4 ± 5 μM (n = 3) for the control and yohimbine experiments, respectively. Both data sets were normalized to percent maximal response. Error bars are ± 1 SD.

Two control experiments were used to ensure that the observed BGTPase activity was due to specific (i.e., receptor-mediated) agonist stimulated effects. In the first, similar experiments were performed using membranes of HEK293T without the

receptor being expressed. Without receptor, BGDP formation in presence of 100 μM UK14,304 was 100 ± 3% of that without drug (n = 5), indicating no stimulation of BGDP formation over background. Similar results were obtained in the presence of 10 μM GTP. In the second control, stimulation in the presence of 10 μM GTP was tested in membranes expressing the α_{2A}AR-C351I fusion protein. In these experiments, BGDP formation rate with drug was 97 ± 2% (n = 5) of that without drug, indicating no stimulation of high K_M GTPase activity by the α_{2A}AR agonist. This latter result also demonstrates the effectiveness of the unlabeled GTP in suppressing receptor-mediated GTPase activity.

Assay Reproducibility

The relative standard deviation (RSD) of the BGDP/IS ratio within a sample was <5% (for an average of 10 electropherograms), suggesting good reproducibility in the measurement of activity in one sample. This reproducibility was similar for standards and is inherent in the CE-LIF measurement. Total BGTPase activity measured in samples prepared for a given condition (e.g., drug concentration) from the same membrane preparation on different days had relative standard deviations <8% (n = 3 for each condition). Specific activity had higher RSDs, especially at low drug concentrations (see Figure 2-2), as a direct result of the background subtraction. The average nonspecific or background GTPase activity that was subtracted was 80 ± 3 pmol of BGDP (mg of protein)$^{-1}$ min^{-1} (n = 6) whereas the activity recorded for the maximum agonist concentration was 104 ± 2 pmol of BGDP (mg of protein)$^{-1}$ min^{-1}

and for the lowest agonist concentrations it was barely above 80 pmol of BGDP (mg of protein)$^{-1}$ min^{-1}. Subtracting two similar numbers with small variability resulted in relatively larger errors for specific activity measurements.

Assays with Wild-Type $G_{\alpha o1}$ and RGS Protein

Agonist-stimulated GTPase activity was also detected for membranes expressing α_{2A}AR-wt $G_{\alpha o1}$ fusion (Figure 2-3). Basal levels of specific G protein GTPase were 7.0 ± 3 pmol (mg of protein)$^{-1}$ min^{-1} (n = 10) for samples containing 58.6 fmol of fusion protein. Addition of 10 μM UK14,304 resulted in a increase to 145% of basal levels (11 ± 2 pmol (mg of protein)$^{-1}$ min^{-1}, n = 9, $p < 0.0025$). The extent of stimulation is less than the maximal agonist-stimulated increase detected in membranes containing an equivalent amount (58.6 fmol) of C351I fusion protein (basal: 4.8 ± 1 pmol (mg of protein)$^{-1}$ min^{-1}; stimulated: 24 ± 3 pmol (mg of protein)$^{-1}$ min^{-1}). This result is consistent with less efficient stimulation of wt as compared to C351I fusion proteins for equivalent amounts of receptor as reported previously using radiolabeled GTP as the substrate[121].

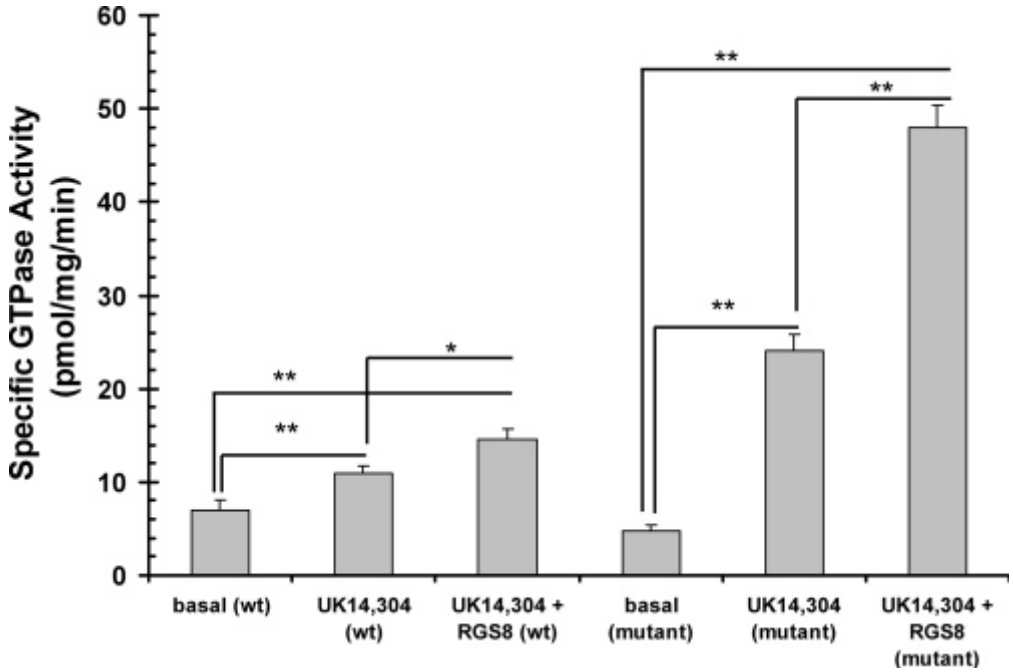

Figure 2-3. Agonist-stimulated specific GTPase activity can be modulated with RGS8. Data shown are for membranes expressing the wt and mutant fusion protein. Stimulation in the presence of 10 μM UK14,304 and 10 μM UK14,304 + RGS8. Differences with ** are significant with $p < 0.001$ and with * are significant with $p = 0.0025$. Error bars are 1 standard error of the mean.

RGS proteins modulate GPCR signaling by binding G proteins and accelerating the hydrolysis of bound GTP and inactivating the G protein. Because of this effect, these proteins are an emerging drug target (e.g., RGS inhibitors are expected to greatly enhance the effect of a GPCR agonist)[50]. To determine if we could detect modulation of the GPCR activity by RGS, we measured agonist-stimulated GTPase activity in the wt fusion membrane samples in the presence of RGS8. As shown in Figure 2-3, agonist-stimulated GTPase activity was amplified to 210% of basal levels (14.6 ± 3 pmol (mg of protein)$^{-1}$ min^{-1}, $n = 7$) by the addition of GTPase-accelerating protein RGS8 to the sample. For mutant G protein, even greater levels of stimulation were achieved (Figure 2-3). The ability to separately detect the effect of RGS proteins highlights an important advantage of this in vitro approach over

cell-based assays (i.e., reagents or intracellular modulators can be added directly to solution to monitor their effect on the reaction), meaning that interactions downstream of the GPCR (such as the RGS−G protein interaction used here) can be monitored. Thus, the developed assay could also potentially be used to screen for RGS inhibitors, in addition to novel GPCR ligands.

Direct Injection Assays

The results from these experiments illustrate that the CE-LIF assay can be used to detect agonist-stimulated GTPase activity. Significant improvements would be required for the assay to be considered suitable for high-throughput screening. One area of improvement is assay reproducibility. The reproducibility of assays used in high-throughput screening may be assessed using the Z'-factor, which is calculated as $Z' = 1.0 - (3.0 \times (s_{neg} + s_{pos})/R)$ where s_{neg} is the standard deviation of the response of a negative control (no drug), s_{pos} is the standard deviation of the response to a positive control (active drug), and R is the difference in signal between the mean of positive and negative controls[45, 121-124]. The maximum Z' is 1.0, and Z' over 0.5 is considered necessary for high-throughput screens. The assay described had a Z' = 0.4 suggesting that improvements were needed to make this assay viable for high-throughput screens.

We therefore investigated modifications of the assay aimed at improving reproducibility. To improve the assay, we focused on eliminating the membrane filtration step because not only did it seem likely to be a source of error, but it also

made the assay more complex and slower. To avoid the membrane filtration step, we directly injected without filtering using the flow-gated interface. The resulting electropherograms were cluttered with spikes, apparently associated with injection of the membrane particles. The nucleotide peaks could be resolved from the spikes using a modified electrophoresis buffer as shown in Figure 2-4. These conditions resulted in loss of resolution of the BGTP and BDP isomers; however, the loss of resolution was considered inconsequential given the similar behavior of the isomers in the assay. To better suppress background, we added 0.53 mM App(NH)p to the incubation media. This reagent has been shown to help reduce the high K_M GTPase activity[122]. A dose−response curve using these modifications is shown in Figure 2-5. The data shown in Figure 2-5 illustrate the curves with and without the background subtraction. Using this approach, the Z' factor was improved to 0.8. Even without the background subtraction step, the Z' factor was 0.7. Similar Z' factors were obtained when using the α_{2A}AR-wt $G_{\alpha o1}$ fusion. We conclude that the use of direct injection simplified the assay, improved the reproducibility, eased the potential for automation, and allowed a nearly 10-fold reduction in the amount of protein used for the assay.

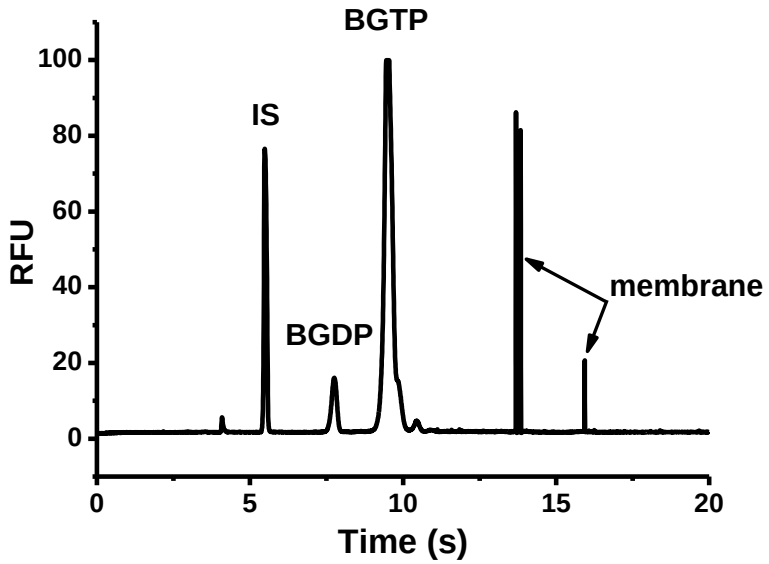

Figure 2-4. Electropherogram obtained using the direct injection assay conditions. Sample shown was for basal conditions (i.e., without drug) following 10 min incubation. Signal is plotted as relative fluorescence units (RFU).

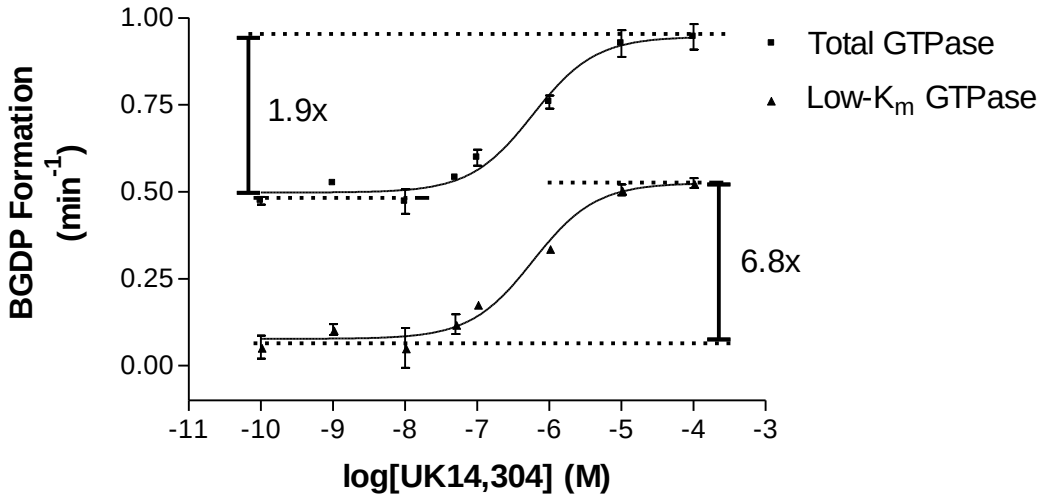

Figure 2-5. Dose−response curve obtained using direct assay conditions. Both background subtracted (low K_M GTPase) and raw data (total GTPase) activities are shown. Total GTPase was observed to increase 1.9-fold over basal levels when 0.1 mM UK14,304 was present. When the nonspecific, high K_M GTPase activity was subtracted out, the increase was 6.8-fold. Error bars are ± 1 SD (n = 3).

Conclusions

The success of the assay is perhaps surprising in view of previous work suggesting that the bulky BODIPY moiety reduces the affinity of guanosine nucleotide analogues GppNHp and $GTP_{\gamma}S$ for membrane-bound G proteins 17- to 55-fold and 1100- to 5600-fold respectively[125]. These prior results led to the conclusion that BODIPY-labeled nucleotides would be unsuitable for fluorescence studies in native membranes. The discrepancies between the two results may arise from the difference between the two techniques used. We directly measured consumption of BGTP and formation of BGDP, whereas previous studies indirectly assessed fluorescent nucleotide binding by measuring how effectively their presence blocked the receptor-stimulated hydrolysis of [γ^{32}P]GTP. It is possible, for example, that unaccounted for hydrolysis of the $BGTP_{\gamma}S$[107] and BGppNHp contributed to apparent lower affinities in these competition experiments.

The results presented herein demonstrate the use of fluorescent GTP analogues to study receptor-mediated GTPase activity in cell membranes. The method yielded expected responses in the presence of GPCR agonist and antagonist, with EC_{50}s comparable to those obtained from traditional techniques using [γ^{32}-P]GTP as substrate, without the drawbacks associated with radioactivity. In the direct injection format, the assay also has potential to serve as the basis for high-throughput screening applications. Use of the assay for high-throughput screens would require adaptation to array CE-LIF systems[16] or microchip formats[35, 126] that would offer parallel analysis and increased throughput. Another area of exploration is how versatile the

approach would be for different G protein systems. These data were obtained using a G_o coupled GPCR, but this approach may not be applicable to other G proteins.

CHAPTER 3

MICROFABRICATED CHANNEL ARRAY ELECTROPHORESIS FOR RAPID CHARACTERIZATION AND SCREENING OF ENZYMES USING RGS-G PROTEIN INTERACTIONS AS A MODEL SYSTEM

Introduction

Determination of enzymes and their kinetics is important in biotechnology, biochemistry, clinical chemistry, and pharmaceutical development[127-129]. Increasingly, high-throughput characterization of enzymes is important. This is especially true in drug discovery where chemical libraries are commonly screened for potential drugs that inhibit or activate enzymes that are therapeutic targets[127, 130]. Where feasible, enzyme activity is assessed using photometric or fluorometric methods to measure changes in substrate and product concentrations[131, 132]. If it is not possible to distinguish substrate and product by those techniques, then other methods such as radiochemical assays or HPLC may be used[133]. While these latter methods are acceptable in many cases, they are not well-suited for high-throughput applications.

Capillary electrophoresis (CE) has emerged as a promising means to detect and monitor enzyme activity as an alternative to HPLC or radiochemistry[134-136]. Advantages of CE include low sample consumption, rapid analysis, high sensitivity,

and efficient separation of product from substrate for detection and quantification CE enzyme assays can take several forms based on how the enzyme and substrate are mixed including: 1) pre-column mixing where CE is used to analyze reaction mixtures; and 2) on-column mixing, also called enzyme-mediated microanalysis, where substrate and product are mixed electrophoretically within the capillary[128, 135, 136]. With pre-capillary mixing, it is possible to use rapid CE to continually monitor a reaction and determine enzyme kinetics[112].

The throughput of enzyme assay by CE can be increased by performing separations in parallel using capillary bundles[16, 58, 137-139]. In most cases, capillaries used in array instruments are 40-80 cm long and have 50-100 μm i.d. These capillary dimensions are suitable for high efficiency, but cannot deliver high-speed analysis[15]. Slow separation compromises the improvement of throughput brought about by using large number of capillaries and precludes experiments aimed at monitoring reaction kinetics.

A promising alternative to capillary-array devices is chip-based CE[140-144]. Separation channels a few centimeters long can be easily fabricated on a glass substrate allowing rapid separations. Assays of a variety of enzymes including β-galactosidase[145], protein kinase A[146], and acetylcholinesterase[147] have been demonstrated on single-channel chips. Increasing the number of channels can be achieved for significantly improved throughput. Chips with as many as 384 channels have been demonstrated for genetic analysis[148]; however, relatively few applications have been reported demonstrating enzyme assays on multi-channel CE

devices. Increased throughput for electrophoretic enzyme assay has been demonstrated on a 4-channel, optically-gated CE device[35]. In that study, β-galactosidase was screened against a few inhibitors demonstrating modest throughput. A commercial system (Caliper HTS) is available with 4 parallel channels (now also available with 12 channels) to generate throughput of 384 samples in 80 min for kinase assays[36, 37]. This sophisticated device also incorporates automated sampling from multi-well plates and automated chip conditioning. In this work we explore the use of 16- and 36-channel chips that are suitable both for monitoring reactions on the second time scale to determine kinetics and for analyzing quenched reactions.

We use an assay of G protein GTPase activity as a model because of its significance in intracellular signaling[42, 149]. When a G protein-coupled receptor (GPCR) is activated, it stimulates exchange of GDP for GTP in the G_α subunit of the heterotrimeric G protein associated with the GPCR. The G_α-GTP complex is active, sending signals to downstream effectors such as adenylyl cyclase. Hydrolysis of GTP to GDP by the G protein terminates the signal. It has been shown that GTPase activity can be accelerated by Regulators of G protein Signaling (RGS) proteins which bind the G protein[49, 50, 150]. G protein hydrolysis activity and its regulation by RGS have emerged as interesting drug targets. Low RGS activity is associated with high blood pressure[151], schizophrenia[152], and drug addiction[153] suggesting that agents that increase RGS activity may be useful in treating these conditions. Substances that inhibit RGS activity may be useful in increasing the potency of GPCR ligands[43].

Currently available assays for GTPase activity and its modulation by RGS are not ideal. The most common GTPase assay uses [γ-^{32}P]GTP as G protein substrate[154]. A fluorescence assay based on changes of G protein intrinsic fluorescence during hydrolysis was also demonstrated[52]. Binding of G protein and RGS protein has been detected by flow cytometry and used in screening for potential RGS inhibitors[155]. These methods are either inconvenient for high-throughput or do not report on actual hydrolysis activity. Recently we demonstrated that GTPase activity and modulation by RGS could be detected by using BODIPY® FL GTP (BGTP) as substrate and rapid CE to detection conversion to the product BODIPY® FL GDP (BGDP)[112].

In this work, we used multi-channel electrophoresis chips to monitor GTPase activity in real-time for kinetics determinations. Potential applications include rapid determination of kinetics, determination of enzyme concentrations, and optimization of reaction conditions. In addition, we mimicked drug screening against G protein and RGS protein and characterized dose-response curves.

Experimental Section

Materials

BGTP and BGDP were obtained from Molecular Probes, Inc. (Eugene, OR). $G_{\alpha o}$ and RGS8 were expressed and purified as described previously and stored at -80℃ until used[112]. The peptide Ac-Val-Lys-c(Et)[Cys-Thr-Gly-Ile-Cys]-Glu-NH_2 (YJ34), where c(Et) designates cyclization via an ethylene dithioether linking the Cys side chains, was synthesized and purified as previously described[156], dissolved in

DMSO and stored as 2 mM aliquots at -20 °C. Methyl N-[(4-chlorophenyl)sulfonyl]-4-nitrobenzenesulfinimidoate (CCG-4986) was from the screening compound library from the Chembridge screening collection (hit2lead.com)[155]. All other chemicals were purchased from Sigma. All buffers were made using Milli-Q (Millipore, Bedford, MA) 18-MΩ deionized water and filtered using 0.2-μm SFCA membrane filters (Nalgene Labware, Rochester, NY).

All BGTP hydrolysis experiments were performed with Tris-Glycine buffer supplemented with 1 mM EDTA and 10 mM $MgCl_2$ (TGEM buffer) as the solvent except for those studying the effect of Mg^{2+} on $G_{\alpha o}$ GTPase activity. Electrophoresis buffer was Tris-Glycine buffer (pH 8.3) supplemented with 8 mM $MgSO_4$.

Microfluidic Chip Fabrication

Microfluidic networks consisting of either 16 or 36 separation channels were fabricated on a 76 mm × 76 mm borofloat glass substrate according to a previously described procedure[157]. Briefly, 0.7 mm thick borofloat glass photomask blanks pre-coated with a 530-nm layer of AZ1518 positive photoresist on top of another 120-nm layer of chrome were purchased from Telic Co. (Santa Monica, CA). A custom-made photomask (Fineline Imaging, Colorado Springs, CO) patterned with the microfluidic network (Figure 3-1 (a) and (b)) was used to transfer the network design onto the photomask blanks by exposing for 4 s at 26 W cm^{-2}. The exposed photomask blanks were developed in AZ915 MIF developer (Clariant Corp., Sommerville, NJ) and then treated with CEP-200 chrome etchant (Microchrome

Technologies, Inc., San Jose, CA). 12 μm deep channels were then formed by etching the exposed glass in 14:20:66 (v/v/v) HNO_3/HF/H_2O for 20 min. 360 μm diameter access holes were drilled onto the etched plate with diamond-tipped drill bits (Kyocera, Ervine, CA). Both the etched and another blank substrate were thoroughly cleaned in Piranha solution (3:1 v/v H_2SO_4/H_2O_2) for 20 min and then with RCA solution (5:1:1 v/v/v $H_2O/NH_4OH/H_2O_2$) for 40 min at 60 ℃. The cleaned substrates were pressed together when wet and bonded at 610 ℃ for 8 h in a Neytech Centurian Qex furnace (Pacific Combustion, Los Angeles, CA). Sample and buffer reservoirs were attached to the bonded chip using epoxy (Epo-Tech., Bellerica, MA). Figure 3-1 (c) shows the completed 36-channel chip.

Mircrofluidic Chip Operation

Before use, chips were conditioned with 0.1 M NaOH in 50:50 (v/v) H_2O/methanol by electrophoretically perfusing the solution through all channels for 30 min. This treatment was followed by conditioning channels with deionized water and electrophoresis buffer for 5 min each. To prepare the chip for CE separation, samples were loaded onto sample reservoirs which were grounded using a platinum electrode array fabricated in-house. As shown in Figure 3-1 (e), samples were driven towards the injection cross channel by voltage 1 (-4 kV and -2.5 kV for 16 and 36 channel designs respectively) at the chip center. Sample loading onto the separation channel at the injection cross was controlled by voltage 2 and the relay (Kilovac, Santa Barbara, CA) connected at the waste 1 and gate reservoirs

respectively. (These reservoirs were common to all electrophoresis units as shown in 3-1 (b)). With the relay closed sample was shunted to waste 1 while opening the relay for 0.5 to 1.0 s allowed a plug of sample to be injected onto the separation channel. All voltages were applied with a Spellman High Voltage Electronics CZE1000R power supply (Happauge, NY). Applied voltage and frequency of injection were controlled by a personal computer equipped with a multi-function board (AT-MIIO-16, National Instruments, Austin, TX) using software written in-house.

Fluorescence Detection and Data Analysis

Excitation light from a 300 W Xe arc lamp (LB-LS/30, Sutter Instrument Company, Novato, CA) was filtered through a FITC filter cube (Semrock, Rochester, NY) before it was focused onto the chip detection region at the center of the chip (Figure 3-1 (d)) with an objective lens (Olympus America Inc., Melville, NY). Emission light was collimated with the same objective and detected using an electron-multiplying CCD camera (C9100-13, Hamamatsu Photonic Systems, Bridgewater, NJ). Time-lapse fluorescence images of the detection region were collected using an inverted epi-fluorescence microscope (IX71, Olympus America, Inc., Melville, NY) at ~15 Hz and analyzed with Slidebook software (Intelligent Imaging Innovations, Inc., Denver, CO). Electropherograms from individual channels were reconstructed from the images before they were analyzed using software written in-house[158]. To test this system for cross-talk between channels,

solutions without fluorophore were injected into channels parallel to those with fluorophore. No peaks were detected in the blank channels. In addition, no signal was detected when imaging the area between channels when all channels had fluorophore pumped through them. From these results we concluded that no detectable cross-talk occurred between channels.

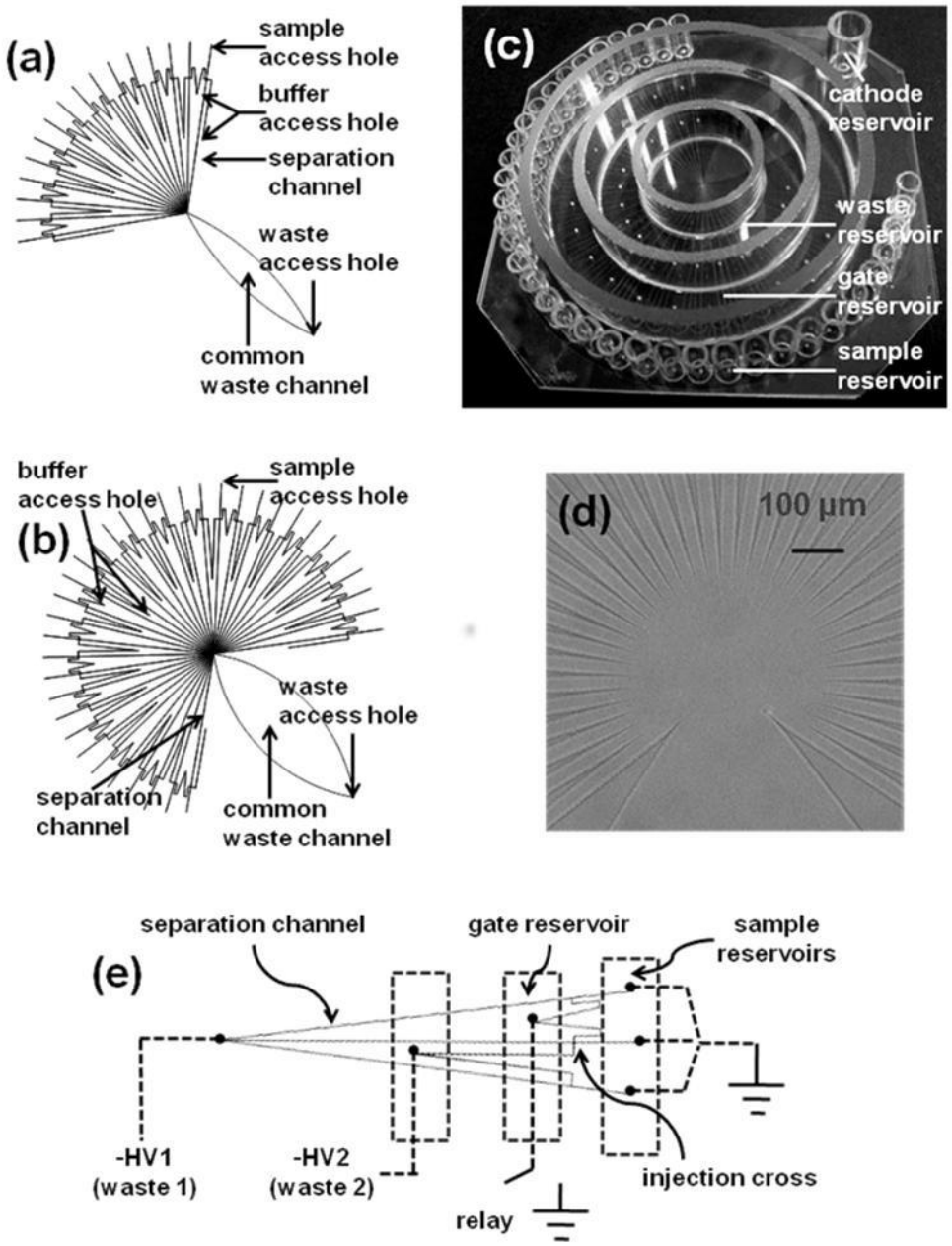

Figure 3-1. Microfluidic devices used for parallel electrophoretic enzyme assays. (a). Design of microfluidic network containing 16 parallel separation channels. Dimensions of each section were as follows: 7 mm from sample access hole to injection cross; 27 mm for separation channel (from injection cross to center where all separation channels converge); 8 and 13 mm for two other channels connecting the injection cross; 35 mm long and 6 mm wide at the widest point for the common waste channel. (b) Design of 36-channel network. Dimensions were similar to the 16-channel chip except the common waste channel was 40 mm long and 13 mm wide at the widest point. (c) Photograph of finished 36-channel chip. 1 cm long glass tubes of volume of 50 µL each were used for individual sample reservoirs. Two groups of access holes were separately connected to gate reservoir and waste reservoir which were formed by using three glass rings. Common waste channel led to another cathode reservoir to which –HV was applied. (d). Bright-field image of the

detection area on the 36-channel chip. (e) Repetitive units of microfluidic network. Electrokinetic injection procedure is described in experimental section.

G protein assay and drug screening

Assays were done in a real-time monitoring format on the 16-channel chip. Hydrolysis was initiated by mixing G protein and BGTP in reaction buffer and then loading 50 μL of the sample into sample reservoirs on the chip. Periodic injections were then made to track the evolution of BGDP peak. The initial portion of BGDP peak growth was fitted to a linear equation and the resulting slope converted to hydrolysis rate using a previously acquired calibration curve. Derived hydrolysis rates were used as indications of G protein enzymatic activities. On the 36-channel chip, all assays were performed on quenched reactions. G protein, BGTP and other modulators as indicated were incubated in the TGEM buffer at room temperature for specific period before reactions were quenched by adding excess $GTP_{\gamma}S$. The quenched reactions were stored on ice prior to loading on chip for analysis. The final BGDP concentrations were derived and quantified from the acquired electropherograms and calibration curves. BGDP formation was calculated by subtracting out the initial BGDP residue existing in the BGTP sample. The calculated BGTP turnover rates were used to determine the stimulatory or inhibitory effects of test substances.

Results and Discussion

Chip Performance

Electrophoretic assay of GTPase activity requires separation and quantification of the G protein substrate BGTP, the product BGDP, and the internal standard rhodamine 110 (R110). To determine kinetics by monitoring the enzyme reaction, it is necessary to perform serial injections from a given sample at a rate sufficient to achieve adequate temporal resolution. Separation time also affects the ability to perform high throughput assays. To implement parallel enzyme assays on chip, reliable and reproducible channel performance, including reproducible migration times across channels, is required. We therefore tested the 16- and 36-channel devices for their suitability for serial separation of substrate, product, and internal standards.

Typical serial electropherograms on a 16-channel chip are shown in Figure 3-2. As shown, the substrate, product, and internal standard were well-resolved in 18 s and injections could be reliably performed serially across all channels. The separation time is limited by the electric field applied to the separation channel. In the 16-channel design, electrical resistance of separation channel is about 250-fold that of the common waste channel. The total resistance of 16 parallel separation channels is about 15-fold that of the common channel. Therefore, with -4 kV applied to the cathode reservoir an electric field of -1.1 kV/cm was developed in the separation channels. In the 36-channel design, electrical resistance of a single separation channel is about 470-fold that of the common channel. So the total resistance of 36 parallel separation channels is about 13-fold higher than that of the common channel. In similar experiments with 36-channel chips, -2.5 kV was applied to the cathode

resulting in – 0.68 kV/cm electrical field. As a result, the separation of R110, BGDP and BGTP took longer, about 30 s. At these voltages Joule heating, evidenced by non-linear Ohm plots, was not observed. Rather, voltages applied in both cases were limited by the maximal current allowed by the high-voltage power supply. Should higher current power supplies be available a higher separation voltage could be applied to attain even faster and higher resolution separation.

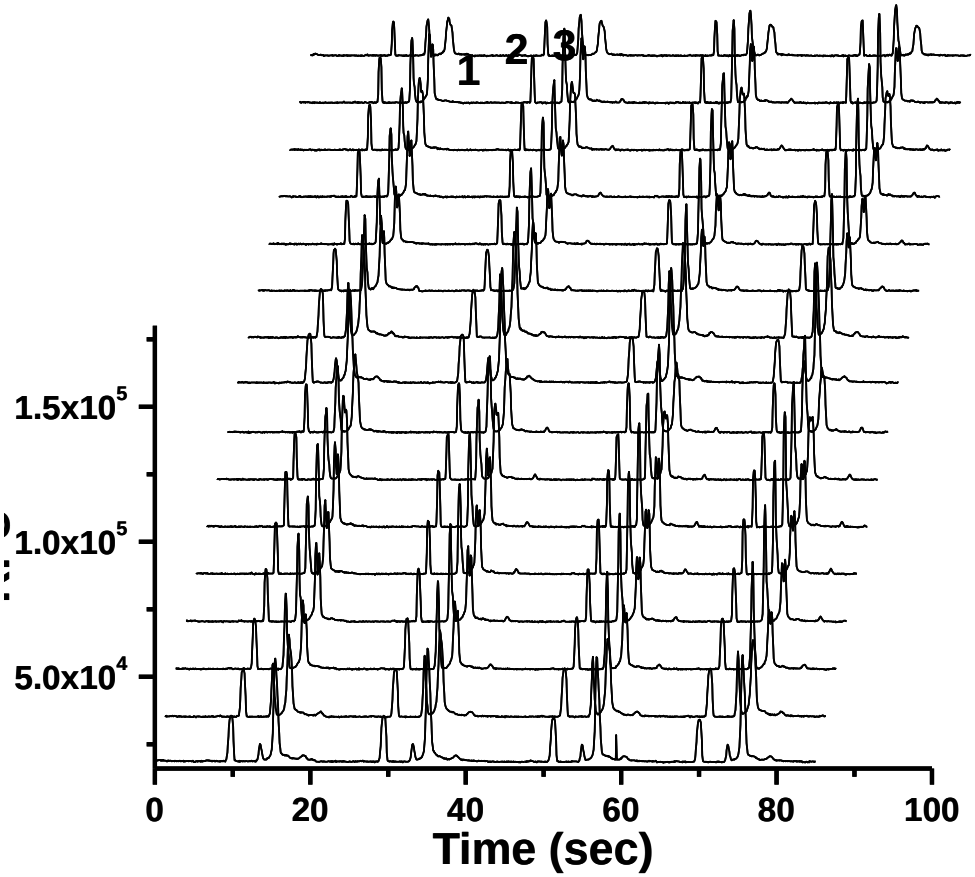

Figure 3-2. Typical serial electropherograms acquired in parallel from a 16 channel-chip. Solution containing 26.2 nM rhodamine 110 (peak 1), 1.0 μM BGTP (peak 3) and trace amount of BGDP (peak 2) was serially injected 4 times onto each channel at 20 s intervals.

The reproducibility of migration times for both the 16- and 36-channel chips was excellent with RSDs of 1.5% (n = 6) and 2.5% (n = 6) respectively. Good reproducibility allowed for controlling injection on all channels using a single high-voltage relay because the injections could be performed simultaneously. This simplified instrumentation as well as computer control of the relay.

Within a single channel, RSDs of peak area of R110 and BGDP were about 1.5% and 2.0% respectively, and that of the peak area ratio BGDP/R110 was around 3%. Absolute peak areas across all channels were not reproducible enough to achieve quantification (relative standard deviation could be as high as 33%). Therefore relative peak area of BGDP to R110 was always used for quantification. In the 16-channel design, the relative standard deviation of BGDP peak area normalized to internal standard R110 was around 5% across all channels. However, in the 36-channel design, the RSD was increased 11%. This RSD is acceptable for quantification in some cases, but the best quantitative results were obtained by calibrating each channel individually.

We next compared calibration curves across different channels by plotting BGDP/R110 peak area ratios as a function of BGDP concentration from 100 to 800 nM. Linear response was found for all channels with variation of 5.1% in slope for both the 16- and 36-channel designs indicating good channel-to-channel homogeneity. Therefore all channels had similar sensitivity and detection limit of GTPase activity.

It is desirable that chips maintain their performance as long as possible. The most common reason for chip failure was particle accumulation, especially around the

common outlet. In preliminary experiments, we found that a wide common waste channel was essential in preventing particulates from accumulating at the outlets of separation channels. This is probably because the wide channel helps decrease pressure build-up at the center of the chip and facilitates particles and fluid passing through the waste channel. With the wide channel, small particles could be observed passing through the common channel and clogging rarely happened in the separation process. Precipitate that did build up during chip storage could be easily removed by perfusing diluted nitric acid, water, and then NaOH through channels by vacuum. By using these procedures a chip could be used daily for at least 2 weeks (~400 electrophoresis injections per channel per week) without significant loss of performance. As the chip was used, the differences in migration times were large enough to make parallel analysis difficult. Even after this time, however, intrachannel reproducibility for migration time and peak areas was sufficient for quantitative analysis.

Parallel Kinetic Enzyme Assays on Chip

We next explored the possibility of using multiplexed channel chip to monitor GTPase hydrolysis kinetics of multiple samples simultaneously. For these kinetics experiments, the 16-channel chip was used because of the better temporal resolution. In initial experiments, BGTP hydrolysis rates at different concentrations of G protein were examined. G protein at 8 different concentrations from 10 to 125 nM was mixed with a fixed concentration of substrate BGTP. Immediately after mixing the

mixtures were loaded into separate sample chambers on the chip (each concentration of G protein was loaded onto and analyzed by two different channels) and monitored by serial electropherograms acquired at 20 s intervals. The resulting hydrolysis rates from those two channels were averaged to generate calibration curves for G protein concentration. These curves could be fit by linear regression (slope = 0.0087 ± 0.0008 nM BGDP formed per nM G protein/s, r^2 = 0.83 for n=4 calibrations). The linear fit could be improved by using only the G protein concentrations from 10 to 60 nM (r^2 = 0.94) due to nonlinearity and lower reproducibility at high G protein concentrations. These effects at higher G protein concentrations occurred because it took about 5 min to load the samples into the chip and during this time rapid hydrolysis that occurred at higher protein concentrations consumed sufficient BGTP to affect the rate measurement. Variation in time of sample loading would directly lead to variation in measured rates. Automated loading or on-chip mixing would alleviate this problem. Channel-to-channel reproducibility at low G protein concentrations was generally good, below 15%. Under conditions used in the experiments, the limit of detection (LOD) for G protein by its enzymatic activity was 10 nM. This detection limit could easily be improved by increasing the incubation time using off-line assay.

For characterizing enzymes, it is often necessary to vary buffer composition to identify how different factors affect enzyme behavior and to optimize conditions. For example, G protein hydrolysis is dependent upon Mg^{2+} which is required for BGTP to effectively bind to G protein. Optimizing conditions can be a slow process

if performed serially. To demonstrate rapid reaction optimization using the 16-channel chip, we varied the Mg^{2+} concentration and monitored hydrolysis kinetics. By monitoring BGTP hydrolysis by G protein at 8 concentrations of Mg^{2+} in duplicate on the 16-channnel chip, the optimization could be accomplished in a single experiment (Figure 3-3). The results showing a linear increase up to 2 mM Mg^{2+} are in good agreement with previous studies[112].

The multi-channel chip also allows kinetic parameters of enzymes to be rapidly determined. For example, measuring enzymatic activity across a range of substrate concentration is used to determine K_M. This process can be greatly shortened by running assays on the 16-channel chip. In our experiment, BGTP of concentrations ranging from 50 nM to 2.5 μM was mixed with 42 nM G protein and loaded onto the 16-channel chip. The hydrolysis rate at each BGTP concentration was monitored in two separate channels. As shown in figure 3-4, BGTP turnover rates can be fitted to the Michaelis-Menton equation. K_M and k_{cat} calculated by curve fitting were 305 ± 85 nM and 0.015 ± 0.001 sec^{-1} respectively. These results are comparable to previously reported K_M of 300 nM and k_{cat} of 3.6×10^{-2} s^{-1} for GTP [159, 160] and 120 nM and 8.3×10^{-3} s^{-1} for BGTP[112].

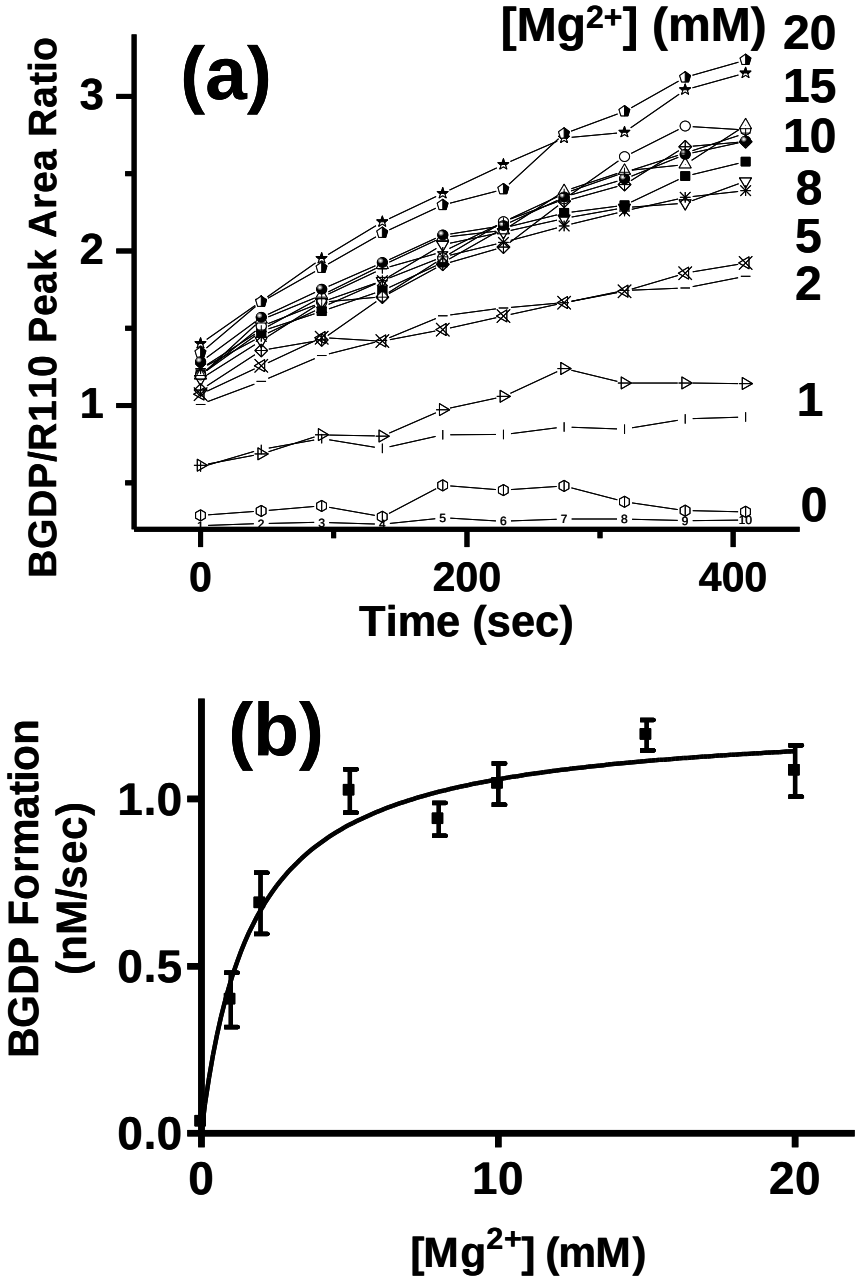

Figure 3-3. Optimizing enzyme assay conditions. (a) BGDP peak heights recorded by serial electrophoresis from 16-channels when BGTP was hydrolyzed by $G_{\alpha o}$ at various Mg^{2+} concentrations. Each sample reservoir was filled with a solution of 83.3 nM $G_{\alpha o}$, 1 μM BGTP, and 21.8 nM R110 in TGE buffer spiked with Mg^{2+} concentrations as shown. Each Mg^{2+} concentration was used in two separate channels. BGDP formation was monitored and BGDP/R110 ratios were used to indicate the real-time concentrations of BGDP in the reaction mixtures. (b) Plot showing $G_{\alpha o}$ hydrolytic activities at different Mg^{2+} concentrations. Hydrolysis rates indicated by BGDP formation (nM/sec) were derived from linear fitting of Figure 4 (a). The rates were fitted to a one-site binding function versus Mg^{2+}.

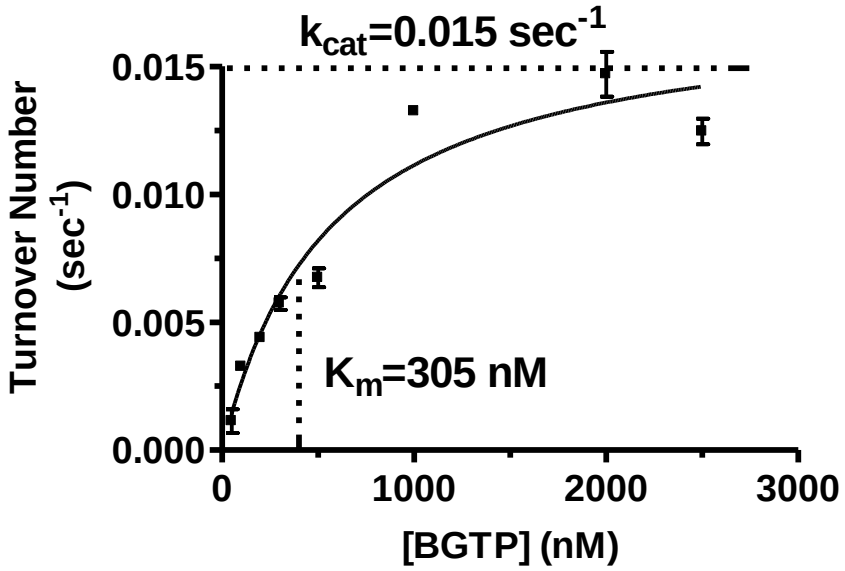

Figure 3-4. Determination of Enzyme Kinetics. 20.8 nM $G_{\alpha o}$ was incubated with 0.05, 0.1, 0.2, 0.3, 0.5, 1.0, 2.0, and 2.5 μM BGTP respectively in TGEM buffer at room temperature. Hydrolysis rates expressed in turnover number were calculated by real-time monitoring and plotted against BGTP concentrations. Data were fit to the Michaelis-Menton function.

Although enzyme kinetics can be measured by a variety of analytical techniques, the results shown here illustrate a unique potential for rapid separations in parallel channel electrophoresis. Optical methods in principle could be operated in parallel, but they require changes in optical properties upon conversion from substrate to product which is not always the case, as is true here for GTP with the BODIPY label on the sugar ring. Radiochemical methods require hazardous substances and frequent multiple washing and rinsing steps. Slower parallel CE methods are not well-suited for on-line kinetics measurements. Thus, the combination of rapid measurement in parallel with electrophoretic separation allows kinetics to be measured in parallel even for enzymes where the substrate and product are indistinguishable by optical methods.

Parallel Analysis of Quenched Reaction Mixtures: Drug Screening and Dose Response Curves

In addition to the multi-point kinetic data, it is also frequently of interest to measure the extent of reaction at a fixed time point. For example, dose response curves for compounds that affect enzyme activity are typically measured at fixed times. Similarly, in combinatorial screening for enzymatic activators or inhibitors, the extent of reaction at a single time point is often measured. We therefore examined the possibility of performing such measurements using the multiplexed chip. In this experiment, serial analysis was less important than parallel measurements so the 36-channel chip was used.

Because RGS has become an interesting drug target, we tested the possibility of screening against RGS protein effects on GTPase activity. The principle of the assay is illustrated in Fig. 3-5. G protein was mixed with substrate for a fixed period and the hydrolysis reaction was then quenched by addition of an excess of the non-hydrolyzable GTP analog $GTP_{\gamma}S$ (see Experimental section for details). As shown in Fig. 3-5, the extent of hydrolysis reaction is increased by the presence of RGS protein in the reaction mixture. Inhibition of RGS activity results in less net hydrolysis. Therefore, comparison of BGDP formation with and without test compound in the presence of RGS allowed detection of inhibitors. The steady state assay used here is made possible by the rapid dissociation of BGDP from G protein. RGS assays normally require a single turnover format, which is requires more sophisticated mixing because the RGS effect is masked by slow dissociation of GDP

from the G protein.

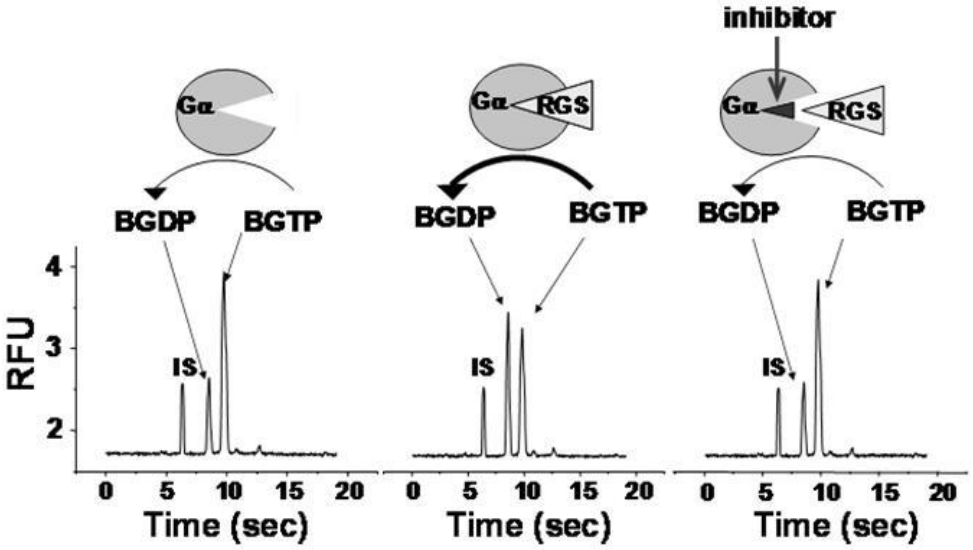

Figure 3-5. Electrophoretic assay for RGS GTPase accelerating activity and its inhibition. (left) Basal hydrolysis by G_α alone results in formation of BGDP from BGTP; (middle) RGS protein accelerates the GTPase activity of G_α resulting in a larger BGDP peak formation; (right) addition of an inhibitor interferes with RGS and G_α interaction and thus diminishes the acceleratory effect of RGS protein resulting in a smaller BGDP peak in the electropherogram. All solutions were incubated for 20 min and then quenched with 10 μM $GTP_\gamma S$ before electrophoretic analysis.

For the screen we tested the effect of 11 compounds. YJ34 had previously been shown to interfere with G protein-RGS8 binding and would therefore be expected to inhibit BGTP hydrolysis[161]. CCG-4986 was reported to interfere with G protein-RGS4 binding but not G protein-RGS8 binding and was expected to not have an effect[155]. The other 9 compounds were known drugs but not expected to have any activity on this system. Each reaction mixture containing one drug was analyzed in triplicate using three separate channels. The results are summarized in Figure 3-6. As shown, the expected inhibitory effect of YJ34 was detected and the 9 negative

controls gave similar responses to each other. Interestingly, CCG-4986 showed an inhibitory effect. This could be due to several possibilities including: 1) inhibition of hydrolysis activity independent of inhibition of binding, which is one of the reasons for using activity instead of binding assays or 2) an artifact of using BGTP instead of GTP in the assay. While further work would be required to resolve this issue, the data overall illustrate the potential for screening with the chip-based system. We used Z' value to evaluate the reproducibility of the assay. The Z' is by definition = $1.0 - (3.0 \times (s_{neg} + s_{pos}) / R)$ where s_{neg} and s_{pos} are the standard deviation of the signal of negative and positive controls respectively, and R is the difference between the mean of positive and negative controls[162]. We determined a Z' = 0.7 for the assay which is well above the 0.5 considered necessary for high-throughput screening. Also, the assay only required 30 s (the separation time) for 11 compounds to be analyzed (in addition to one control sample) in triplicate corresponding to a throughput of 1,440 samples per hour. If only single samples were analyzed the throughput could be 4,320 samples per hour. Naturally, achieving throughput this high would require a means of introducing new samples to the chip rapidly and automated sample preparation procedures.

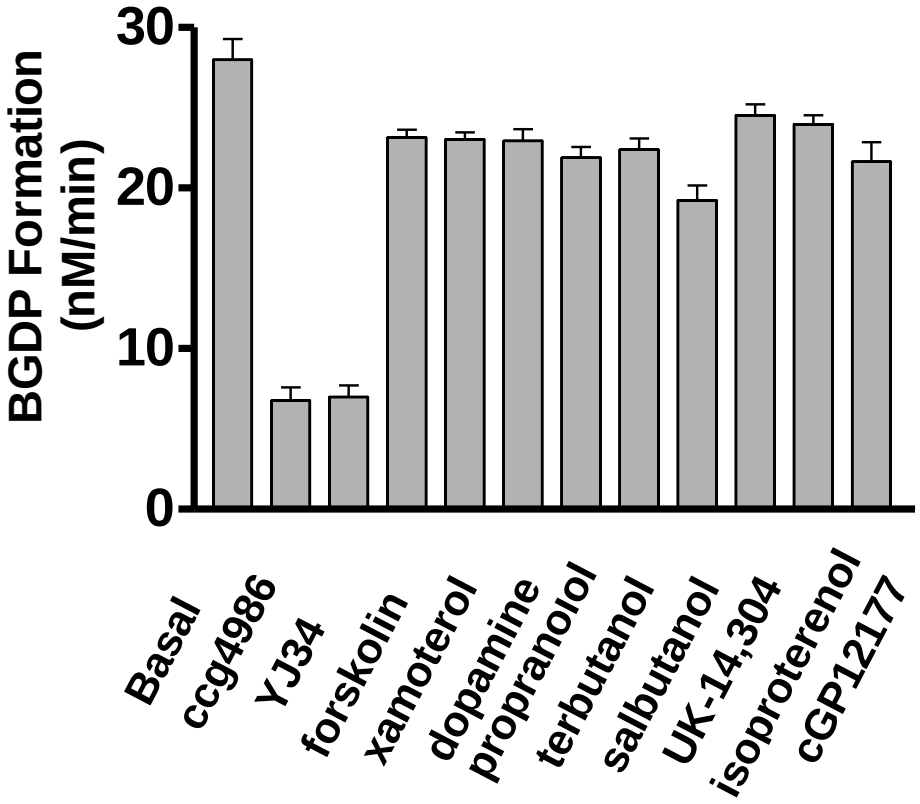

Figure 3-6. GTPase accelerating activity of RGS8 in the presence of test compounds. 1 μM BGTP was incubated with 20 nM $G_{\alpha o}$ and 321 nM RGS8 in the presence of 11 different compounds. BGDP formation rates were used indicate RGS8 activities. All compounds were at 102 μM except YJ34 which was at 40.8 μM.

We also tested the ability to quantitatively determine dose-response curves across channels with a single experiment. Nine concentrations of $G_{\alpha o}$ inhibitor $GTP_{\gamma}S$ and activator RGS8 separately were included in the reaction mixtures containing G protein and BGTP. After incubation of 30 and 15 min respectively, reactions were quenched with $GTP_{\gamma}S$ and put on ice before analysis. Each reaction mixture was analyzed in two separate channels and BGDP formation was quantified (Figure 3-7). $GTP_{\gamma}S$ showed IC_{50} of 18.8 nM and a maximal inhibition of 97.7% of

basal GTPase activity.

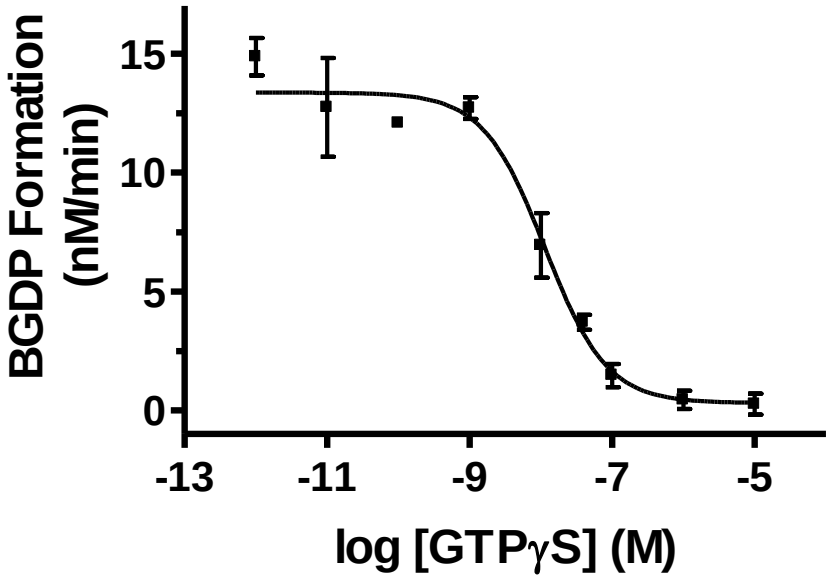

Figure 3-7. Dose response curve for GTP$_\gamma$S inhibiting $G_{\alpha o}$ GTPase activity. Nine concentrations of GTP$_\gamma$S were tested for the effect on basal BGTP hydrolysis rate. Reaction mixture containing each concentration of GTP$_\gamma$S was analyzed in 2 separate channels. The calculated IC_{50} value was 18.8 ± 8 nM. At maximal inhibition GTPase was 2.3% of basal level. Error bars are ±1 SD.

Conclusions

The microfabricated channel-array electrophoresis device described here is suitable for parallel enzyme assays. The combination of fast separations and parallel operation yields a versatile platform for determining kinetics, enzyme concentrations, optimizing reactions, screening inhibitors, and determining dose response curves. Although the system has the potential for high throughput screening assays, the development of improved sample introduction will be required for this system to be

used for such applications. The assay for RGS-G proteins appears to be sufficiently sensitive for drug screening.

CHAPTER 4

PARALLEL ELECTROPHORETIC ANALYSIS OF SEGMENTED SAMPLES ON CHIP FOR HIGH THROUGHPUT DETERMINATION OF ENZYME ACTIVITIES

Introduction

Capillary electrophoresis (CE)-based micro-total analysis system (μTAS) has greatly evolved since the first demonstration of CE separation on microfluidic devices in 1992[21]. CE is by far the dominant separation technique for on-chip analysis not only because it is the easiest to impletment but it also enables fast analysis, low sample consumption and requires no external pumping. A broad spectrum of analytes including DNAs, proteins and small molecules have been separated by CE on chip[22, 23]. Until recently, research interest in this area has mostly been focused on improving separation efficiency and integrating other laboratory functionalities such as mixing and reaction. Achieving high throughput using such electrophoresis devices has also gained attention. Performing parallel CE separation on devices consisting of multiple separation channels is the most prominent approach to this end. Initially parallel CE separation was demonstrated for DNA sequencing and genotyping by Mathies' group[38]. Up to 384 separation lanes have been microfabricated on a single device for high-throughput genetic analysis[40]. Parallel

CE separation has also found applications in immunoassays[163, 164] and enzyme assays[30, 35-37]. For example, we previously developed a microfluidic device which consisted of up to 36 parallel electrophoretic channels. With fast separation in each channel, 36 enzyme assay mixtures could be analyzed in 30 seconds[30]. However, in most of the above works, samples were loaded into the reservoirs manually. When a different set of samples were to be analyzed, it required that reservoirs be emptied, cleaned, and re-loaded. This time-consuming step undermined the high throughput achieved by parallel separation. Therefore further improvement in sample handling is required to achieve real high throughput and enable applications such as high-throughput screening (HTS). Even though robotic systems have been built for automated sample loading and changing, the overall throughput still fell short of HTS requirements.

Effort has been devoted to devising so-called world-to-chip interfaces which would allow delivering discrete samples to the inlet of the CE channels for continuous analysis[165]. Most of the designs utilized a sample introduction channel which had a much lower flow resistance than the separation channels. Samples were perfused through this channel without causing significant pressure-driven flow in the rest of the chip. A fraction of the sample flow was pulled by electroosmotic flow into the separation channel for injection. To change samples, the previous sample was completely flushed out by the next sample before analysis so that low cross-contamination was possible. An alternative to such flow-through sample reservoir was shown by He et al. where the sampling tip of the CE device was

inserted alternatively into samples and electrophoresis buffer stored in microvials fixed on a computer controlled autosampler platform[166]. A similar but simpler sampling method that allowed direct CE injection was also reported[167]. All these sample introduction schemes facilitated sample changing and increased analysis throughput; however, they did not address the issue as to how to transfer samples to chip. Pipetting individual samples to the chip inlet was unavoidable. Other disadvantages of these approaches included low sample utilization rate, complicated power control and external moving parts. For example, tens of microliters of sample was required to flush out previous sample and fill the sample introduction channel while only nanoliters of sample was injected[165]. Therefore more than 99% of the sample was wasted. The moving stage for sample changing in another case added complexity to the instrumentation and compromised the benefits of microfluidic devices[166]. An alternative sample introduction method to pipetting is transporting and feeding serial samples entrained in a multiphase flow to the analyzer. These so called continuous flow analysis techniques have been around for decades but until recently have not migrated to the microfluidic regime[168, 169]. It has been shown that sample droplets or plugs on the nanoliter scale separated by an immiscible phase (such as gas or fluorinated oil) can be transported in an automatic fashion without significant cross contamination. Various pre-analysis sample processing methods such as reagent mixing[76, 91], dilution[81] and concentration[170, 171] have also been demonstrated. However, methods for chemically analyzing segmented sample droplets have been largely limited to spectroscopic techniques such as absorbance and

fluorescence. Only recently analyzing segmented flow using information-rich methods such as CE[85, 86] and mass spectrometry (MS)[87, 172] was demonstrated. Roman et al developed a microfluidic device for sampling and electrophretically analyzing aqueous samples segmented in an immiscible oil phase. However manually aligning two microfluidic networks of different depths was required for the chip fabrication, which made it difficult to construct more than one of such unit on a single device. Here we described a novel microfabricated interface to microchip CE for extracting and injecting samples from segmented flow. This way multiple interfaces could be fabricated on a single chip allowing parallel analysis of segmented sample streams. The entire analysis was automated with no need for power manipulation. We envision the utilization of this device for automated high-throughput analysis such as HTS for drug discovery.

Experimental Section

Materials

BODIPY® FL GTP (BGTP) and BODIPY® FL GDP (BGDP) were obtained from Molecular Probes, Inc. (Eugene, OR). $G_{\alpha o}$ was expressed and purified as described previously and stored at -80℃ until used[30]. All other chemicals were purchased from Sigma. All buffers were made using Milli-Q (Millipore, Bedford, MA) 18-MΩ deionized water and filtered using 0.2-μm SFCA membrane filters (Nalgene Labware, Rochester, NY).

BGTP hydrolysis experiment was performed in Tris-Glycine buffer

(containing 25 mM Tris and 192 mM glycine, pH 8.3) supplemented with 1 mM EDTA and 10 mM $MgCl_2$ (TGEM buffer). Electrophoresis buffer was Tris-Glycine buffer supplemented with 5 mM $MgSO_4$ (TGM buffer).

Microfluidic Chip Fabrication

Microfluidic channels of two different depths were fabricated on two separate 76 mm × 76 mm borosilicate (D263) glass substrate according to standard photolithographic procedure. Briefly, 0.5 mm thick borosilicate glass pre-coated with a 530-nm layer of AZ1518 positive photoresist on top of another 120-nm layer of chrome were purchased from Telic Co. (Santa Monica, CA). A custom-made photomask (Fineline Imaging, Colorado Springs, CO) patterned with the microfluidic network (Figure 4-1 (a) and (b)) was used to transfer the network design onto the photomask blanks by exposing for 6 s at 26 W cm^{-2}. The exposed photomask blanks were developed in AZ915 MIF developer (Clariant Corp., Summerville, NJ) and then treated with CEP-200 chrome etchant (Microchrome Technologies, Inc., San Jose, CA). 80 μm deep channels were then formed on one glass by etching the exposed glass in 50:50 (v:v) HCl/HF for 5 min and 45 sec. 360 μm diameter access holes were drilled onto this etched plate with diamond-tipped drill bits (Kyocera, Ervine, CA). 18 μm deep separation channels were created on another glass by etching in the same solution for 100 sec. Both glass substrates were thoroughly cleaned in Piranha solution (3:1 v:v H_2SO_4/H_2O_2) for 30 min and then 60 °C in RCA solution (5:1:1 v/v/v $H_2O/NH_4OH/H_2O_2$) for 40 min. The cleaned substrates were pressed

together when wet and bonded at 606 °C for 8 h in a Neytech Centurian Qex furnace (Pacific Combustion, Los Angeles, CA). Nanoport® microfluidic reservoirs (Upchurch Scientific, Oak Harbor, WA) were attached to the bonded chip over the access holes after bonding. Additional 360 μm access holes were drilled from the side of the chip using flat-tipped drill bits from Kyocera so that they connect with the segmented-flow channels. Water was perfused through the channels during drilling to prevent debris from clogging the channels. The chip was thoroughly sonicated after drilling to clean out all remaining debris. 360 μm o.d. / 150 μm i.d. fused-silica capillaries (pre-treated with octadecyltrichlorosilane (OTCS) to make inner wall hydrophobic) were inserted into the access holes and glued in place using fast setting epoxy (Royal Adhesives & Sealants, Belleville, NJ) as the inlet of segmented flow. Figure 4-2 (a) shows the completed device.

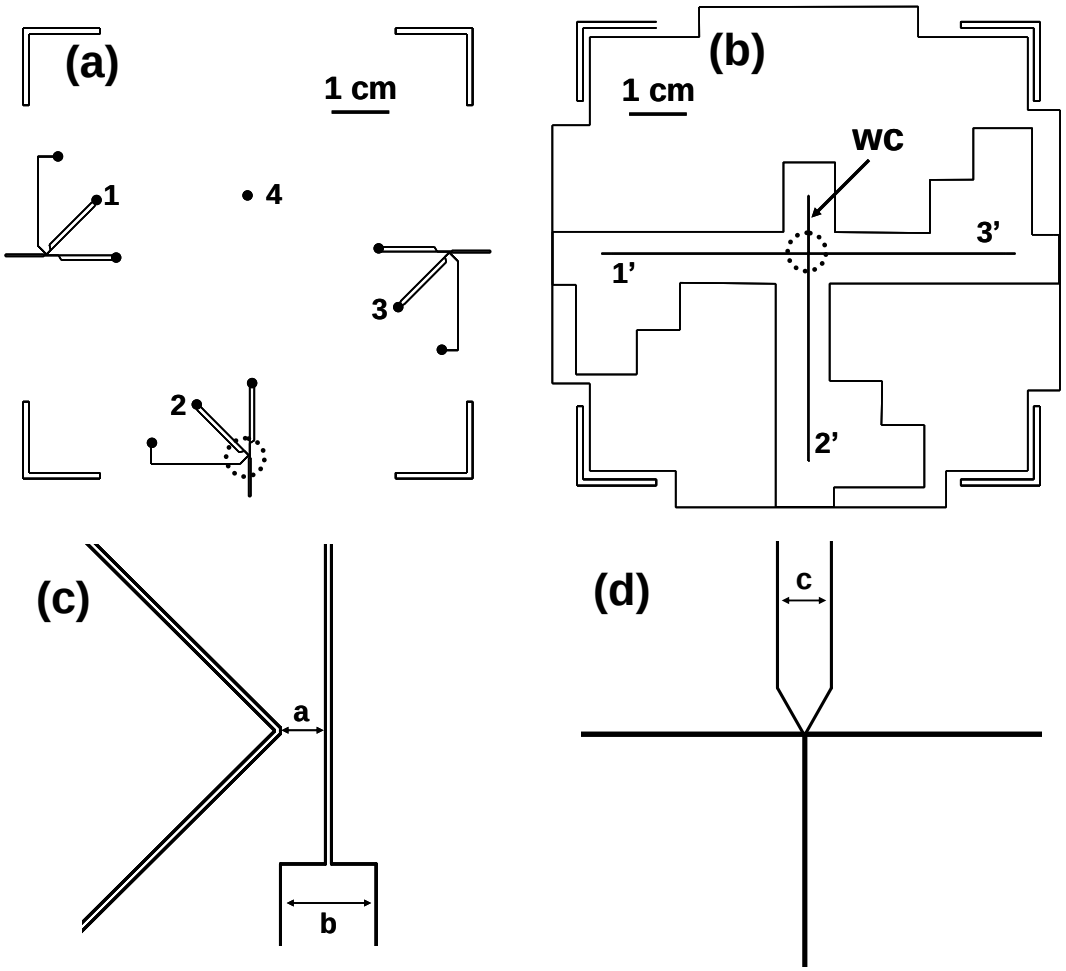

Figure 4-1. Design of a microfluidic device for parallel segmented flow analysis. (a) Three parallel designs of an interface for extracting aqueous sample droplets form the segmented flow. Black dots will become access holes during fabrication. Positions 1-3 are buffer flow wastes and will be grounded. Position 4 is common waste and will be biased to a negative high voltage; (b) Three parallel separation channels (labeled 1'-3'). The channels have a length of 3.4 cm and they converge at the center and connect with a common waste channel (wc); (c) blow up of circled region of one of the interfaces in (a). a and b are 150 µm and 320 µm respectively; (d) blow up of the center of design (b). Three separation channels are 5 µm wide by design and the wc is 120 µm wide.

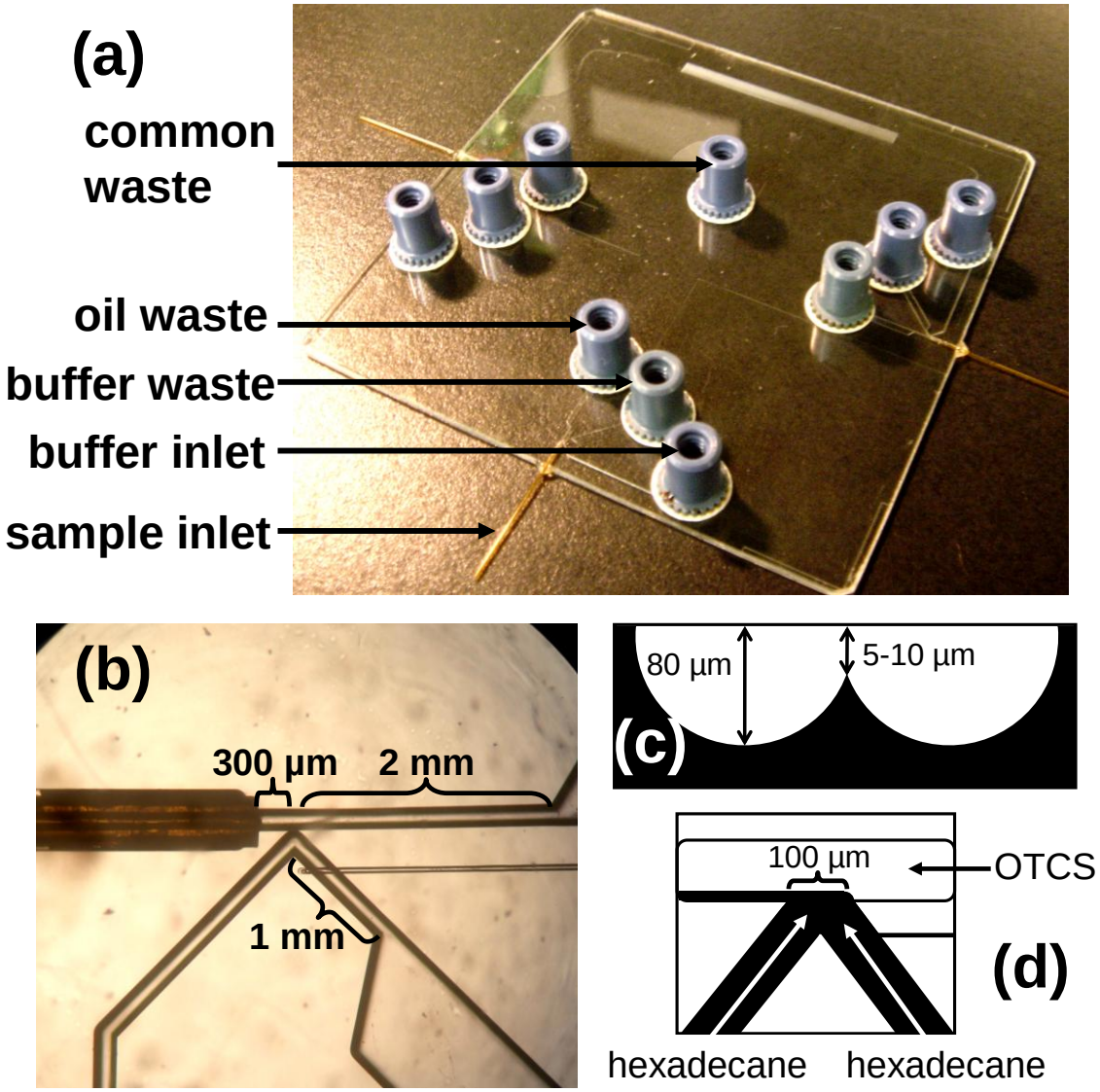

Figure 4-2. Specifications of the finished chip. (a). A picture of the completed device. Segmented flow enters the chip via the capillary labeled sample inlet. Buffer flow enters via buffer inlet using a nanoport connection unit. Buffer waste is grounded and a negative separation voltage is applied to common waste; (b). A close-up look of the extraction interface. The sample inlet capillary forms a dead volume-free connection with the microfluidic channel. The end of the capillary is only 300 µm from where two channels connect. Separation channel connects to the buffer channel at 300 µm downstream of the interface; (c) Cross section of the interface (not drawn to scale). Both channels are 80 µm deep while the gap between them is only 5-10 µm deep; (d) Channel modification procedure. The clear part shows the OTCS hexadecane solution flow profile (at 10 µL/min) while the dark part shows the hexadecane flow (at 2 µL/min from each direction).

Channel Wall Modification

In order to achieve phase separation for extracting aqueous droplets from the segmented flow, the microfluidic channels were selectively modified and made hydrophobic with OTCS[86, 173]. The chip was kept dry in a desiccator until channel wall derivatization. As shown in figure 4-2 (d), 0.5% OTCS solution in anhydrous hexadecane was flown through the segmented flow channel at 10 µL/min. Hexadecane was flown at the indicated directions at 2 µL/min. A Valco 6 port valve (VICI Valco Instruments Co. Inc., Houston, TX) was used for switching the flow through the segmented flow channel between OTCS solution and hexadecane without interrupting the flow profile. Stable flow was maintained for 4 min and bubbles flushed out before the flow was switched from hexadecane to OTCS solution for 7 min. The flow was switched back to hexadecane for another 14 min in order to flush out all residual OTCS. After derivatization, all channels were flushed three times with 200 µL anhydrous hexane and then thoroughly dried under vacuum.

Sample Preparation

GTPase assay for G protein α unit ($G_{\alpha o}$) was performed according to conditions reported before with some minor modifications[30]. The hydrolysis was initiated by mixing 2 µM BGTP with 100 nM $G_{\alpha o}$ in the TGEM buffer and the mixture was incubated at room temperature for some amount of time before it was quenched by adding 20 µM GTP. To generate cartridges containing nanoliter sample droplets, a 96-well plate the surface of which was modified according to a previously reported

method was used[174]. In brief, 60 µL of deionized water was placed in all the wells of the 96-well plate before the whole plate was sprayed with MS-122DF PTFE release agent (Miller-Stephenson Chemical Co. Inc., Danbury, CT). The water was then decanted and the plate dried before use. 60 µL of the quenched reaction mixtures were then placed in the plate and covered with an immiscible phase consisting of Fluorinert® FC-40 (Sigma) supplemented with 1% perfluoro-1-octanol. The modified plate surface kept the oil phase stable and on top of the aqueous samples even though it had a higher density. A Teflon tube of 150 µm i.d. and 360 µm o.d. (IDEX Health & Science, Oak Harbor, WA) was used to sample from the well plate and store the sample droplets. One end of this tubing was connected to a 100 µL syringe (Hamilton, Fisher Scientific, Pittsburg, PA) using a 250 µm bore PEEK union (Valco Instruments, Houston, TX). The syringe and Teflon tubing was pre-filled with the immiscible phase and a PHD 200 programmable syringe pump (Harvard Apparatus, Holliston, MA) in refill mode was used for sampling. An in-house built xyz-micropositioner (assembled from XSlide® assemblies, Velmex Inc., Bloomfield, NY) controlled by a Labview program written in-house (National Instruments, Austin, TX) was used to maneuver the inlet of the Teflon tubing and sample from each well. An aspiration rate of 1 µL/min was used to form the samples. Sample plugs were measured under a fluorescence microscope when they passed through the field of view and their sizes were estimated to have a variance of ±7%.

Mircrofluidic Chip Operation

Before use, chips were conditioned with 0.1 M NaOH in 50:50 (v:v) H_2O/Methanol by perfusing the solution through separation channels for 10 min. Care was taken so that the solution did not go into the hydrophobic channels. This was followed by conditioning channels with deionized water and electrophoresis buffer for 5 min each. Sample cartridges were connected to the chip inlet capillaries using 360 i.d. Teflon connectors. To start sample analysis, both buffer and segmented-flow were initiated while cathode reservoir was electrically connected to a negative high voltage (–HV) power supply (CZE1000R, Spellman High Voltage Electronics, Hauppauge, NY) and buffer waste reservoirs grounded. Voltage applied was controlled by a personal computer equipped with a multi-function board (AT-MIIO-16, National Instruments, Austin, TX) using software written in-house.

Fluorescence Detection and Data Analysis

Fluorescence detection of all separation channels was accomplished by collecting time-lapse intervals of fluorescence images using an inverted epi-fluorescence microscope (IX71, Olympus America, Inc., Melville, NY) as described before[30]. Briefly, light from a 300 W Xe arc lamp (LB-LS/30, Sutter Instrument Company, Novato, CA) was passed through a FITC filter cube (Semrock, Rochester, NY) before being focused on the chip detection region (Figure 4-1 (d)) with an objective lens (Olympus America Inc., Melville, NY). Fluorescent emission was collected with the same objective and detected using an electron-multiplying CCD camera (C9100-13,

Hamamatsu Photonic Systems, Bridgewater, NJ). Images were collected at ~10 Hz, stored, and analyzed with Slidebook software (Intelligent Imaging Innovations, Inc., Denver, CO). Fluorescence intensity corresponding to each separation channel was extracted from the images to produce parallel electropherograms that were analyzed using software written in-house[158].

Results and Discussion

Interface for droplet extraction

A microfluidic interface was designed and fabricated for extracting aqueous sample droplets from a bi-phase segmented flow. Previously an interface for this purpose was fabricated by manually aligning two microfluidic structures of different depths under microscope[86]. The wall of the deeper channel which segmented flow passed through was selectively rendered hydrophobic by derivatizing with OTCS. Electrophoresis buffer stream flowed through the shallower channel. It was found that it required a combination of channel wall modification and difference in channel depths to form a stable oil/aqueous interface. Otherwise the oil phase would easily invade the electrophoretic channel and interrupt with the separation. A potential use of this interface was to serially analyze samples stored in the droplet format. This way all other sample manipulations such as pipetting or injecting could be circumvented and the whole process automated. Only an external syringe pump would be required for sample delivery. In order to obtain higher throughput by processing multiple segmented flow streams simultaneously, it would be beneficial to

incorporate multiple such interfaces on a single microfluidic device, each interface assigned to a separation channel. However, the difficulty in the aligning step made the fabrication of parallel interfaces almost impossible. In this work, we developed a new approach. We found that geometrical restriction could be created by well-controlled isotropic etching. As shown in figure 4-1 (c), two channels were originally 150 μm apart in the photomask. During wet etching in a buffered hydrofluoric acid solution, these two channels would grown in both depth and width and eventually connect with each other. The etching was stopped when the gap between two channels was about 5 - 10 μm high (Figure 4-2 (c)).

Transfer of Droplets to Chip

A key requirement of the system is a suitable method for transferring sample plugs stored in Teflon tubing to the glass electrophoresis chip. For this purpose a commercial fitting (Upchurch nanoport) was initially evaluated. This way the Teflon tubing was connected to the microfluidic channel via a 360 μm o.d., 0.5 mm depth-access hole. Nanoports are convenient for fluidic connections when there is only one single phase. However, when used for segmented flow, the large dead volume of the access hole underneath the nanoports caused serious problems for the stability of the flow. Droplet coalescence and high cross contamination were observed.

To circumvent this problem, a zero-dead volume connection was made by directly connecting a flat-end capillary to the microfluidic channel via an access hole

drilled from the side of the chip. This piece of capillary was pre-treated with OTCS and then connected to the droplet-containing Teflon tubing using a home-made Teflon connector. Smooth droplet transferring without any coalescence was achieved using this method.

To pattern segmented-flow channel with a self-assembled monolayer of OTCS, it was found that the flow rate of hexadecane needed to be at least 1/5 of that of OTCS solution to prevent any accidental derivatization of the buffer flow channel caused by flow fluctuation. Accidental derivatization could cause oil phase entering buffer flow channel and failure of droplet extraction and was detrimental to chip performance. However, a higher hexadecane : OTCS solution ratio would create larger underivatized region in the segmented flow channel. Even though this region was found to be essential for droplet extraction, it was also a source of cross-contamination. Therefore, to minimize this region while establish a stable aqueous/oil interface, a flow rate ratio (OTCS : hexadecane) of 5 : 1 was used in all our experiments. A short width of the interface was also found helpful in preventing flow fluctuation during derivatization probably because the increased flow resistance kept OTCS from crossing the interface. In our design, the width of the interface was 20 μm in the photomask and 100 μm after etching (see Figure 4-2 (d)). Decreased interface width; however, was not observed to affect efficiency of droplet extraction. To further reduce the size of the underivatized region in the segmented flow channel, the side access hole was drilled as close as possible to the interface under a microscope so that the final length of this region was only about 300 μm (labeled in

Figure 4-2 (b)).

Conditions affecting quality of OTCS derivatization were also studied. Initially we found that even though most interfaces worked for the first few injections, performance of a significant portion of units deteriorated with time. In some cases, injection was no longer observed. By observing droplet extraction at the interface, we found that in these cases the aqueous layer in the segmented flow channel no longer existed and whole channel was taken over by the immiscible phase. Even though the oil phase did not cross the interface and enter the buffer channel, droplets would pass by the interface without being extracted. Reason for this was ascribed to instability of the OTCS/hexadecane interface during channel modification. This caused accidental but incomplete derivatization of the region which was supposed to be underivatized. Therefore the aqueous layer critical to droplet extraction was unstable and was gradually expelled by the oil phase. We found that air bubbles were the main cause of unstable flow interface during derivatization. Purging all air bubbles with hexadecane and establishing stable flow before switching to OTCS was found to greatly improve the success rate. In some other cases, peaks in the electropherograms gradually became broadened and resolution was lost. This was due to imperfect silane reaction which resulted in large underivatized areas in the segmented flow channel. Droplets would adhere to these areas and then slowly merge into the buffer stream thus broadening the injected plugs. As noted in literatures, silane reaction is extremely sensitive to moisture. To reduce moisture, we stored the chip in a desiccator until derivatization. Also all the solvents used

were dried with molecular sieves. However, even with all these precautions, the success rate was only 70%.

Separation channels which were 41 µm wide on top and 18 µm deep were fabricated on a different glass wafer. Deeper separation channels were used here because they were less prone to clogging when drilling the side access holes. In addition, water was perfused against the direction of the drilling so that most debris was flushed out. Connecting separation channels to the buffer channels was very simple and could be easily done with manual alignment under naked eye. Variation of the superimposed area of the two networks was found to have no significant effect on sample injection. Width of buffer flow channel was increased from 180 µm to 960 µm 1 cm after its interface with the segmented flow channel. This was found to be necessary to reduce the flow resistance after the inlet to the separation channel and minimize flow splitting which could compromise CE separation efficiency. Detection region was shown in Figure 4-1 (d) where three separation channels converged and connected to a common waste channel. This common waste channel had a width of 156 µm on top. This was found to efficiently prevent separation channels from being clogged. Also higher electric field could be generated along separation channels because less voltage was distributed across the waste channel (more details in the next part).

Chip performance

Sample injection control is essential for speed and quality of CE operation and

performance. Several factors such as sample size, flow rate and voltage were expected to affect injection and separation efficiency and thus studied in detail. Effects of channel modification and cross contamination were also studied.

1. Effect of interface modification. Two different modification patterns were created and compared. In figure 4-3 (b), the underivatized region in the segmented flow channel extended toward the same direction of segmented flow, while in figure 4-3 (a), the direction of this region was reversed. Sample droplet extraction was done using interfaces patterned both ways and electropherograms were compared (figure 4-3 (c)). Under the same experiment conditions, the interface in figure 4-3 (b) resulted in worse separation efficiency and resolution. By observing the extraction process it was found that this was caused by multiple injections from a single droplet. When a droplet reached the interface, a portion of it was extracted into the buffer stream but the other half merged into the aqueous layer. Since this layer was relatively stagnant the sample content was not flushed out to the waste. Instead a fraction of this layer would gradually leak into the buffer stream until it returned to its original volume. The result of this was either multiple injections or prolonged injection. Interestingly with interface 4-3 (a) this was not observed and complete extraction and clean injection were obtained. This was probably because in this case the aqueous layer acted as a path into the buffer stream which facilitated droplet transferring. Electropherograms showing better resolution were shown in the top panel of figure 4-3 (c). In all other studies, only interface with this pattern was used.

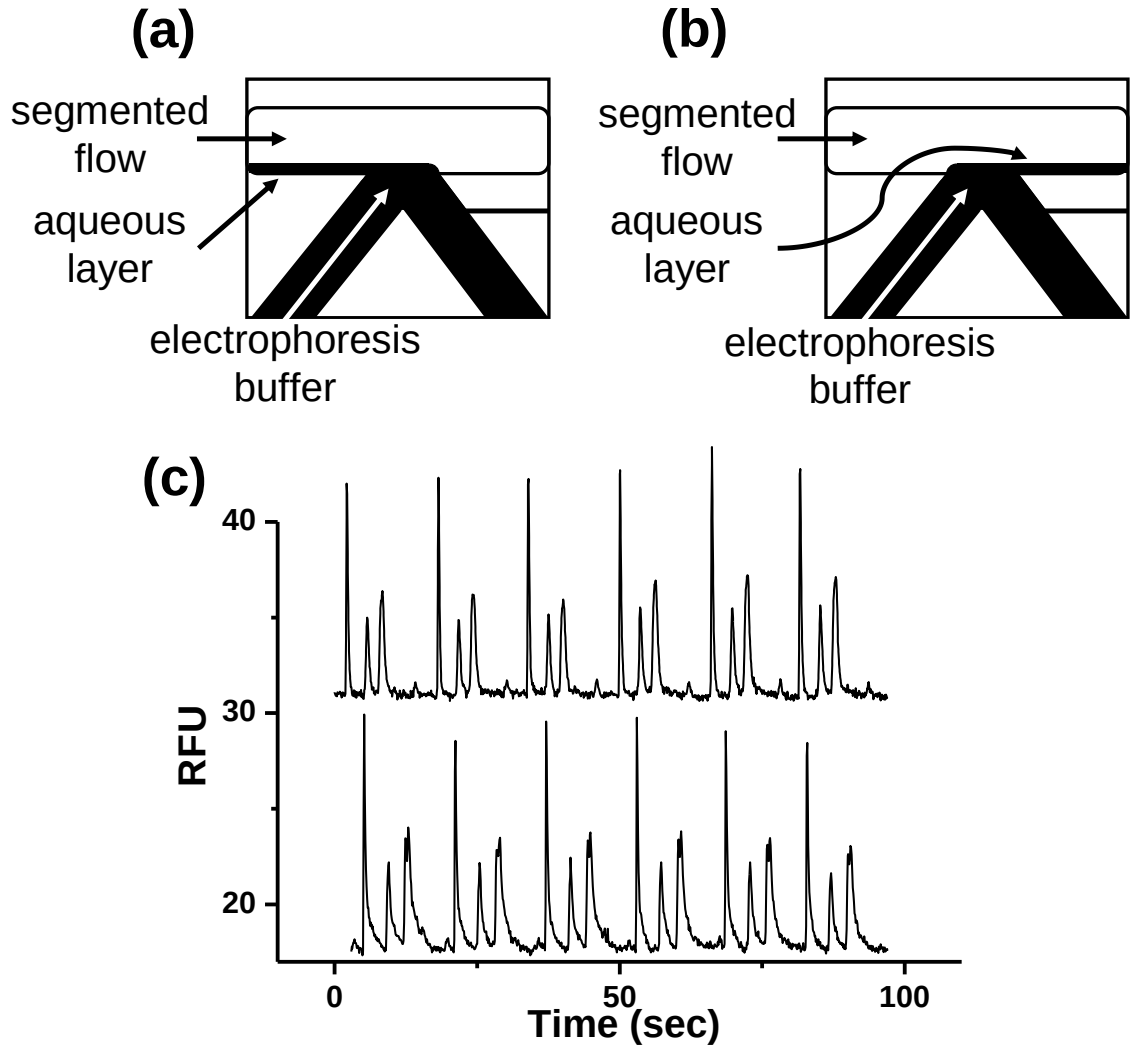

Figure 4-3. Two different channel modification patterns for droplet extraction. The clear region is modified with OTCS and therefore is hydrophobic. The dark region is underivatized and remains hydrophilic. (a). The hydrophilic region extends toward the inlet of the segmented flow. Once droplets enter the microfluidic channel they immediately merge into this region and are extracted into the electrophoresis buffer stream. A fraction of the droplet is then injected onto the separation channel positioned downstream; (b). The hydrophilic region points away from the inlet of the segmented flow channel. Droplet extraction doesn't happen until droplets reach the interface; (c). Typical electropherograms acquired from interface shown in (a) and (b) respectively. Top panel corresponds to interface (a) and shows better separation efficiency while bottom panel from interface (b) has broader peaks and worse resolution.

2. Cross contamination. With the interface shown in figure 4-3 (a), the biggest source of cross contamination was the aqueous layer in the segmented flow channel

because sample droplets merged into this layer before they enter the buffer stream. To minimize the volume of this layer, we have tried to decrease its length during fabrication as discussed earlier. In addition we have found that by supplementing the FC-40 with 1% (v/v) perfluoro-1-octanol the oil phase would expand and displace part of the aqueous layer thus further decreasing its volume. To evaluate cross contamination, two sample droplets followed by three blank droplets, each was about 9 nL, were serially analyzed on chip (Figure 4-4). Cross contamination in this case was 7%. After the first blank droplet, signals from the other two blanks did not drop significantly, which indicated that there might be other sources for cross contamination. Also since the source of cross contamination, the aqueous layer, had a constant volume, lower cross contamination should be possible if larger sample droplets are to be used.

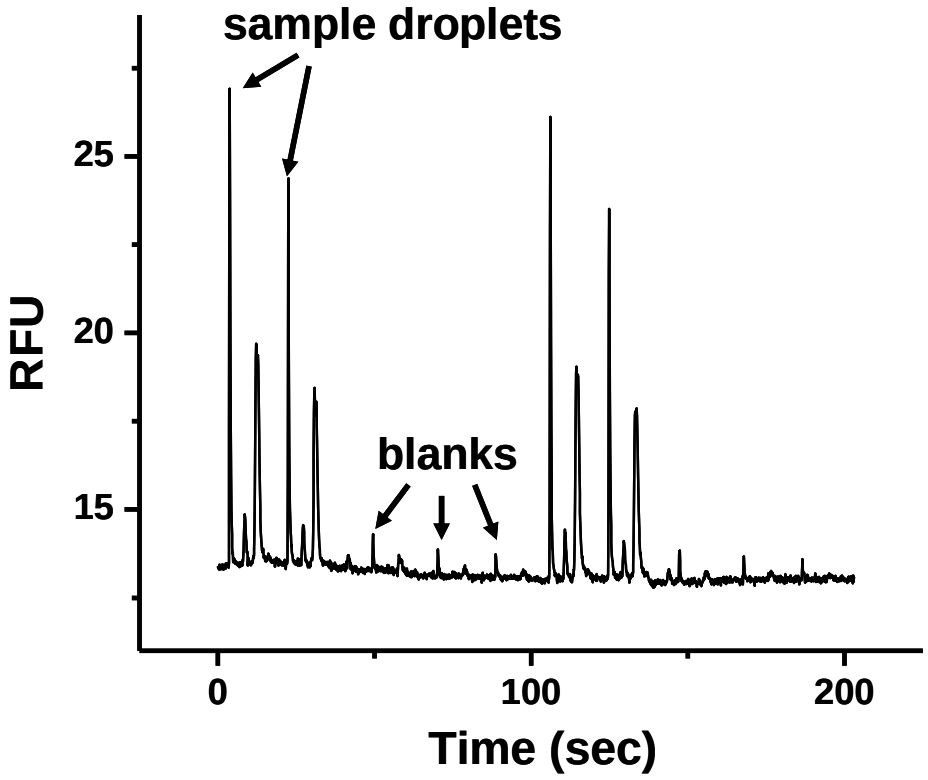

Figure 4-4. Typical electropherograms showing cross contamination. Two sample droplets containing 65.4 nM rhodamine 110 internal standard and 2 µM BGTP in TGEM followed by three blank droplets were extracted and injected. Each droplet was about 9 nL. Immiscible phase was Fluorinert® FC-40 supplemented with 1% perfluoro-1-octanol. Both segmented flow and buffer flow rates were 4 µL/min and separation voltage was 6 kV here. Cross contamination was evaluated using rhodamine 110 peak height and was about 7.3%.

3. Effect of sample size. It was expected that the size of the sample droplet should be proportional to amount of injection. Therefore an optimal sample size would be desirable to obtain the optimal combination of signal intensity and separation efficiency. Groups of sample droplets of different sizes were generated and then analyzed on chip (Figure 4-5 (a)). Peak width at half peak height was used to evaluate peak broadening. Determining actual separation efficiency (e.g. plate number) was difficult in this case because it was hard to determine to the time when

injections happened which was required to calculate migration time. As shown in Figure 4-5 (b), peak height increased with droplet size while peak broadening only worsened marginally. These results suggested that for the volumes used, the droplet volume was not a significant contributor to band broadening.

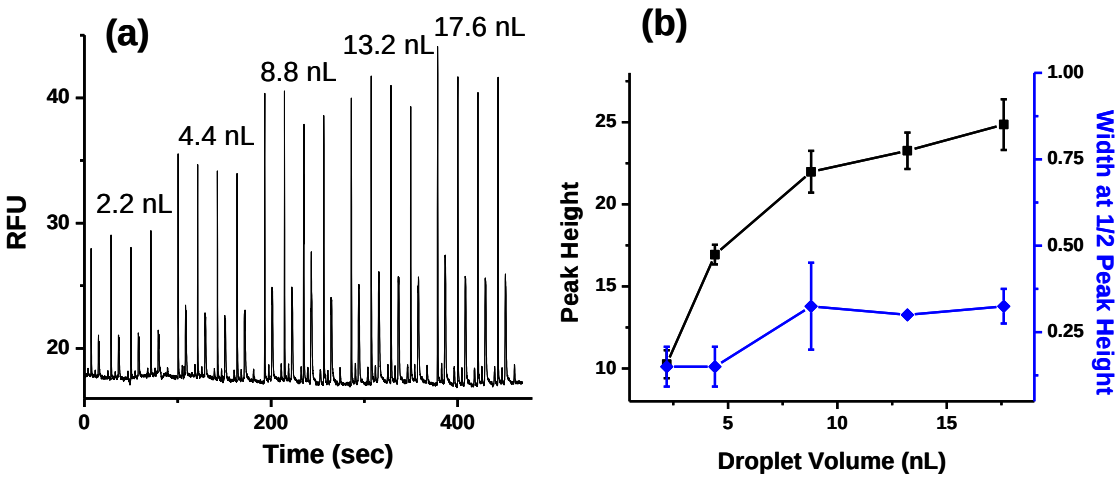

Figure 4-5. Effect of sample droplet size on CE separation. (a). Five groups of sample droplets of different sizes were analyzed on chip. Each group had four droplets of the same size as indicated in the figure. Each droplet contained 65.4 nM rhodamine 110 internal standard and 2 µM BGTP in TGEM buffer. Flow rate was 4 µL/min and separation voltage was 7 kV; (b). Rhodamine 110 peak heights (squares) and peak widths at half peak height (diamonds) were plotted against droplet sizes. Peak heights increased with droplet volumes indicating more injection at larger volume. Peak widths at half peak height only increased slightly from 2.2 nL droplets to 17.6 nL droplets, which meant that separation efficiency was not lost in this droplet size range. Error bars are ±1 SD and n=4.

4. Effect of flow rate. Effect of flow rate of segmented flow on sample injection and separation efficiency was evaluated. Segmented flow rate was varied from 2 to 5 µL/min while the buffer flow rate was varied accordingly and kept the same as the segmented flow. This way neither of the flow rates would be rate limiting and the segmented flow rate would be equal to how fast sample was swept across separation

channel inlet. As could be seen in Figure 4-6 (a), increasing flow rate directly resulted in higher injection frequency and thus higher throughput. Peak intensity decreased with increasing flow rate but peak broadening was not affected (Figure 4-6 (b)). This result again suggested that the volume injected was not a significant contributor to overall bandwidth. Thus, with this system a trade-off between throughput and efficiency could be made by varying sample and buffer flow rates.

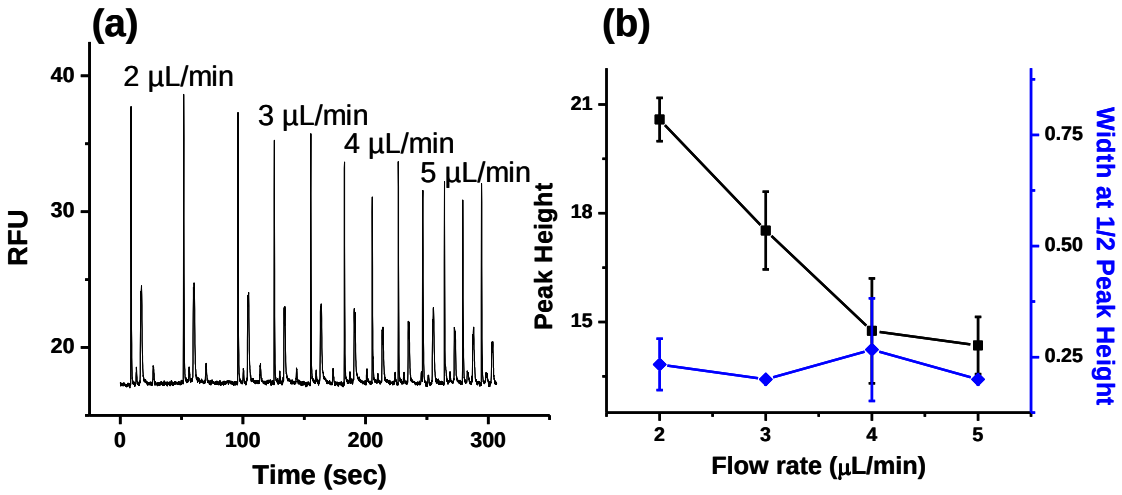

Figure 4-6. Effect of flow rate on CE separation. (a). Sample droplets of the same size and content were analyzed on chip but with varied flow rates as indicated. Three droplets were injected at each flow rate. Each droplet was about 9 nL and contained 65.4 nM rhodamine 110 internal standard and 2 µM BGTP in TGEM buffer. Separation voltage was 7 kV; (b). Rhodamine 110 peak heights (squares) and peak widths at half peak height (diamonds) were plotted against flow rates. Peak heights decreased with flow rates indicating less injection at high flow rate because sample passed by the separation channel inlet at a faster speed which meant less injection time. Peak width at half peak height which is inversely proportional to separation efficiency did not change in the flow rate range tested here. Error bars are ± 1 SD and n=3.

5. Effect of voltage. Since voltage was kept constant during chip operation, it acted as both injection voltage and separation voltage. Therefore its effect on separation efficiency was studied. As shown in figure 4-7 (a), voltage was varied

while other experiment conditions were kept constant. Four sample droplets were electrophoretially analyzed at each voltage. Intensity of electric field was estimated by calculating the ratio of resistance of separation channels and waste channel. Since the ratio was about 7.2:1, the electric field was 1 kV/cm when 4 kV was applied and 1.8 kV/cm when 7 kV was applied. As shown in Figure 4-7 (b), peak height increased with voltage while the peak broadening increased at first and then leveled off probably due to overinjection. Higher voltage was not tested due to arcing and possible Joule heating.

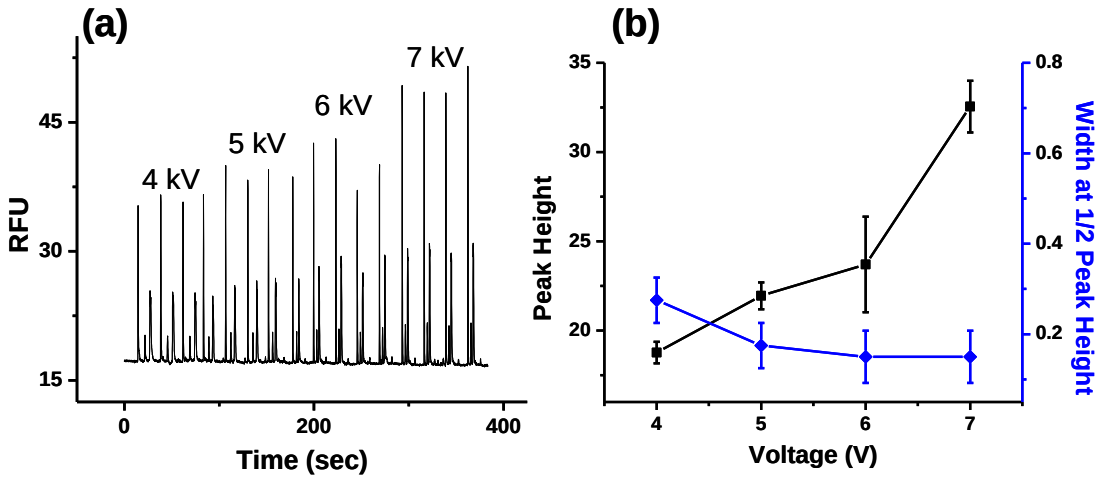

Figure 4-7. Effect of separation voltage on CE separation. (a). Sample droplets of the same size and content were analyzed on chip with different separation voltage applied. Four droplets were injected at each voltage. Each droplet was about 9 nL and contained 65.4 nM rhodamine 110 internal standard and 2 µM BGTP in TGEM buffer. Flow rate was 4 µL/min; (b). Rhodamine 110 peak heights (squares) and peak widths at half peak height (diamonds) were plotted against voltages. Peak heights increased with voltage indicating more injection. Peak width at half peak height first decreased from 4 kV to 5 kV indicating increased separation efficiency. But it leveled off at higher voltage gradually. Error bars are ± 1SD and n=4.

As could be seen in the discussion above, injection control with the device presented here was totally different than previously reported electrophoretic devices. In traditional CE instrument, inlet of the capillary is moved between sample vials and electrophoresis buffer vial to switch between injection mode and separation mode. Voltage control is required for turning on and off power supply during the operation. Besides adding complexity to the operation, it also affects the instrument's duty cycle. Flow-gated CE obviates mechanical control of the CE capillary, but it requires additional control (e.g. high-speed solenoid valve) for the gating flow. CE on chip is more simplified and injection is solely controlled by manipulating potentials at different reservoirs. Two injections modes i.e. pinched injection and gated injection are most commonly used and electroosmotic flow is main driving force for injection control. At least one power supply and one high-voltage relay are required for operation. With our microfluidic device, samples in droplet format were continuously transported onto chip and extracted when they approached the interface. An electric field was applied at all time across the separation channels. When a sample droplet was extracted and swept past the inlet of the separation channel a fraction of it would be injected for separation. This way only a syringe pump was required for sample introduction. No external computer program was necessary to control the power supply. This largely simplified the operation of the device.

Parallel Analysis of Segmented Samples

Our goal was to achieve high sample throughput that might be attractive to HTS

applications by electrophoretically analyzing segmented samples in parallel. One way to perform drug screening is to measure end-point reaction extent, i.e. amount of product formed or reactant consumed at fixed reaction times. By including test compounds in the reaction, the effect of active compounds can be detected. We have previously developed a CE-based enzyme assay for G protein GTPase activity. A fluorescent GTP analog BGTP was used as the surrogate enzyme substrate in the assay and its hydrolysis product BGDP was separated by CE from remaining BGTP. BGDP formation was thus used to determine GTPase activities. By performing the assay on chip in parallel, we have demonstrated inhibitor screening for *in vitro* modulator of G protein, RGS protein. However the overall throughput obtainable was limited by the speed of sample introduction. In this work, multiple streams of segmented samples consisting of the assay mixtures were fed to parallel separation channels via the interfaces described above to achieve high-throughput and automated analysis.

In an initial test of the system, we evaluated injection and separation stability within single unit and reproducibility across three parallel units. We first tested stability of single unit by serially extracting and analyzing droplets containing 65.4 nM rhodamine 110 and 2 μM BGTP in GTPase assay buffer. With a unit that continuously made 40 consecutive injections, the RSDs of absolute and relative (to internal standard rhodamine 110) peak areas of BGDP were estimated to be 15% and 6% respectively. We believe that improved derivatization procedures would enable longer term operation and lower RSDs. Glass surface activation using Piranha

solution prior to OTCS treatment might improve the derivatization quality[175]. Other surface patterning methods such as photocatalytic patterning[173, 176] might also turn out to be superior even though it requires special equipment such as a mask aligner.

Reproducibility across three parallel units was also evaluated. Sample droplets of the same size (9 nL) and content (65.4 nM rhodamine 110 and 2 µM BGTP) were analyzed at flow rate of 5 µL/min and voltage of 7 kV. Absolute peak area had high variation across three channels. RSD of R110 peak area was as high as 29% and BGDP 30%. Relative BGDP peak area to R110 was more suitable for quantification. Average relative BGDP peak areas from three units had an rsd of 2%. One-way ANOVA test showed that measurements by the three units were not significantly different from each other.

To demonstrate high throughput analysis of enzyme reactions for the purpose of HTS, 100 nM $G_{\alpha o}$ was incubated with 2 µM BGTP for 0, 15 and 30 minutes at room temperature. Three cartridges were generated each containing 40 9 nL droplets of one of the three quenched reaction mixtures. Content of all three cartridges was pumped out at 4.5 µL/min to chip for separation at a voltage of -7 kV. Figure 4-8 shows the typical parallel electropherograms. Each separation took 15 seconds and 120 samples were analyzed by CE within 10 minutes. Different levels of BGDP formation could be observed in the inset on the right. The throughput achieved here was equivalent to 720 samples/hr or 17,280 samples/day. We envision that even higher throughput could be achieved with more channels; however, fabrication difficulty and success rate have prevented us from going to higher numbers.

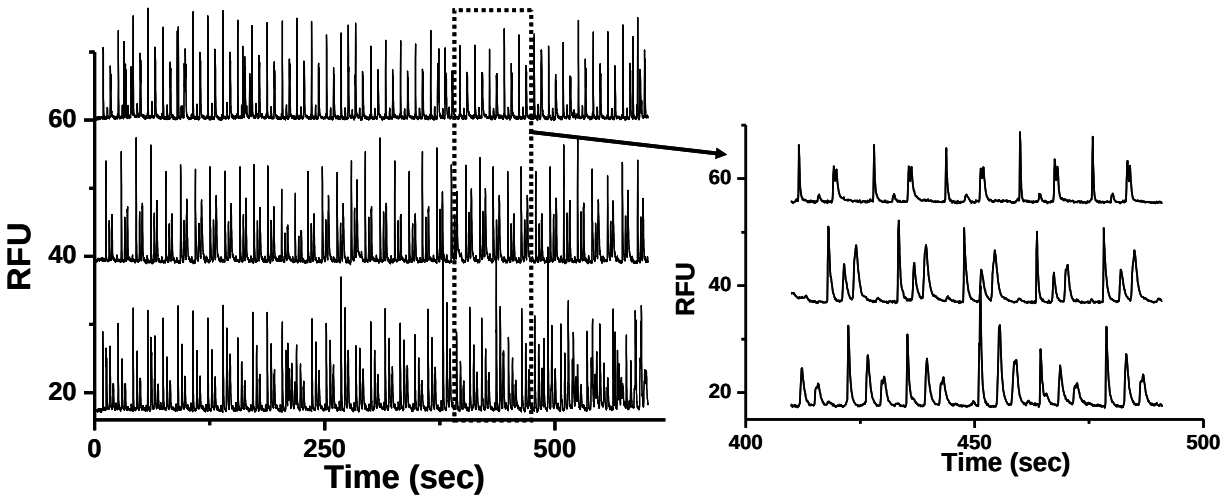

Figure 4-8. Parallel analyses of segmented samples. 100 nM $G_{\alpha o}$ was incubated with 2 μM BGTP in TGEM buffer at room temperature for 0, 15 and 30 minutes before the reactions were quenched by spiking in 10 μM GTP. 40 droplets, each having a volume of 9 nL, were generated from each reaction mixture and stored in a 150 μm inner diameter Teflon tubing. Gap between two neighbor droplets was about 1.42 μL of immiscible phase. All three sets of samples were analyzed simultaneously at 4.5 μL/min. -7 kV was applied for separation. 10 minutes analysis time was used to analyze all 120 samples. Different hydrolysis extent indicated by various BGDP peak heights could be observed in the close-up on the right.

Conclusions

We developed a microfabricated world-to-chip interface which coupled streams of segmented nanoliter samples to on-chip CE separation. Multiple such interfaces could be integrated on a single device which further increased the throughput. Chip operation required no sample pipetting and external control program and thus was highly automated. CE separation of discrete samples containing GTPase assay mixtures was demonstrated and throughput of 720 samples/hr was obtained. Despite the high throughput, life time of the device which was limited by the stability of the

modified channel wall remained to be improved. Also higher separation efficiency which is desirable when analyzing more complex samples might require more sophisticated sample injection control. One possible way to do so is to use fluorescence-activated voltage control. Fluorescence from a sample droplet will trigger a lower voltage for sample injection. A higher voltage will then be applied for high speed separation.

CHAPTER 5

RAPID ANALYSIS OF SAMPLES STORED AS INDIVIDUAL PLUGS IN A CAPILLARY BY ELECTROSPRAY IONIZATION MASS SPECTROMETRY AND APPLICATION IN HIGH-THROUGHPUT LABEL-FREE ENZYME INHIBITOR SCREENING

Introduction

Drug discovery often requires identification of lead compounds from combinatorial libraries containing millions of candidates. High-throughput screening (HTS) is necessary for such large scale sample handling and measurement[177]. *In vitro* biochemical assay in multi-well plates with optical detection[178-181] has been the primary format for HTS. A drawback of optical detection is that usually either labels or indicator reactions must be incorporated into the assay to generate detectable signal. This requirement results in several problems including increased difficulty of developing the assay, increased cost because of added or complex reagents, and greater potential for inaccurate results if test compounds affect the label or indicator reaction rather than the test reaction. High-throughput assays that can be performed without labels or indicator reactions are therefore of great interest[182].

A potentially powerful label-free detection system is electrospray ionization

mass spectrometry (ESI-MS). Indeed, a variety of ESI-MS assays for enzymes and non-covalent biomolecule binding have been developed and explored for screening applications[182-184]. The throughput achievable by ESI-MS is limited by the need to interface the mass spectrometer to multi-well plates and perform individual injections for each assay. (This limit assumes the standard procedure of testing one compound at a time. For certain assays, MS can analyze a mixture of test compounds at one time[96, 102]). Currently, individual samples are most often introduced to a mass spectrometer by flow injection, i.e. loading sample into an HPLC-style injection valve and then pumping it through the ESI emitter. It is a significant challenge to engineer a rapid injection system that uses small volumes, has low carry-over between injections, uses low flow rates, and is reliable. A rapid system that requires just 4-5 s per analysis and consumes 1-5 microliters of sample has been commercialized[185]; however, more common systems are considerably slower, having an average speed of 5-10 min/sample.

In this work, we forwent flow injection and utilized segmented flow analysis for high-throughput ESI-MS. Segmented flow has long been a popular method for high-throughput analysis in clinical settings[168]. In the classical scheme, individual samples are segmented by air in a tube, reagents added for colorimetric or fluorescent assays, and the samples passed through an optical detector[168, 169]. The last few years have seen a resurgence of interest in segmented flow with the advent of sophisticated microfluidics that allow miniaturization (femtoliter to nanoliter samples) and new methods for manipulating droplets[73, 91]. The sophistication of these methods has

rapidly increased so that it is now possible to perform many common laboratory functions such as sampling[74], splitting[75, 78, 186], reagent addition[76, 77], concentration[170, 171] and dilution[81] on plugs in microfluidic systems. A frequent emphasis is that such manipulations can be performed automatically at high-throughput. A limiting factor in using and studying multi-phase flows is the paucity of methods to chemically analyze the contents of plugs. Optical methods such as colorimetry[168] and fluorescence[81] are most commonly used. Systems for electrophoretic analysis of segmented flows have also been developed[85, 86]. Drawbacks of these methods are that they require that the analytes be labeled to render them detectable and they provide little information on chemical identity of plug contents. NMR has been used for analysis of plugs, but poor sensitivity of this method limits its potential applications[89]. Mass spectrometry has been coupled to segmented flow by collecting samples onto a plate for MALDI-MS[82] or a moving belt interface for electron impact ionization-MS[187]. ICP-MS of air-segmented samples has been demonstrated on a relatively large sample format (0.2 mL samples)[188]. MS analysis of acoustically levitated droplets using charge and matrix-assisted laser desorption/ionization has also been demonstrated[189]. Recently, a method to perform electrospray ionization (ESI)-MS of a stream of segmented flow has been reported[87]. In this method, a stream of aqueous droplets segmented by immiscible oil was periodically sampled by using electrical pulses to transfer the droplet into an aqueous stream that was directed to an electrospray source. This proof-of-concept report showed the feasibility of on-line droplet analysis; however, the limit of detection (LOD) for peptide was ~500

μM. The high LOD was due at least in part to dilution of droplets once transferred to the aqueous stream and the high flow rate (~3 μL/min) for the electrosprayed solution. The dispersion of droplets after transfer to the aqueous stream also limited the throughput of this approach.

We have found that a cartridge of 10 to 50 nL samples segmented by gas within a Teflon tube can be pumped directly into a electrospray source to yield a simple, robust and sensitive method for analyzing droplet content. This method can also be considered a novel approach to sample introduction for MS. As a test system we demonstrate screening for inhibitors of acetylcholinesterase (AchE). AchE catalyzes conversion of acetylcholine (Ach) to choline and is the primary way of terminating Ach signaling at synapses. Inhibition of AchE is a possible treatment for Alzheimer's disease (AD) and other related dementia[55-57, 59]. While a handful of AchE inhibitors have been approved for AD treatment, searching for compounds with improved pharmacological and toxicological properties remains an active pursuit[60-63].

Because the AchE reaction does not generate components that are easily detected optically, screening has required coupling the enzyme with indicator reactions[64-68, 71]. It has also been demonstrated that AchE assays can be performed using flow-injection ESI-MS[71] and HPLC-MS[72] to directly detect substrate and/or product of the reaction. Throughput of 0.2 Hz with 1-5 μL of sample consumption was possible when using an automated sampling and injection[72]. In this work, we demonstrate that with direct ESI-MS of segmented flow, we can generate an analysis rate of 0.65 Hz while consuming only 10 nL of samples.

Experimental Section

Chemicals and Reagents

Water and methanol were purchased from Burdick & Jackson (Muskegon, MI). Acetic acid was purchased from Fisher Scientific (Pittsburgh, PA). All other chemicals were obtained from Sigma.

AchE Activity Measurement

10 mM NH_4HCO_3 was used as reaction buffer for all AchE experiments. AchE (from Electrophorus electricus, Type VI-S) was prepared daily from lyophilized powder at 90 µg/mL solution. 2 µL solution of drug to be tested was mixed with 20 µL AchE solution and incubated on ice for 30 min before being brought to room temperature. 20 µL 200 mM acetylcholine iodide solution was then added to above AchE solution to start hydrolysis. After incubation, 180 µL of an ice-cold mixture containing 1 mM chlormequat, 60% (v/v) methanol and 1.5% (v/v) acetic acid was then rapidly mixed with 20 µL of the enzyme mixture to terminate the reaction. 30 µL of each final quenched reaction mixtures were pipetted into a 384-well plate (Corning, Fisher Scientific, Pittsburg, PA) for loading into sample tube for analysis.

Sample Droplet Generation

Air-segmented sample droplets were generated using the system illustrated in Figure 5-1 A. A Teflon tube of 75 µm inner diameter (i.d.) and 360 µm outer

diameter (o.d) (IDEX Health & Science, Oak Harbor, WA) was used for sampling and storing sample plugs. One end of this tubing was connected to a 100 µL syringe (Hamilton, Fisher Scientific, Pittsburg, PA) using a 250 µm bore PEEK union (Valco Instruments, Houston, TX). The syringe and Teflon tubing were intially filled with Fluorinert® FC-40 (Sigma). The syringe was mounted onto A PHD 200 programmable syringe pump (Harvard Apparatus, Holliston, MA). To fill the tube with air-segmented samples, a computer-controlled xyz-micropositioner (assembled from XSlide® assemblies, Velmex Inc., Bloomfield, NY) was used to move the inlet of the Teflon tubing from sample-to-sample on the multi-well plate while the pump was operated at a fixed aspiration rate. By using an aspiration rate of 200 nL/min, 10 nL sample plugs and 4 mm long air plugs were produced. Using this procedure, a tube could be filled with 100 samples in ~10 min. The relative standard deviation of sample plug size was 25%. It was also observed that FC-40 formed a thin film covering the tubing wall and this was found to help decrease droplet-to-droplet carry over. Figure 5-1 B and C compared droplets generated with and without FC-40 coating.

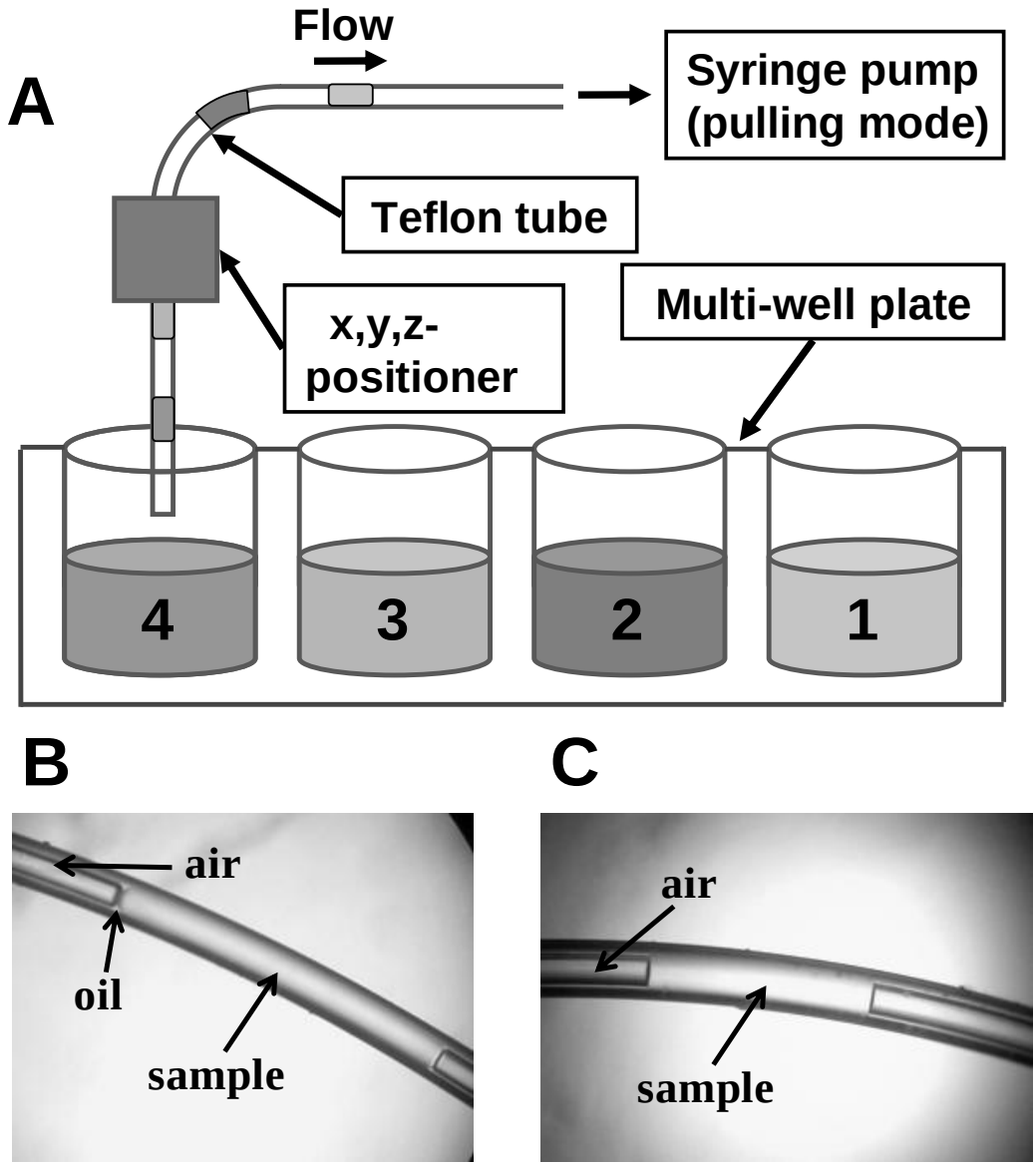

Figure 5-1. Generation of air-segmented sample plugs. A. Scheme showing generating air-segmented sample droplets from a multi-well plate. Cartridges of sample droplets were prepared by dipping the tip of a 75 μm i.d. Teflon tubing prefilled with Fluorinert FC-40 into sample solution stored in a multi-well plate, withdrawing a desired volume, retrieving the tube, withdrawing a desired volume of air, and moving to the next well until all samples were loaded. Movement of the tubing was controlled with an automated micropositioner and sample flow was controlled with a syringe pump connected to the opposite end of the tubing; B. Photograph of a 3 mm long (50 nL) plug stored in a 150 μm i.d. Teflon tube. Plug was created by withdrawing sample and air alternately into the tube prefilled with Fluorinert FC-40. Cross contamination was less than 0.1% in this case; C. Same as B except the tube was prefilled with air instead of oil. Cross contamination could be as high as 4%.

ESI-MS and Data Analysis

After sample plug generation, the inlet end of the Teflon tubing was connected to a Pt-coated fused-silica electrospray emitter (FS 360-50-8-CE, New Objective, Woburn, MA), which was 50 µm i.d. and pulled to 8 µm i.d. at the tip, using a 360 i.d. Teflon connector (Figure 5-2 A). The emitter was mounted in a nanospray source (PV-550, New Objective). Sample plugs were pumped at 1.0 µL/min using a syringe pump through the emitter poised at +1.7 kV for ESI-MS analysis. Electrospray plume could be seen when sample droplets arrived at the emitter tip (Figure 5-2 B) while there was no signal when air plugs exit (Figure 5-2 C). The MS used was a LTQ XL linear ion trap MS (Thermo Fisher Scientific, Waltham, MA) operated in single-stage, full-scan mode with following settings: automatic gain control (AGC) on, negative mode, 50 – 300 m/z scan range and micro scan number = 1. Scan time was approximately 0.1 s. Reconstructed ion current traces (RIC) of choline (m/z 104) and chlormequat (m/z 122) were extracted from total ion current (TIC). Peak marking and analysis were performed automatically by Qual Browser.

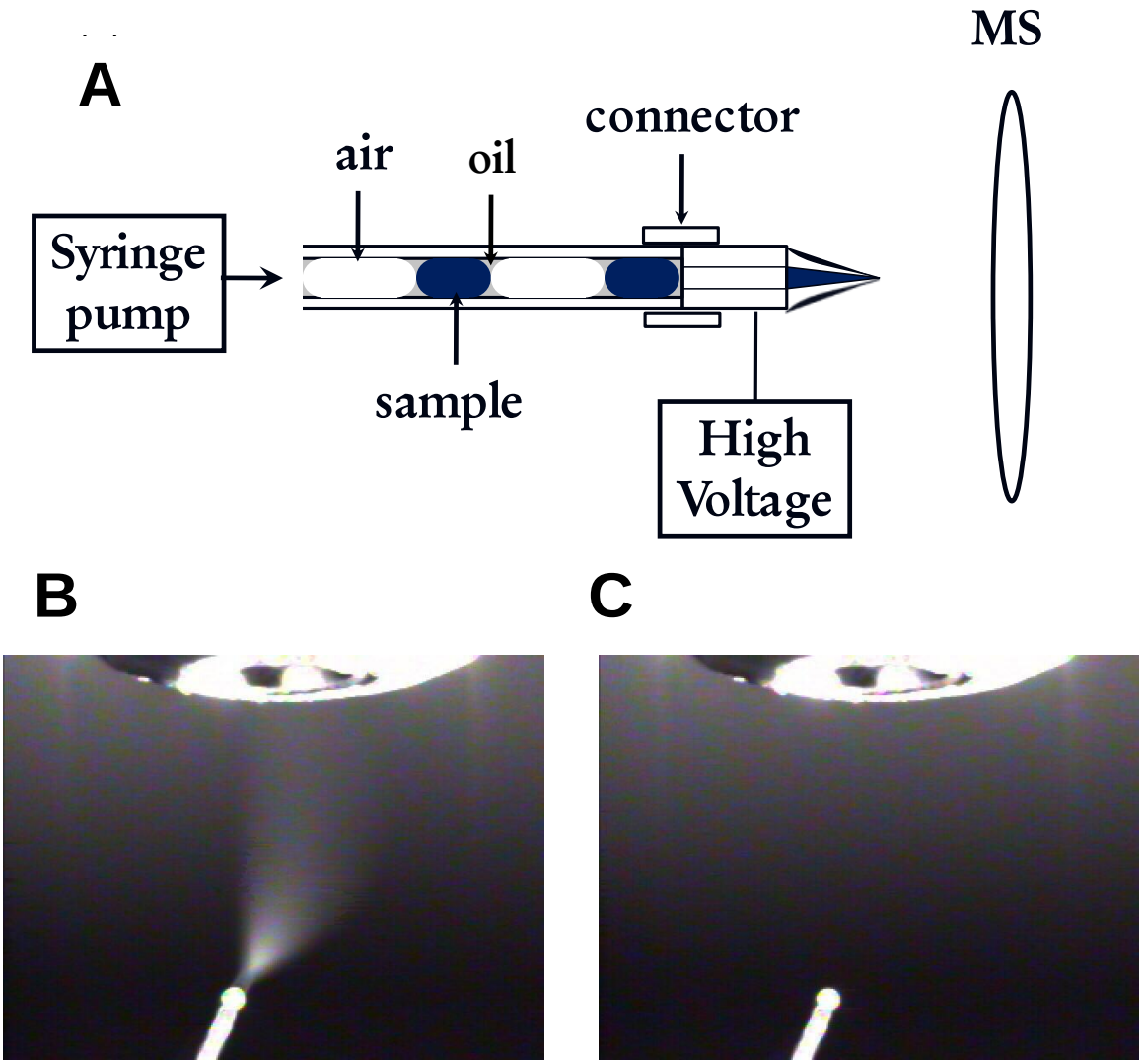

Figure 5-2. Direct ESI-MS analysis of air-segmented samples. A. Overview of scheme for analyzing a train of plugs stored in the Teflon tube. +1.7 kV is applied at the spray tip. Connector is a Teflon tube that fits snugly over the cartridge tube and emitter tip; B. A picture showing the electrospray plume when sample is emerging; C. A picture showing no electrospray when air is emerging.

Results and Discussion

Acetylcholinesterase assay

Initial experiments were directed at determining AchE assay conditions that would be compatible with ESI-MS. Incubating acetylcholine with AchE in 10 mM NH_4HCO_3 buffer for 20 min at room temperature followed by quenching of the

reaction by addition of a methanol and acetic acid mixture was found to be suitable. With this incubation time, less than 10% of the original acetylcholine was consumed thus ensuring linear hydrolysis rates. The quenching solvent was found to completely stop the enzymatic reaction and be compatible with MS. NH_4HCO_3 provided adequate buffering while being compatible with ESI and providing low ion suppression. To improve quantification, chlormequat was included in the quenching solution to act as an internal standard[71]. Typical MS spectra illustrating detection of substrate (acetylcholine), product (choline), and internal standard are shown in Figure 5-3. Under the electrospray conditions used, the spectra are free from interfering peaks from the Fluorinert® FC-40 used for coating the Teflon tubing. Inhibitors added to the assay reduced the choline signal as shown by Figure 5-3 A.

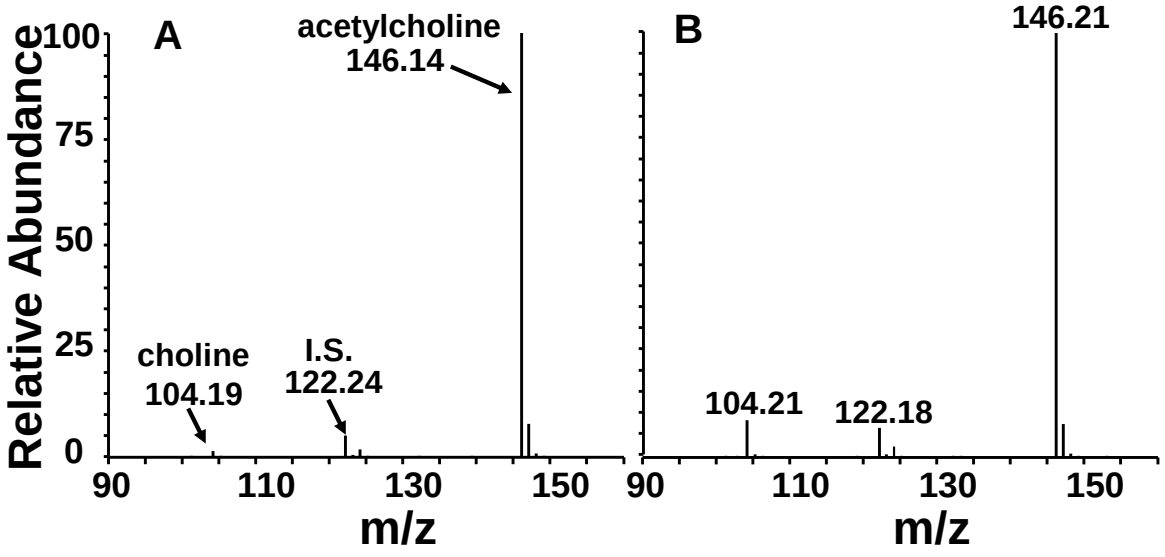

Figure 5-3. Typical mass spectra of AchE assay. Analysis of quenched AchE assay mixtures after incubating 100 mM acetylcholine with 45 µg/mL AchE with or without 100 µM neostigmine at room temperature for 20 minutes. Mass spectra showing inhibited (A) and basal (B) AchE activities. Compared to the basal spectrum, choline (m/z 104) production from hydrolyzing acetylcholine (m/z 146) is decreased and shows smaller MS intensity.

Rapid Screening

To demonstrate rapid screening of AchE inhibitors, a set of 32 compounds including 4 known AchE inhibitors and 28 randomly picked compounds were tested at 100 μM each in the AchE assay mixtures. For screening, each compound was tested in triplicate resulting in a total of 102 samples (96 assay samples, plus 3 blanks with no enzyme added, and 3 controls with no test compound added). These samples were loaded into a Teflon tube as a linear array using the procedure described in the Experimental Section. Throughput of analysis is determined by sample plug volume and flow rate into the ESI source so that small sample volumes and high flow rates generate higher throughput. For this work, 10 nL sample plugs with 17 nL air gaps (or 4 mm spacing in a 150 μm i.d. tubing) were chosen as a small volume that was convenient to produce. Samples were pumped through the emitter at 1 μL/min, which was the highest flow rate that did not cause the samples to merge in the emitter tip because of compression of the air segment.

These conditions allowed the 102 samples to be analyzed in 2.6 min, corresponding to an analysis rate of 0.65 Hz, as illustrated by ion current traces for the analysis shown in Figure 5-4 A. Each sample was detected as a current burst followed by a period of zero current corresponding to the air segment passing through the emitter. As shown, the current rapidly stabilized for each sample and remained steady as the sample passed through the emitter. The presence of inhibitors was easily visualized by the reduced choline signal relative to internal standard signal in these traces. The inconsequential carry-over between samples was illustrated by the

immediate step change in signal between samples of different choline concentrations.

The throughput of the segmented flow method compares favorably to previously reported flow injection AchE assays[65, 67, 72]. The speed of these methods was limited by the need to inject individual samples or additional separation steps when assay buffer was not directly compatible with ESI-MS. Other approaches for ESI-MS analysis of droplet or segmented flow samples have also been reported[87, 88]. These methods involve using microfluidics to extract the aqueous sample from an oil stream and transferring to a secondary aqueous stream before passing through the ESI emitter. The resulting band broadening and carry-over effects would likely keep throughput from being as good as that reported here.

Further improvements in throughput using the method reported here are feasible. One way is to generate smaller samples segmented by smaller air gaps by using smaller i.d. sample tubing and more sophisticated positioner that can move faster from well to well. This would be able to decrease the time required to analyze each sample. Higher flow rates may be possible by using fluorocarbon oil to segment samples to avoid the effect of air compressibility. Ultimately the analysis rate would be limited by the scan time of the mass spectrometer used.

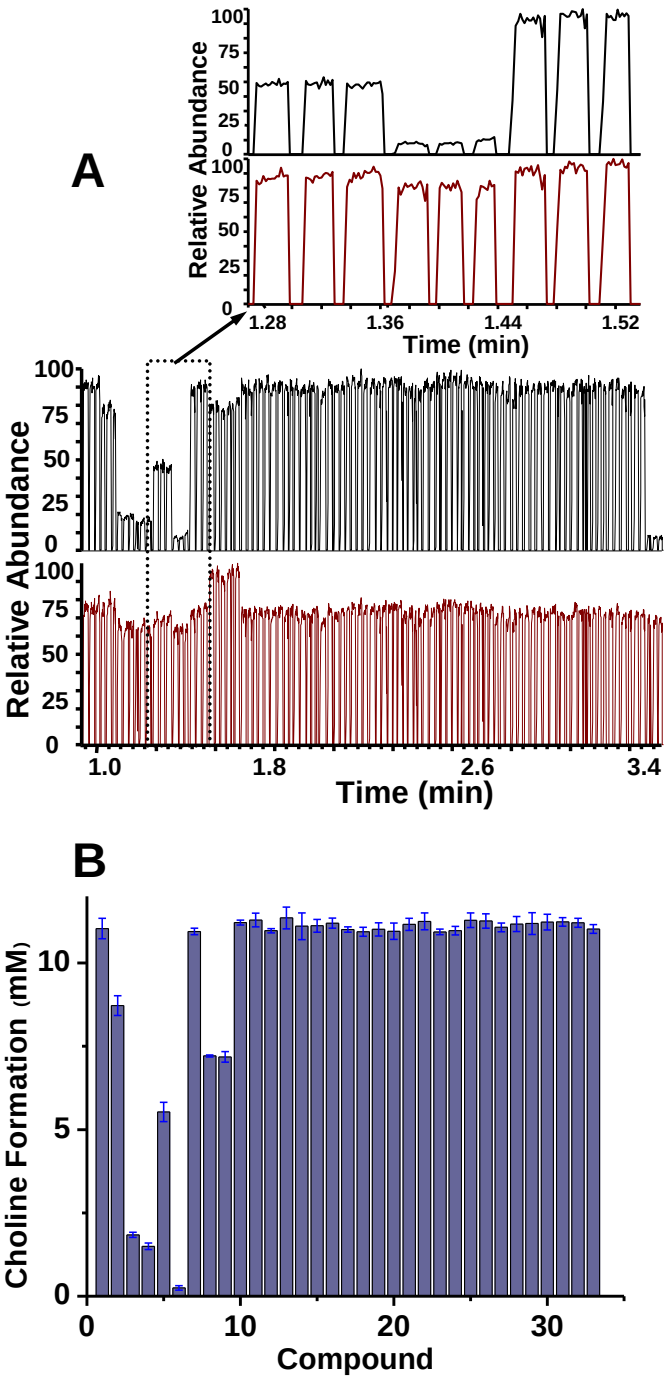

Figure 5-4. Screening of AchE inhibitors by droplet-ESI-MS. A. 32 compounds were tested for their activity toward AchE. Each compound had three replicates. 102 sample droplets were generated including these 32 compounds (96 droplets) and two controls (6 droplets). RICs of choline and clormequat from analyzing all 102 sample droplets in 2.5 min. Compounds tested from left to right were control 1 (no drug added), malathion, neostigmine, eserine, edrophonium, isoproterenol, yohimbine, UK14,304, DMSO, serine, adenosine, thyronine, GABA, phenylalanine, alanine, proline, arginine, cysteine, lysine, tyrosine, glycine, arginine, glutamine, methionine, leucine, tryptophan, isoleucine, histidine, glutamic acid, aspartic acid, taurine, dopamine, valine, control 2 (no enzyme added); B. After subtracting the background

choline, choline formation was calculated from the three replicates for each compound.

Quantification

To quantify choline production in the enzyme reaction, four different measurements were evaluated as shown in Figure 5-5 A. Absolute choline peak area had the most variability which was not surprising because the size of sample plugs had 25% variability. Peak heights were less variable but could sometimes be affected by fluctuation in electrospray stability. Choline peak area and height relative to the internal standard had low variability and both proved to be equally acceptable for quantification.

Charge competition between choline and internal standard chlormequat during electrospray and its effect on quantification was also evaluated. Choline signal intensity was measured at various choline concentrations with a fixed chlormequat concentration. As shown in figure 5-5 B, choline signal increased with its concentration non-linearly while chlormequat signal decreased with increasing choline concentration. By using choline signal relative to the internal standard, a linear calibration curve could be obtained demonstrating that the use of internal standard also helped to correct for charge competition during ESI at different choline concentrations.

Figure 5-4 B summarizes quantification of the assay screen shown in Figure 5-4 A using peak area ratio for choline and internal standard. Four of the known AchE inhibitors showed reduced choline production as expected. Interestingly,

isoproterenol and DMSO also showed some inhibition at this concentration. DMSO increased signal of both choline and chlormequat; however, quantification was not affected since relative signal intensities were used. This result indicates that the assay should be resistant to compounds that have generalized effects on the ESI-MS process. The reproducibility of the assay can be evaluated using the Z'-factor[45, 121]. Z'-factor is defined as $Z' = 1.0 - (3.0 \times (s_{neg} + s_{pos}) / R$ where s_{neg} is the standard deviation of the response of a negative control (no inhibitor) and s_{pos} in the standard deviation of the response of a positive control (with inhibitor) and R is the difference in signal between the mean of positive and negative controls. Z' over 0.5 is generally considered necessary for HTS. Z' values in experiments for neostigmine, eserine, malathion and edrophonium were 0.84, 0.83, 0.87 and 0.85 respectively. High Z' values were the direct result of excellent reproducibility.

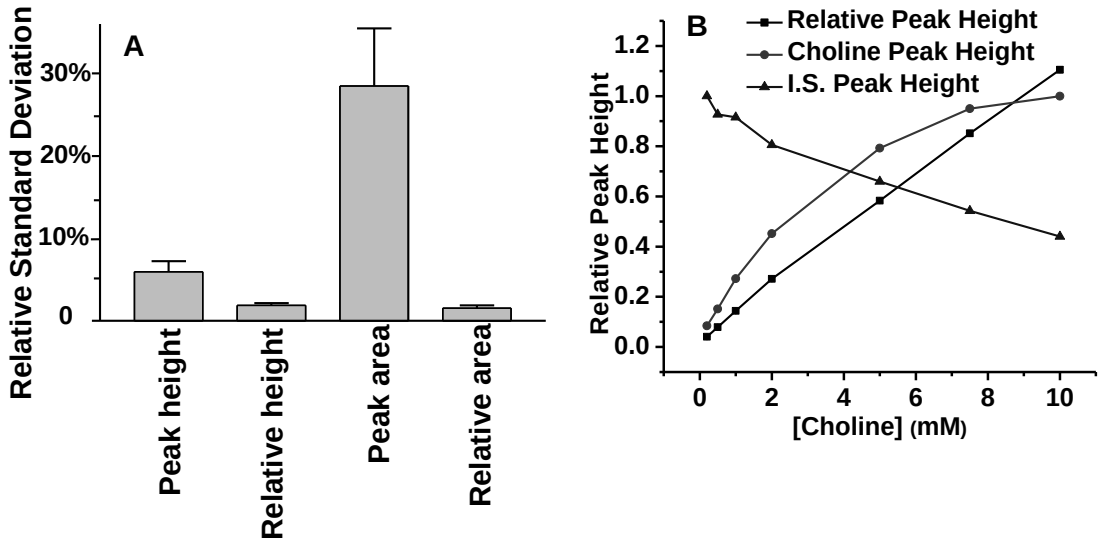

Figure 5-5. Quantification of AchE hydrolysis. A. Evaluating quantification of choline formation by four parameters: peak height is the highest choline ion intensity of all the scans over a sample droplet; relative height is the ratio of peak height of choline to that of chlormequat; peak area is the area under all the MS scans of a sample droplet; relative area is ratio of the peak area of choline to that of chlormequat.

Relative standard deviations of these four parameters from 7 separate experiments were used to generate the above figure. The average RSDs were 5.9%, 28.5%, 1.9% and 1.5% for calculation based on peak height, peak area, relative height and relative area respectively (n=7); B. Calibration curve for choline. Solutions containing 0.9 mM chlormequat and various concentrations of choline (200 µM to 10 mM) were infused for ESI-MS analysis. Choline peak intensity increased with its concentration non-linearly while chlormequat peak intensity decreased with higher choline concentration. Using ratio of the two peak heights corrected the effect caused by charge competition during electrospray ionization and the ratio increased linearly with choline concentration. The calibration curve had a slope of 0.1083 (mM^{-1}) and a y intercept of 0.03412. r^2=0.9991.

AchE inhibitor characterization

Another use of the assay is for rapid determination of dose-response relationships for known inhibitors as illustrated for neostigmine, eserine, malathion, and edrophonium in figure 5-6. For this experiment, 10 different concentrations of each inhibitor ranging from 10 mM to 0 nM were incubated with the assay mixtures for 20 min at room temperature. The quenched reaction mixtures were analyzed as described earlier and absolute choline formation was derived from the choline calibration curve. Three replicates were taken for each inhibitor concentration. IC_{50}s of eserine, malathion and edrophonium were calculated to be 63 ± 13 nM, 480 ± 70 µM, 63 ± 11 µM respectively. Neostigmine resulted in two IC_{50} values, 50 ± 25 µM and 38 ± 10 nM, based on two-site competition fitting. These number generally agreed well with previously reported values(eserine 72-109 nM[190], malathion 370 µM[191], neostigmine 11.3 nM[192] and edrophonium 5.4 µM[193]). However, direct comparison of these numbers might not be appropriate because the experiment conditions were not identical (e.g. use of surrogate substrate and different AchE).

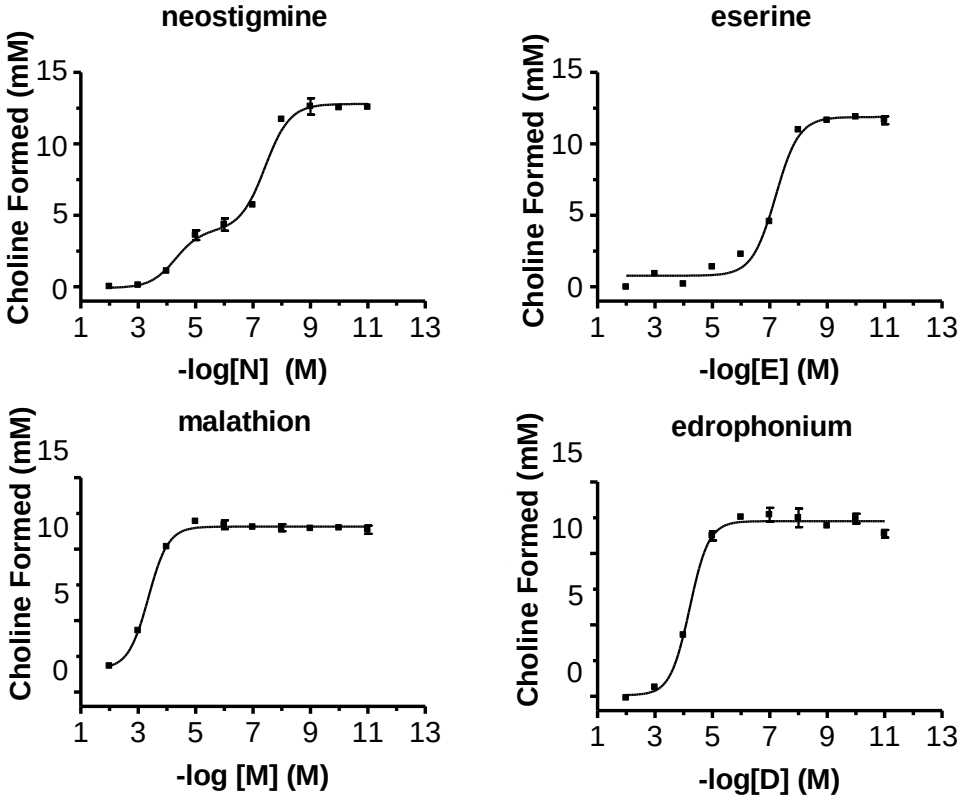

Figure 5-6. Dose-response curves of four AchE inhibtors: neostigmine, eserine, malathion, and edrophonium. Choline formation when incubated with various inhibitor concentrations were fit to sigmoidal dose-response curves except for neostigime which was fit to a two-site competition curve. Error bars are ±1 SD and n=3.

Conclusions

We demonstrated that AchE inhibitors could be screened at throughput of 1.5 s/sample by preparing samples as individual nanoliter plugs segmented by air and rapidly analyzing them using ESI-MS serially. The throughput achieved here showed a significant improvement over other screening methods since it did not require flow injection of individual samples. Higher throughput is possible by analyzing smaller sample droplets at higher flow rates. Another advantage of segmented flow analysis relative to flow injection approaches is the low sample

volume requirement. Only 10 nL of sample was consumed in this assay because there was no need to fill and rinse an injection loop. Of course, the total sample used depends on the volume required to collect the 10 nL sample. In principle it should be possible to aspirate sample from much lower volume wells than used here.

Although our experiments illustrated the possibility of rapid analysis of assay mixtures by MS, a complete HTS system would require consideration of all aspects of the screen for high-throughput. For example, in the present experiments the overall throughput was limited by loading of samples into the tube for assay. Parallel loading of tubes and higher flow rates during loading are approaches that may be used to improve throughput of this aspect of the method. Alternatively, since only a fraction of the assay mixture was consumed the entire assay approach could be performed in droplets. Several tools for manipulating droplets have been published including mixing with streams, reagent addition, and splitting[76, 78, 81, 91, 186]. Thus, it is possible to envision a system in which a chemical library is stored as a series of droplets that are then tested and assayed by MS and bypass the transfer from multi-well plate to tubing.

Another consideration in overall throughput is sample preparation. The Ach assay was compatible with ESI; however, some assays may require desalting or extraction prior to analysis. Development of such methods that are compatible with multi-well plates or with the segmented flow will be required to further expand the applicability of this approach.

CHAPTER 6

FUTURE DIRECTIONS

In this dissertation, we introduced two approaches to HTS. In the first approach we escalated the throughput of a CE-based fluorescent enzyme assay by performing fast and parallel CE separation. In the second approach, MS was exploited for HTS owing to its fast scanning speed and universal detection capability. One feature shared by these two approaches was the distinct sample introduction method. Instead of pipetting and injecting individual samples, which can be labor-intensive and time-consuming, samples were introduced as a train of droplets segmented by an immiscible phase. This way samples were fed to either CE or MS sequentially without additional sample handling or transferring. The achieved throughput was only limited by the speed of the analyzer.

While these two approaches showed promises for HTS applications, additional features such as on-line reagent addition and reaction, if added to the already developed techniques, could further automate the HTS operation. Also with appropriate modifications to the analytical systems presented herein, we could envision other interesting applications. All these possible routes are discussed in the next few sections.

On-line in-droplet enzyme reactions

In the experiments presented in chapters 2-5, enzyme assays including reagent mixing, incubation and quenching were performed offline. When used in HTS, offline assay format is compatible with how test compounds are currently stored in multi-well plates. Reagent mixing and reactions can take place on plate. This is convenient for direct on-plate readout such as using fluorescence plate reader; however, an additional droplet generation step is required if either of the herein developed methods is to be used. We envision that combinatorial compounds can be stored in tubes as segmented flow format in the future. Since reagent addition[76, 77] and in-droplet reaction[91] have been demonstrated, it will be extremely convenient and attractive to incorporate these operations on-line to achieved automated operations (Figure 6-1). This way enzyme and substrate can be mixed with individual test compounds sequentially and incubation will take place in droplets. Incubation time can be easily adjusted by either controlling the flow rate of the segmented flow or adjusting the tubing length after the second T-junction. Quenching reactions is no longer necessary because essentially all droplets should have the same incubation time. Figure 6-1 illustrates one possible scheme of such on-line ESI-MS-based screening assay. With this system, we can envision fully automated screening with very impressive throughput.

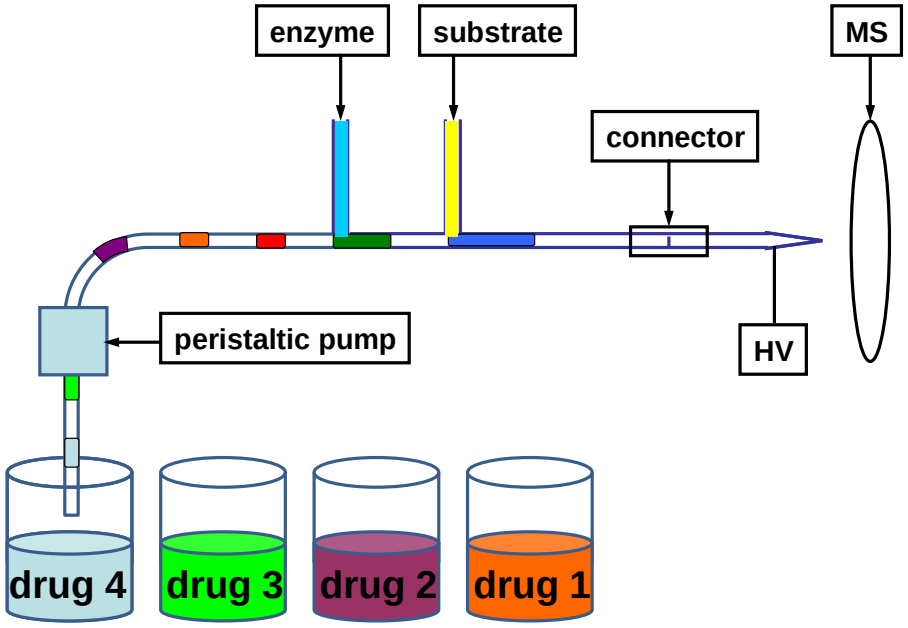

Figure 6-1. On-line droplet-based enzyme assay and MS analysis. A peristaltic pump is used to draw plugs of test compounds (compounds can also be pre-stored in the tubing as the compound library) from well plates. Enzyme and substrate solutions are mixed on-line with the drugs via two T-connectors. After some incubation time, individual droplets consisting of the assay mixture are analyzed by ESI-MS.

Screening using immobilized micro-enzyme reactors

Another alternative to on-line reagent mixing is to immobilize enzymes on the microfluidic channels to form micro-enzyme reactors (Figure 6-2). When droplets containing substrate and test compounds pass through the enzyme reactor, the substrate would be turned over. The reaction product is then detected by downstream analyzer (e.g. CE separation as shown in Figure 6-2). Advantages of using immobilized enzyme reactors include minimized enzyme consumption, improved catalytic efficiency and higher enzyme stability[111, 194].

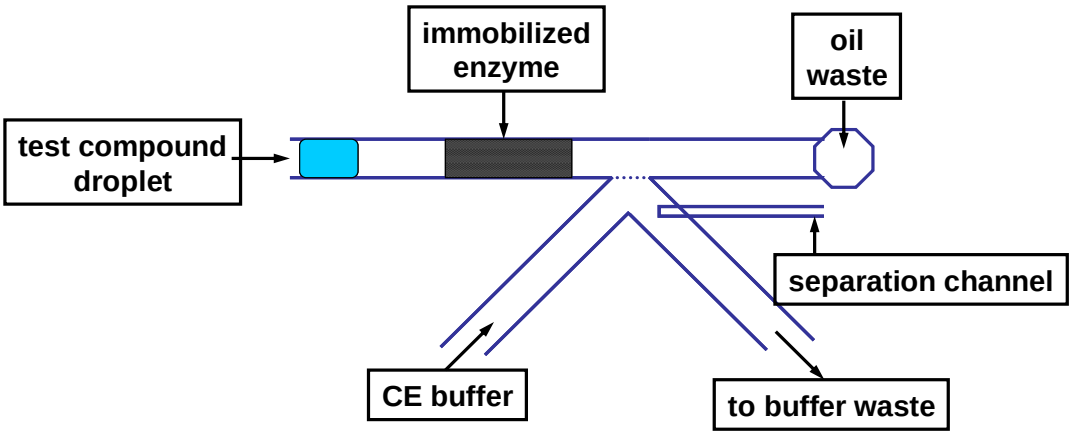

Figure 6-2. Microchannel enzyme reactor for droplet-based enzyme assay. An immobilized enzyme region (the reactor) is constructed before the droplet-to-CE interface described in Chapter 4. Substrate in the droplets are turned over when passing through the reactor and reaction product is separated from substrate by CE.

Single-cell analysis in droplets

Chemical analysis in single cells is of interest for proteomics and metabolomics studies. Due to the small volume of single cells and low concentration of intracellular chemicals, such analysis is difficult. One of the hurdles is that dilution after cell lysis makes the already low-concentration cellular components harder to detect. By encapsulating and lysing single cells in droplets, dilution can be minimized and molecules released from the cells can be more easily detected. In fact this has been reported by Chiu's group[195]. In their work, single-cell enzyme assay was performed in droplet and activity of intracellular β-galactosidase was detected by a fluorescence detector. It can be envisioned that more comprehensive chemical analysis can be achieved by using CE or MS or even CE-MS as the analyzer. Figure 6-3 shows a possible experiment scheme.

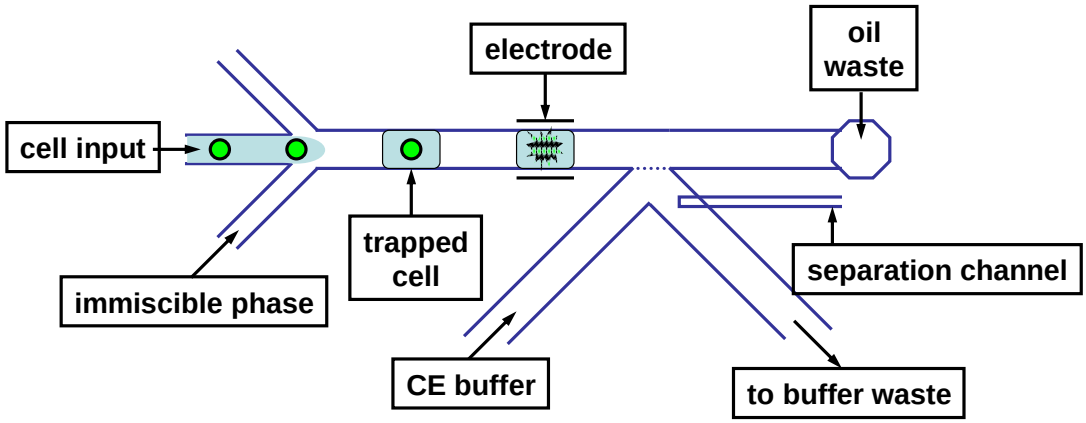

Figure 6-3. Single-cell analysis in droplets. Three steps are incorporated in this scheme. First the cells are encapsulated in individual droplets using a flow focusing device; the cells are then lysed using high electric field[196]; released cellular components remain trapped in droplets and are analyzed by CE (or MS).

LC fraction collection coupled to second-dimension separation

Fraction collection of LC effluent has been practiced extensively. Collected fractions are subjected to all sorts of post-separation analysis such as protein digestion, derivatization and a second-dimension separation step. For HPLC fraction collection can be assisted by commercial fraction collector; however for nano-LC, which is used for analyzing limited amount of samples, fraction collection can be difficult and impractical. We have shown that resolved bands in a nano-LC separation can be collected and stored in discrete droplets using a T-junction shown in Figure 6-4 A. This way LC resolution is preserved as segmented flow and post-analysis can be decoupled from LC separation. Droplet splitting can be used to further divide droplets so that each droplet can be analyzed with different methods (e.g. CE and MS) and results can be correlated (Figure 6-4 B). It is also possible to perform so-called retrospective analysis where the first halves of the droplets are to be analyzed rapidly and only those fractions of interest in the second halves are selected

for detailed analysis which usually takes more time. For example peak parking can be used for perform tandem MS on collected droplets for structural identification etc. A derivatization step can also be incorporated after collecting LC effluent and before further analysis (Figure 6-4 C). Appropriate derivatization agents can be used to enhance sensitivity.

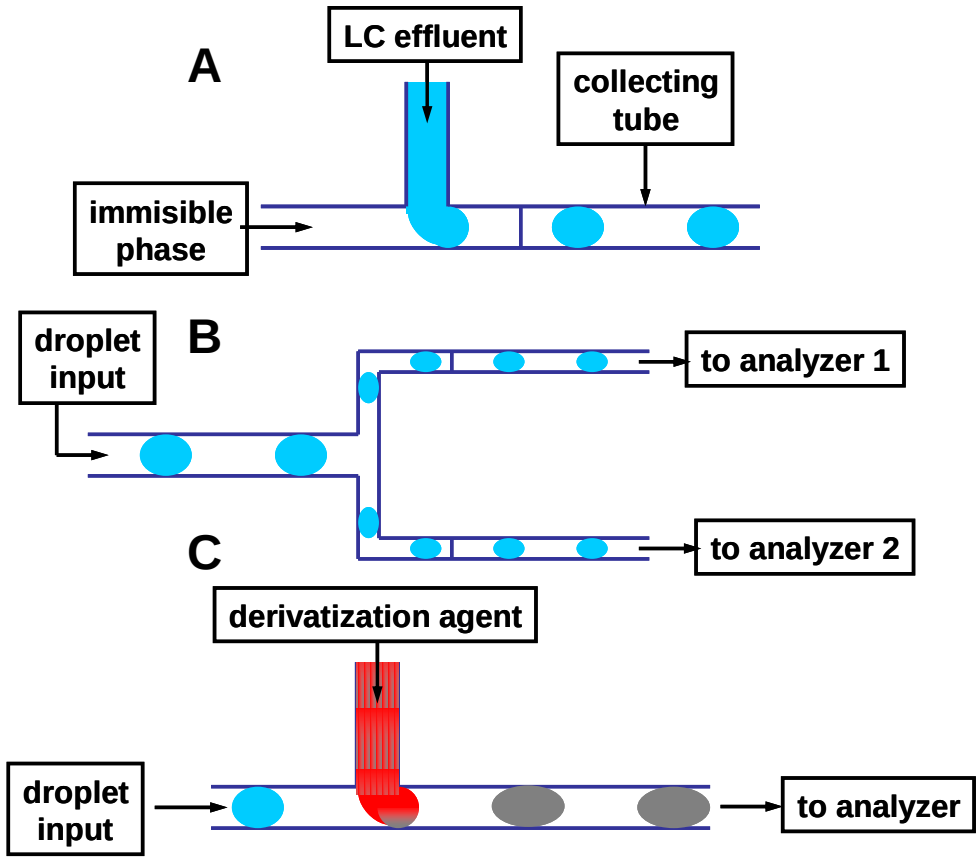

Figure 6-4. LC fraction collection and post-separation fraction processing. A. Effluent from LC separation is fractionized and collected as individual droplets using a T-junction. Droplets are stored in a tubing for later analysis; B. droplet splitting is used to produce two identical cartridges containing the LC fractions; C. derivatizing agent is added into previously collected droplets using a T-junction.

Droplet-based LC separation/desalting

We have demonstrated droplet analysis using CE and MS; however, LC is also of

interest to be applied to droplet analysis. One potential application of a LC separation step is desalting. Biological samples such as microdialysate and cell extract contain large amount of inorganic salts which can interfere with ESI by causing ion suppression. Generating a series of droplets as illustrated in Figure 6-5 and passing them sequentially through a reverse-phase packed column can be used for sample desalting and improve MS sensitivity. Difficulties of this project might include choosing the right immiscible phase and generating droplets of different contents.

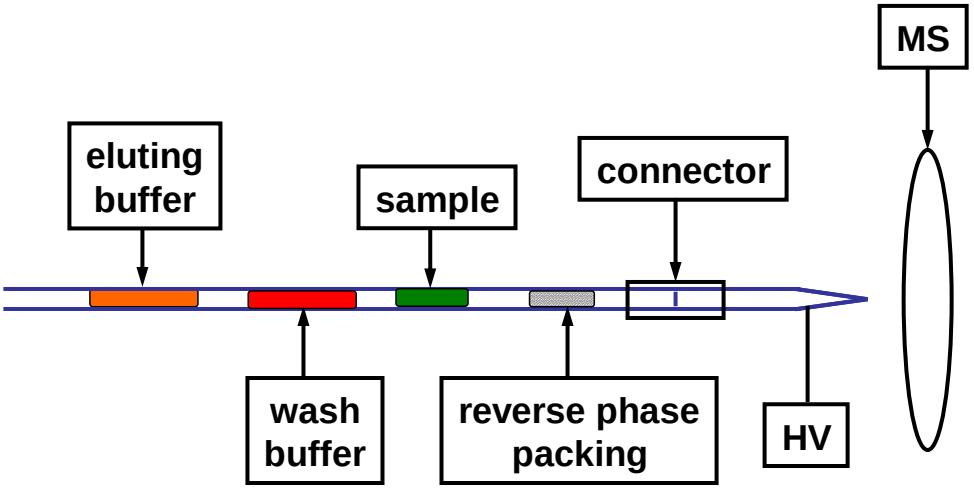

Figure 6-5. Droplet-based LC separation for desalting. A sample droplet, a wash droplet and an eluting solution droplet are pumped through a reverse-phase packed column sequentially. The outlet of the column is connected to a ESI emitter tip for ESI-MS analysis.

LITERATURE CITED

(1) Hertzberg, R. P.; Pope, A. J. *Current Opinion in Chemical Biology* **2000**, *4*, 445-451.

(2) Oldenburg, K. R.; Zhang, J. H.; Chen, T. M.; Maffia, A.; Blom, K. F.; Combs, A. P.; Chung, T. D. Y. *Journal of Biomolecular Screening* **1998**, *3*, 55-62.

(3) Wolcke, J.; Ullmann, D. *Drug Discovery Today* **2001**, *6*, 637-646.

(4) Rose, D. *Drug Discovery Today* **1999**, *4*, 411-419.

(5) Pope, A. J.; Haupts, U. M.; Moore, K. J. *Drug Discovery Today* **1999**, *4*, 350-362.

(6) Haupts, U.; Rudiger, M.; Pope, A. J. *Drug Discovery Today* **2000**, 3-9.

(7) Ramm, P. *Current Opinion in Biotechnology* **2005**, *16*, 41-48.

(8) Michaelis, L. *Biochemische Zeitschrift* **1909**, *16*, 81-86.

(9) Landers, J. P. *Handbook of Capillary Electrophoresis - second edition*, 1997.

(10) Krueger, R. J.; Hobbs, T. R.; Mihal, K. A.; Tehrani, J.; Zeece, M. G. *Journal of Chromatography* **1991**, *543*, 451-461.

(11) Van Dyck, S.; Kaale, E.; Novakova, S.; Glatz, Z.; Hoogmartens, J.; Van Schepdael, A. *Electrophoresis* **2003**, *24*, 3868-3878.

(12) Novakova, S.; Van Dyck, S.; Van Schepdael, A.; Hoogmartens, J.; Glatz, Z. *Journal of Chromatography A* **2004**, *1032*, 173-184.

(13) Glatz, Z. *Journal of Chromatography B-Analytical Technologies in the Biomedical and Life Sciences* **2006**, *841*, 23-37.

(14) Chen, D. Y.; Dovichi, N. J., Frederick, Md, Oct 19-20 1993; Elsevier Science Bv; 265-269.

(15) Ma, L.; Gong, X.; Yeung, E. S. *Anal. Chem.* **2000**, *72*, 3383-3387.

(16) Tu, J.; Anderson, L. N.; Dai, J.; Peters, K.; Carr, A.; Loos, P.; Buchanan, D.; Bao, J. J.; Liu, C.; Wehmeyer, K. R. *J. Chromatogr. B* **2003**, *789*, 323-335.

(17) Terry, S. C.; Jerman, J. H.; Angell, J. B. *Ieee Transactions on Electron Devices* **1979**, *26*, 1880-1886.

(18) Voldman, J.; Gray, M. L.; Schmidt, M. A. *Annual Review of Biomedical Engineering* **1999**, *1*, 401-425.

(19) Lagally, E. T.; Paegel, B. M.; Mathies, R. A., Enschede, Netherlands, May 14-18 2000; Springer; 217-220.

(20) Dolnik, V.; Liu, S. R.; Jovanovich, S. *Electrophoresis* **2000**, *21*, 41-54.

(21) Manz, A.; Harrison, D. J.; Verpoorte, E. M. J.; Fettinger, J. C.; Paulus, A.; Ludi, H.; Widmer, H. M., Basel, Switzerland, Jun 03-07 1991; Elsevier Science Bv; 253-258.

(22) Dolnik, V.; Liu, S. R. *Journal of Separation Science* **2005**, *28*, 1994-2009.

(23) Wu, D. P.; Qin, J. H.; Lin, B. C. *Journal of Chromatography A* **2008**, *1184*, 542-559.

(24) Hadd, A. G.; Raymond, D. E.; Halliwell, J. W.; Jacobson, S. C.; Ramsey, J. M. *Analytical Chemistry* **1997**, *69*, 3407-3412.

(25) Hadd, A. G.; Jacobson, S. C.; Ramsey, J. M. *Analytical Chemistry* **1999**, *71*, 5206-5212.

(26) Wang, J.; Chatrathi, M. P.; Tian, B. M. *Analytical Chemistry* **2001**, *73*, 1296-1300.

(27) Zugel, S. A.; Burke, B. J.; Regnier, F. E.; Lytle, F. E. *Analytical Chemistry* **2000**, *72*, 5731-5735.

(28) Cohen, C. B.; Chin-Dixon, E.; Jeong, S.; Nikiforov, T. T. *Analytical Biochemistry* **1999**, *273*, 89-97.

(29) Wang, J.; Ibanez, A.; Chatrathi, M. P.; Escarpa, A. *Analytical Chemistry* **2001**, *73*, 5323-5327.

(30) Pei, J.; Dishinger, J. F.; Roman, D. L.; Rungwanitcha, C.; Neubig, R. R.; Kennedy, R. T. *Analytical Chemistry* **2008**, *80*, 5225-5231.

(31) Dishinger, J. F.; Reid, K. R.; Kennedy, R. T. *Analytical Chemistry* **2009**, *81*, 3119-3127.

(32) Xu, H.; Roddy, T. P.; Lapos, J. A.; Ewing, A. G. *Anal Chem* **2002**, *74*, 5517-5522.

(33) Shen, Z.; Liu, X. J.; Long, Z. C.; Liu, D. Y.; Ye, N. N.; Qin, J. H.; Dai, Z. P.; Lin, B. C. *Electrophoresis* **2006**, *27*, 1084-1092.

(34) Shadpour, H.; Hupert, M. L.; Patterson, D.; Liu, C. G.; Galloway, M.; Stryjewski, W.; Goettert, J.; Soper, S. A. *Analytical Chemistry* **2007**, *79*, 870-878.

(35) Xu, H.; Ewing, A. G. *Electrophoresis* **2005**, *26*, 4711-4717.

(36) Lin, S.; Fischl, A. S.; Bi, X.; Parce, W. *Anal. Biochem.* **2003**, *314*, 97-107.

(37) Perrin, D.; Fremaux, C.; Scheer, A. *J. BIOMOL. SCREEN.* **2006**, *11*, 359-368.

(38) Woolley, A. T.; Mathies, R. A. *Proceedings of the National Academy of Sciences of the United States of America* **1994**, *91*, 11348-11352.

(39) Simpson, P. C.; Roach, D.; Woolley, A. T.; Thorsen, T.; Johnston, R.; Sensabaugh, G. F.; Mathies, R. A. *Proceedings of the National Academy of Sciences of the United States of America* **1998**, *95*, 2256-2261.

(40) Emrich, C. A.; Tian, H. J.; Medintz, I. L.; Mathies, R. A. *Analytical Chemistry* **2002**, *74*, 5076-5083.

(41) Aborn, J. H.; El-Difrawy, S. A.; Novotny, M.; Gismondi, E. A.; Lam, R.; Matsudaira, P.; McKenna, B. K.; O'Neil, T.; Streechon, P.; Ehrlich, D. J. *Lab on a Chip* **2005**, *5*, 669-674.

(42) Milligan, G.; Wakelam, M. *G proteins: signal transduction and disease*; Academic Press Limited: San Diego, CA, 1992.

(43) Thomsen, W.; Frazer, J.; Unett, D. *Curr. Opin. Biotechnol.* **2005**, *16*, 655-665.

(44) Milligan, G.; Kostenis, E. *British Journal of Pharmacology* **2006**, *147*, S46-S55.

(45) Neubig, R. R., Bethesda, Maryland, May 08-10 2002; Blackwell Munksgaard; 312-316.

(46) Thomsen, W.; Frazer, J.; Unett, D. *Current Opinion in Biotechnology* **2005**, *16*, 655-665.

(47) Marinissen, M. J.; Gutkind, J. S. *Trends in Pharmacological Sciences* **2001**, *22*, 368-376.

(48) Flower, D. R. *Biochimica Et Biophysica Acta-Reviews on Biomembranes* **1999**, *1422*, 207-234.

(49) Neubig, R. R.; Siderovski, D. *Nat. Rev.* **2002**, *1*, 187-197.

(50) Neubig, R. R. *J. Pept. Res.* **2002**, *60*, 312-316.

(51) Lan, K.; Sarvazyan, N. A.; Taussig, R.; Mackenzie, R. G.; Dohlman, H. G.; Neubig, R. R. *Faseb Journal* **1998**, *12*, 721.

(52) Lan, K.; Zhong, H.; Nanamori, M.; Neubig, R. R. *J. Biol. Chem* **2000**, *275*, 33497-33503.

(53) Roman, D. L.; Neubig, R. R., San Diego, CA, Mar 31-Apr 06 2005; Federation Amer Soc Exp

Biol; A1099-A1099.

(54) Jameson, E. E.; Roof, R. A.; Whorton, M. R.; Mosberg, H. I.; Sunahara, R. K.; Neubig, R. R.; Kennedy, R. T. *Journal of Biological Chemistry* **2005**, *280*, 7712-7719.

(55) Bartus, R. T.; Dean, R. L.; Beer, B.; Lippa, A. S. *Science* **1982**, *217*, 408-417.

(56) Perry, E. *British Journal of Psychiatry* **1988**, *152*, 737-740.

(57) Winkler, J.; Thal, L. J.; Gage, F. H.; Fisher, L. J. *Journal of Molecular Medicine-Jmm* **1998**, *76*, 555-567.

(58) Pang, H.; Kenseth, J.; Coldiron, S. *Drug Discovery Today* **2004**, *9*, 1072-1080.

(59) Greenblatt, H. M.; Dvir, H.; Silman, I.; Sussman, J. L. *Journal of Molecular Neuroscience* **2003**, *20*, 369-383.

(60) Zangara, A. *Pharmacology Biochemistry and Behavior* **2003**, *75*, 675-686.

(61) Livingston, G.; Katona, C. *International Journal of Geriatric Psychiatry* **2004**, *19*, 919-925.

(62) Maidment, I.; Fox, C.; Livingston, G.; Katona, C. *International Journal of Geriatric Psychiatry* **2006**, *21*, 6-8.

(63) Yamanishi, Y.; Kosasa, T.; Ogura, H.; Sugimoto, H. *Japanese Journal of Pharmacology* **2000**, *82*, 29P.

(64) Ellman, G. L.; Courtney, K. D.; Andres, V.; Featherstone, R. M. *Biochemical Pharmacology* **1961**, *7*, 88-&.

(65) Ingkaninan, K.; de Best, C. M.; van der Heijden, R.; Hofte, A. J. P.; Karabatak, B.; Irth, H.; Tjaden, U. R.; van der Greef, J.; Verpoorte, R. *Journal of Chromatography A* **2000**, *872*, 61-73.

(66) Ingkaninan, K.; Temkitthawon, P.; Chuenchom, K.; Yuyaem, T.; Thongnoi, W. *Journal of Ethnopharmacology* **2003**, *89*, 261-264.

(67) Andrisano, V.; Bartolini, M.; Gotti, R.; Cavrini, V.; Felix, G. *Journal of Chromatography B* **2001**, *753*, 375-383.

(68) Rhee, I. K.; Appels, N.; Luijendijk, T.; Irth, H.; Verpoorte, R. *Phytochemical Analysis* **2003**, *14*, 145-149.

(69) Guardigli, M.; Pasini, P.; Mirasoli, M.; Leoni, A.; Andreani, A.; Roda, A. *Analytica Chimica Acta* **2005**, *535*, 139-144.

(70) Guilarte, T. R.; Burns, H. D.; Dannals, R. F.; Wagner, H. N. *Journal of Pharmaceutical Sciences* **1983**, *72*, 90-92.

(71) Hu, F. L.; Zhang, H. Y.; Lin, H. Q.; Deng, C. H.; Zhang, X. M. *Journal of the American Society for Mass Spectrometry* **2008**, *19*, 865-873.

(72) Ozbal, C. C.; LaMarr, W. A.; Linton, J. R.; Green, D. F.; Katz, A.; Morrison, T. B.; Brenan, C. J. H. *Assay and Drug Development Technologies* **2004**, *2*, 373-381.

(73) Chen, D. L. L.; Ismagilov, R. F. *Current Opinion in Chemical Biology* **2006**, *10*, 226-231.

(74) Chen, D.; Du, W. B.; Liu, Y.; Liu, W. S.; Kuznetsov, A.; Mendez, F. E.; Philipson, L. H.; Ismagilov, R. F. *Proceedings of the National Academy of Sciences of the United States of America* **2008**, *105*, 16843-16848.

(75) Song, H.; Tice, J. D.; Ismagilov, R. F. *Angewandte Chemie-International Edition* **2003**, *42*,

768-772.

(76) Shestopalov, I.; Tice, J. D.; Ismagilov, R. F. *Lab on a Chip* **2004**, *4*, 316-321.

(77) Song, H.; Li, H. W.; Munson, M. S.; Van Ha, T. G.; Ismagilov, R. F. *Analytical Chemistry* **2006**, *78*, 4839-4849.

(78) Adamson, D. N.; Mustafi, D.; Zhang, J. X. J.; Zheng, B.; Ismagilov, R. F. *Lab on a Chip* **2006**, *6*, 1178-1186.

(79) Song, H.; Bringer, M. R.; Tice, J. D.; Gerdts, C. J.; Ismagilov, R. F. *Applied Physics Letters* **2003**, *83*, 4664-4666.

(80) Burns, M. A.; Johnson, B. N.; Brahmasandra, S. N.; Handique, K.; Webster, J. R.; Krishnan, M.; Sammarco, T. S.; Man, P. M.; Jones, D.; Heldsinger, D.; Mastrangelo, C. H.; Burke, D. T. *Science* **1998**, *282*, 484-487.

(81) Song, H.; Ismagilov, R. F. *Journal of the American Chemical Society* **2003**, *125*, 14613-14619.

(82) Hatakeyama, T.; Chen, D. L. L.; Ismagilov, R. F. *Journal of the American Chemical Society* **2006**, *128*, 2518-2519.

(83) Zheng, B.; Roach, L. S.; Tice, J. D.; Gerdts, C. J.; Chen, D.; Ismagilov, R. F., Malmo, SWEDEN, Sep 26-30 2004; Royal Soc Chemistry; 145-147.

(84) Zheng, B.; Ismagilov, R. F. *Angewandte Chemie-International Edition* **2005**, *44*, 2520-2523.

(85) Edgar, J. S.; Pabbati, C. P.; Lorenz, R. M.; He, M. Y.; Fiorini, G. S.; Chiu, D. T. *Analytical Chemistry* **2006**, *78*, 6948-6954.

(86) Roman, G. T.; Wang, M.; Shultz, K. N.; Jennings, C.; Kennedy, R. T. *Analytical Chemistry* **2008**, *80*, 8231-8238.

(87) Fidalgo, L. M.; Whyte, G.; Ruotolo, B. T.; Benesch, J. L. P.; Stengel, F.; Abell, C.; Robinson, C. V.; Huck, W. T. S. *Angewandte Chemie-International Edition* **2009**, *48*, 3665-3668.

(88) Kelly, R. T.; Page, J. S.; Marginean, I.; Tang, K. Q.; Smith, R. D. *Angewandte Chemie-International Edition* **2009**, *48*, 6832-6835.

(89) Kautz, R. A.; Goetzinger, W. K.; Karger, B. L. *Journal of Combinatorial Chemistry* **2005**, *7*, 14-20.

(90) Linder, V.; Sia, S. K.; Whitesides, G. M. *Analytical Chemistry* **2005**, *77*, 64-71.

(91) Song, H.; Chen, D. L.; Ismagilov, R. F. *Angewandte Chemie-International Edition* **2006**, *45*, 7336-7356.

(92) Anna, S. L.; Bontoux, N.; Stone, H. A. *Applied Physics Letters* **2003**, *82*, 364-366.

(93) Roddy, T. P.; Horvath, C. R.; Stout, S. J.; Kenney, K. L.; Ho, P. I.; Zhang, J. H.; Vickers, C.; Kaushik, V.; Hubbard, B.; Wang, Y. K. *Analytical Chemistry* **2007**, *79*, 8207-8213.

(94) Geoghegan, K. F.; Kelly, M. A. *Mass Spectrometry Reviews* **2005**, *24*, 347-366.

(95) Triolo, A.; Altamura, M.; Cardinali, F.; Sisto, A.; Maggi, C. A. *Journal of Mass Spectrometry* **2001**, *36*, 1249-1259.

(96) Mathur, S.; Hassel, M.; Steiner, F.; Hollemeyer, K.; Hartmann, R. W. *Journal of Biomolecular Screening* **2003**, *8*, 136-148.

(97) Hsieh, Y. F.; Gordon, N.; Regnier, F.; Afeyan, N.; Martin, S. A.; Vella, G. J., Osaka, Japan, Nov 07-09 1996; Kluwer Academic Publ; 189-196.

(98) vanBreemen, R. B.; Huang, C. R.; Nikolic, D.; Woodbury, C. P.; Zhao, Y. Z.; Venton, D. L. *Analytical Chemistry* **1997**, *69*, 2159-2164.

(99) Chu, Y. H.; Dunayevskiy, Y. M.; Kirby, D. P.; Vouros, P.; Karger, B. L. *Journal of the American Chemical Society* **1996**, *118*, 7827-7835.

(100) Schriemer, D. C.; Bundle, D. R.; Li, L.; Hindsgaul, O. *Angewandte Chemie-International Edition* **1998**, *37*, 3383-3387.

(101) Calleri, E.; Temporini, C.; Caccialanza, G.; Massolini, G. *Chemmedchem* **2009**, *4*, 905-916.

(102) Gao, J. M.; Cheng, X. H.; Chen, R. D.; Sigal, G. B.; Bruce, J. E.; Schwartz, B. L.; Hofstadler, S. A.; Anderson, G. A.; Smith, R. D.; Whitesides, G. M. *Journal of Medicinal Chemistry* **1996**, *39*, 1949-1955.

(103) Shin, Y. G.; van Breemen, R. B. *Biopharmaceutics & Drug Disposition* **2001**, *22*, 353-372.

(104) Hage, D. S.; Tweed, S. A. *Journal of Chromatography B* **1997**, *699*, 499-525.

(105) Milligan, G.; Feng, G. J.; Ward, R. J.; Sartania, N.; Ramsay, D.; McLean, A. J.; Carrillo, J. J. *Current Pharmaceutical Design* **2004**, *10*, 1989-2001.

(106) Sullivan, E.; Tucker, E. M.; Dale, I. L. *Methods Mol Biol* **1999**, *114*, 125-133.

(107) Frang, H.; Mukkala, V. M.; Syysto, R.; Ollikka, P.; Hurskainen, P.; Scheinin, M.; Hemmila, I. *Assay and Drug Development Technologies* **2003**, *1*, 275-280.

(108) Handl, H. L.; Gillies, R. J. *Life Sciences* **2005**, *77*, 361-371.

(109) Shutes, A.; Der, C. J. *Methods* **2005**, *37*, 183-189.

(110) Willard, F. S.; Kimple, A. J.; Johnston, C. A.; Siderovski, D. P. *Analytical Biochemistry* **2005**, *340*, 341-351.

(111) Bilitewski, U.; Genrich, M.; Kadow, S.; Mersal, G. *Analytical and Bioanalytical Chemistry* **2003**, *377*, 556-569.

(112) Jameson, E. E.; Roof, R. A.; Whorton, M. R.; Hosberg, H. I.; Sunahara, R. K.; Neubig, R. R.; Kennedy, R. T. *J. Biol. Chem.* **2005**, *280*, 7712-7719.

(113) Lee, E.; Linder, M. E.; Gilman, A. G. In *Heterotrimeric G Proteins*; Academic Press Inc: San Diego, 1994; Vol. 237, pp 146-164.

(114) Popov, S.; Yu, K.; Kozasa, T.; Wilkie, T. M. *Proceedings of the National Academy of Sciences of the United States of America* **1997**, *94*, 7216-7220.

(115) Barclay, E.; O'Reilly, M.; Milligan, G. *Biochemical Journal* **2005**, *385*, 197-206.

(116) Neubig, R. R.; Gantzos, R. D.; Brasier, R. S. *Molecular Pharmacology* **1985**, *28*, 475-486.

(117) German, I.; Kennedy, R. T. *Journal of Chromatography B-Analytical Technologies in the Biomedical and Life Sciences* **2000**, *742*, 353-362.

(118) Hooker, T. F.; Jorgenson, J. W. *Analytical Chemistry* **1997**, *69*, 4134-4142.

(119) Tao, L.; Kennedy, R. T. *Analytical Chemistry* **1996**, *68*, 3899-3906.

(120) Shackman, J. G.; Watson, C. J.; Kennedy, R. T. *Journal of Chromatography A* **2004**, *1040*, 273-282.

(121) Klaasse, E.; de Ligt, R. A. F.; Roerink, S. F.; Lorenzen, A.; Milligan, G.; Leurs, R.; Ijzerman, A. P. *European Journal of Pharmacology* **2004**, *499*, 91-98.

(122) Cassel, D.; Selinger, Z. *Biochimica Et Biophysica Acta* **1976**, *452*, 538-551.

(123) Thomsen, W. J.; Jacquez, J. A.; Neubig, R. R. *Molecular Pharmacology* **1988**, *34*, 814-822.
(124) Zhang, J. H.; Chung, T. D. Y.; Oldenburg, K. R. *Journal of Biomolecular Screening* **1999**, *4*, 67-73.
(125) Gille, A.; Seifert, R. *Naunyn-Schmiedebergs Archives of Pharmacology* **2003**, *368*, 210-215.
(126) Paegel, B. M.; Emrich, C. A.; Weyemayer, G. J.; Scherer, J. R.; Mathies, R. A. *Proceedings of the National Academy of Sciences of the United States of America* **2002**, *99*, 574-579.
(127) Goddard, J. P.; Reymond, J. L. *Curr. Opin. Biotechnol.* **2004**, *15*, 314-322.
(128) Eisenthal, R.; Danson, M. *Enzyme assays: a practical approach*; Oxford University Press, 2002.
(129) Inglese, J.; Johnson, R. L.; Simeonov, A.; Xia, M.; Zheng, W.; Austin, C. P.; Auld, D. S. *Nat. Chem. Biol.* **2007**, *3*, 466-479.
(130) Bush, K. *Drug Metab. Rev.* **1983**, *14*, 689-708.
(131) Hennig, A.; Bakirci, H.; Hau, W. M. *Nat. Methods* **2007**, *4*, 629-632.
(132) An, L.; Tang, Y.; Feng, F.; He, F.; Wang, S. *J. Mat. Chem.* **2007**, *17*, 4147-4152.
(133) Rossoando, E. *HPLC in enzymatic analysis*; J. Wiley & Sons: New York, 1998.
(134) Bao, J. J.; Fujima, J. M.; Danielson, N. D. *J. Chromatogr. B* **1997**, *699*, 481-497.
(135) Glatz, Z. *J. Chromatogr. B* **2006**, *841*, 23-37.
(136) Novakova, S.; Dyck, S. V.; Schepdael, A. V.; Hoogmartens, J.; Glatz, Z. *J. Chromatogr. A* **2004**, *1032*, 173-184.
(137) He, Y.; Yeung, E. S. *Electrophoresis* **2003**, *24*, 101-108.
(138) Dai, J.; Tu, J.; Anderson, L. N.; Bao, J. J.; Liu, C.; Quay, B.; Wehmeyer, K. R. *LC-GC N. Am.* **2002**, *20*, 606-612.
(139) Marsh, A.; Altria, K. *Chromatographia* **2006**, *64*, 327-333.
(140) Auroux, P.; Lossifidis, D.; Reyes, D. R.; Manz, A. *Anal. Chem.*. **2002**, *74*, 2637-2652.
(141) Culbertson, C. T.; Jacobson, S. C.; Ramsey, J. M. *Anal. Chem.* **2000**, *72*, 5814-5819.
(142) Dolnik, V.; Liu, S.; Jovanovich, S. *Electrophoresis* **2000**, *21*, 41-45.
(143) Jacobson, S. C.; Hergenroder, R.; Koutny, L. B.; Ramsey, J. M. *Anal. Chem.* **1994**, *66*, 1114-1118.
(144) Weigl, B.; Bardell, R. L.; Cabrera, C. R. *Adv. Drug Deliv. Rev.* **2003**, *55*, 349-377.
(145) Burke, B. J.; Regnier, F. E. *Anal. Chem.* **2003**, *75*, 1786-1791.
(146) Dunne, J.; Reardon, H.; Trinh, V.; Li, E.; Farinas, J. *Assay Drug Dev. Technol.* **2004**, *2*, 121-129.
(147) Hadd, A. G.; Jacobson, S. C.; Ramsey, J. M. *Anal. Chem.* **1999**, *71*, 5206-5212.
(148) Emrich, C. A.; Tian, H.; Medintz, I. L.; Mathies, R. A. *Anal. Chem.* **2002**, *74*, 5076-5083.
(149) Spiegel, A. M. *J. Inherit. Metab. Dis.* **1997**, *20*, 113-121.
(150) Zhong, H. L.; Neubig, R. R. *J. Pharmacol. Exp. Ther.* **2001**, *297*, 837-845.
(151) Heximer, S. P.; Knutsen, R. H.; Sun, X.; Kaltenbronn, K. M.; Rhee, M. H.; Peng, N.; Oliveira-dos-Santos, A.; Penninger, J. M.; Muslin, A. J.; Steinberg, T. H.; Wyss, J. M.; Mecham, R. P.; Blumer, k. J. *J. Clin. Invest.* **2003**, *111*, 1259.
(152) Erdely, H. A.; Tamminga, C. A.; Roberts, R. C.; Vogel, M. W. *Synapse* **2006**, *59*, 472-479.

(153) Traynor, J. R.; Neubig, R. R. *Mol. Interv.* **2005**, *5*, 30-41.
(154) Berman, D. M.; Wikie, T. M.; Gilman., A. G. *Cell* **1996**, *86*, 445-452.
(155) Roman, D. L.; Neubig, R. R. *FASEB J.* **2005**, *19*, A1099-A1099.
(156) Jin, Y.; Zhong, H.; Omnaas, J. R.; Neubig, R. R.; Mosberg, H. I. *J. Pept. Res.* **2004**, *63*, 141-146.
(157) Dishinger, J. F.; Kennedy, R. T. *Anal. Chem.* **2007**, *79*, 947-954.
(158) Shackman, J. G.; Watson, C. J.; Kennedy, R. T. *J. Chromatogr. A* **2004**, *1040*, 273-282.
(159) Gilman, A. G. *Annu. Rev. Biochem* **1987**, *56*, 615-649.
(160) Linder, M. E.; Ewald, D. A.; Miller, R. J.; Gilman, A. G. *J. Biol. Chem* **1990**, *265*, 8243-8251.
(161) Roof, R. A.; Jin, Y.; Roman, D. L.; Sunahara, R. K.; Ishii, M.; Mosberg, H. I.; Neubig, R. R. *Chem. Biol. Drug Des.* **2006**, *67*, 266-274.
(162) Jameson, E. E.; Pei, J.; Wade, S. M.; Neubig, R. R.; Milligan, G.; Kennedy, R. T. *Anal. Chem.* **2007**, *79*, 1158-1163.
(163) Cheng, S. B.; Skinner, C. D.; Taylor, J.; Attiya, S.; Lee, W. E.; Picelli, G.; Harrison, D. J. *Analytical Chemistry* **2001**, *73*, 1472-1479.
(164) Dishinger, J. F.; Kennedy, R. T. *Analytical Chemistry* **2007**, *79*, 947-954.
(165) Fang, Q. *Analytical and Bioanalytical Chemistry* **2004**, *378*, 49-51.
(166) He, Q. H.; Fang, Q.; Du, W. B.; Huang, Y. Z.; Fang, Z. L. *Analyst* **2005**, *130*, 1052-1058.
(167) Chen, G.; Wang, J. *Analyst* **2004**, *129*, 507-511.
(168) Furman, W. B. *Continuous-Flow Analysis. Theory and Practice*: New York, 1976.
(169) Snyder, L. R. *Analytica Chimica Acta* **1980**, *114*, 3-18.
(170) He, M. Y.; Sun, C. H.; Chiu, D. T. *Analytical Chemistry* **2004**, *76*, 1222-1227.
(171) Huang, K. D.; Yang, R. J. *Electrophoresis* **2008**, *29*, 4862-4870.
(172) Pei, J.; Li, Q.; Lee, M. S.; Valaskovic, G. A.; Kennedy, R. T. *Analytical Chemistry* **2009**, *81*, 6558-6561.
(173) Zhao, B.; Moore, J. S.; Beebe, D. J. *Science* **2001**, *291*, 1023-1026.
(174) Chabert, M.; Dorfman, K. D.; de Cremoux, P.; Roeraade, J.; Viovy, J. L. *Analytical Chemistry* **2006**, *78*, 7722-7728.
(175) Darhuber, A. A.; Troian, S. M.; Miller, S. M.; Wagner, S. *Journal of Applied Physics* **2000**, *87*, 7768-7775.
(176) Dulcey, C. S.; Georger, J. H.; Krauthamer, V.; Stenger, D. A.; Fare, T. L.; Calvert, J. M. *Science* **1991**, *252*, 551-554.
(177) Gomez-Hens, A.; Aguilar-Caballos, M. P. *Trac-Trends in Analytical Chemistry* **2007**, *26*, 171-182.
(178) Cockerill, G. S.; Lumley, J.; Bithell, S.; Jennens, L.; Wheeler, K.; Angell, R.; Stables, J.; Charles, I.; Hawkins, A.; Powell, K. *Abstracts of the Interscience Conference on Antimicrobial Agents and Chemotherapy* **2003**, *43*, 250-251.
(179) Hodder, P.; Mull, R.; Cassaday, J.; Berry, K.; Strulovici, B. *Journal of Biomolecular Screening* **2004**, *9*, 417-426.
(180) Miraglia, S.; Swartzman, E. E.; Mellentin-Michelotti, J.; Evangelista, L.; Smith, C.; Gunawan,

I.; Lohman, K.; Goldberg, E. M.; Manian, B.; Yuan, P. M. *Journal of Biomolecular Screening* **1999**, *4*, 193-204.

(181) Hodgson, L. *Acs Chemical Biology* **2008**, *3*, 335-337.

(182) Liesener, A.; Karst, U. *Analytical and Bioanalytical Chemistry* **2005**, *382*, 1451-1464.

(183) Zehender, H.; Mayr, L. M. *Current Opinion in Chemical Biology* **2007**, *11*, 511-517.

(184) Hofstadler, S. A.; Sannes-Lowery, K. A. *Nature Reviews Drug Discovery* **2006**, *5*, 585-595.

(185) Shiau, A. K.; Massari, M. E.; Ozbal, C. C. *Combinatorial Chemistry & High Throughput Screening* **2008**, *11*, 231-237.

(186) Link, D. R.; Anna, S. L.; Weitz, D. A.; Stone, H. A. *Physical Review Letters* **2004**, *92*, 054503.

(187) Karger, B. L.; Kirby, D. P.; Vouros, P.; Foltz, R. L.; Hidy, B. *Analytical Chemistry* **1979**, *51*, 2324-2328.

(188) Noguchi, O.; Oshima, M.; Motomizu, S. *Analytical Sciences* **2008**, *24*, 631-635.

(189) Westphall, M. S.; Jorabchi, K.; Smith, L. M. *Analytical Chemistry* **2008**, *80*, 5847-5853.

(190) Vinutha, B.; Prashanth, D.; Salma, K.; Sreeja, S. L.; Pratiti, D.; Padmaja, R.; Radhika, S.; Amit, A.; Venkateshwarlu, K.; Deepak, M. *Journal of Ethnopharmacology* **2007**, *109*, 359-363.

(191) Krstic, D. Z.; Colovic, M.; Kralj, M. B.; Franko, M.; Krinulovic, K.; Trebse, P.; Vasic, V. *Journal of Enzyme Inhibition and Medicinal Chemistry* **2008**, *23*, 562-573.

(192) Iwanaga, Y.; Kimura, T.; Miyashita, N.; Morikawa, K.; Nagata, O.; Itoh, Z.; Kondo, Y. *Japanese Journal of Pharmacology* **1994**, *66*, 317-322.

(193) Alvarez, A.; Alarcon, R.; Opazo, C.; Campos, E. O.; Munoz, F. J.; Calderon, F. H.; Dajas, F.; Gentry, M. K.; Doctor, B. P.; De Mello, F. G.; Inestrosa, N. C. *Journal of Neuroscience* **1998**, *18*, 3213-3223.

(194) Miyazaki, M.; Maeda, H. *Trends in Biotechnology* **2006**, *24*, 463-470.

(195) He, M. Y.; Edgar, J. S.; Jeffries, G. D. M.; Lorenz, R. M.; Shelby, J. P.; Chiu, D. T. *Analytical Chemistry* **2005**, *77*, 1539-1544.

(196) Brown, R. B.; Audet, J. *Journal of the Royal Society Interface* **2008**, *5*, S131-S138.